Addis Ababa University
Addis Ababa Institute of Technology
School of Electrical and Computer Engineering

DESIGN AND SIMULATION OF A NEURO-FUZZY BASED TEMPERATURE CONTROLLER FOR NEONATAL INCUBATOR

A thesis submitted to Addis Ababa Institute of Technology, School of Graduate Studies, Addis Ababa University

In partial fulfillment of the requirement for the Degree of Master of Science in Electrical Engineering (*Electrical Control Engineering*)

By

Dagmawi Demerwe

Advisor: Dr. Dereje Shiferaw

ADDIS ABABA, ETHIOPIA
DECEMBER 2016

Addis Ababa University
Addis Ababa Institute of Technology
School of Electrical and Computer Engineering

DESIGN AND SIMULATION OF A NEURO-FUZZY BASED TEMPERATURE CONTROLLER FOR NEONATAL INCUBATOR

By Dagmawi Demerwe

APPROVED BY BOARD OF EXAMINERS

Dean, School of Graduate Committee	Signature
Dr. Dereje Shiferaw Advisor	Signature
Mr. Mihreteab Negash Internal Examiner	Signature
Dr. Mengesha Mamo External Examiner	Signature

DECLARATION

I, the undersigned, declare that this thesis work, to the best of my knowledge and belief is my original work, has not been presented for a degree in this or any other universities and all sources of materials used for the thesis work have been fully acknowledged.

Dagmawi Demerwe ______________________
Name Signature

Place: Addis Ababa University, AAU
Addis Ababa Institute of Technology, AAiT
Addis Ababa
Ethiopia.

Submitted in: December, 2016.

This thesis has been submitted for examination with my approval as a university advisor.

Dr. Dereje Shiferaw ______________________
Name Signature

ACKNOWLEDGEMENT

First and foremost, I would like to thank my creator almighty GOD. This thesis would not have been done without His blessing. Secondly, expressing a sincere acknowledgment to my advisor, *Dr.Dereje Shiferaw*, for his guidance, support and encouragement. He has been an excellent advisor and mentor demonstrating high level of patience and continuous help. His deep knowledge to the subject matter contributed a lot in this paper. His guidance was undoubtedly great.

I would like to extend my sincere acknowledgment to Woldia University for supporting my graduate study with full scholarship. I also express my gratitude to AAiT, School of Electrical and Computer Engineering.

Last, but not least, I would like to thank, with all my heart, my wife, my family, my friends and my colleague control engineering students for their patience, encouragement and love.

TABLE OF CONTENTS

LIST OF FIGURES

LIST OF TABLES

LIST OF ABREVIATION

ANN...Artificial Neural Network

FLC...Fuzzy Logic Controller

ANFIS...Adaptive Neuro Fuzzy Inference System

CNS...Central Nervous System

LBW...Low Birth Weight

NICU...Neonatal Intensive Care Unit

PID..Proportional-Integal-Derivative

HVAC...Heating, Ventilation and Air Conditioning

FFNN...Feed-Forward Neural Network

RNN...Recurrent Neural Network

FIS...Fuzzy Inference System

GARIC.. Generalized Approximate Reasoning Based Intelligence Control

FALCON...Fuzzy Adaptive Learning Control Network

NEFCON...Neuronal Fuzzy Controller

FUN...Fuzzy Net

SONFIN..Sulf Constructing Neural Fuzzy Inference Network

FINEST...Fuzzy Inference and Neural Network in Fuzzy Inference Software

EFuNN..Evolving Fuzzy Neural Network

MF...Membership Function

BP..Back Propagation

SISO...Single Input-Single Output

LMS...Least Mean Square

XOR..Exclusive-or

LIST OF NOTATIONS

Qmet : Rate of metabolic heat production of the core.

Qsen : Rate of sensible heat energy due to breathing.

Qlat : Rate of latent heat energy due to breathing.

Qbc : Rate of convection heat transfer between core and skin via blood.

Qcd : Rate of conductive heat transfer between core and skin.

Qscv : Rate of convective heat transfer between skin and incubator air.

Qmc : Rate of conductive heat transfer between skin and mattress.

Qse : Rate of evaporative heat transfer between skin and incubator air.

Qsr : Rate of radiation heat transfer between skin and incubator wall.

Qacv : Rate of convective heat transfer between incubator air and incubator wall.

Qcvo : Rate of convective heat transfer between incubator walls and environment.

Qro : Rate of radiation heat transfer between incubator walls and environment.

Qmat : Rate of convective heat transfer between incubator air and mattress.

Qht : Rate of convective heat energy supplied to hood.

Qic : Rate of conductive heat transfer between mattress and incubator body.

Qheater : Heater rated power.

Sa : Surface area of the local body segment.

Mrst : Resting metabolic rate at thermo neutral zone.

mr_i : Percentage of the total heat production for each segment of the infant.

rr : Respiratory rate.

Tc : Core temperature.

Tex : Exhaled air temperature.

Ta : Air temperature/Inhaled air temperature.

Tw : Wall temperature.

Te : Ambient (room) temperature.

Tm : Mattress temperature.

Ts : Skin temperature.

Tha : Heated air temperature.

Tmx : Mixed air temperature.

$Twet$: Wetted air temperature.

Twa : Water air temperature inside humidification chamber.

Tal : Aluminum block temperature inside humidification chamber

$Tsply$: Supplied air temperature.

v_t : Tidal volume.

Wex : Humidity ratio of the exhaled air.

Wa : Humidity ratio of the inhaled air.

Cp_a : Specific heat of air.

Cp_c : Specific heat of the core.

Cp_s : Specific heat of the skin.

Cp_b : Specific heat of the blood.

Cp_w : Specific heat of the wall.

Cp_{O2} : Specific heat of oxygen.

Cp_{N2} : Specific heat of nitrogen.

Cp_m : Specific heat of mattress.

Cp_{wa}: Specific heat of water.

Cp_{al} : Specific heat of aluminum.

Cp_m : Specific heat of moist air.

Cp_s : Specific heat of vapor.

hfg : Latent heat of water at 35^0C.

hfg_1 : Latent heat of water at 50^0C.

IV : Inspired second volume.

Pt : Atmospheric pressure.

P_{H_2O} : Partial pressure of water-vapor at Ta and Tex.

$Psat$: Saturation pressure at Ta and Tex.

RH: Relative humidity inside incubator.

th_s : Skin thickness.

th_m : Mattress thickness.

th_w : Wall thickness.

ρ_s : Skin density.

ρ_c : Core density.

ρ_a : Air density.

ρ_{H2O} : Water density.

ρ_{bl} : Blood density.

ρ_w : Wall density.

ρ_{ha} : Heated air density.

ρ_{wet} : Wetted air density.

m_s : Mass of the skin.

m : Mass of the infant.

m_c : Mass of the core.

M_w : Mass of the wall.

M_a : Mass of the incubator air.

M_m : Mass of mattress.

M_{al} : Mass of the aluminum.

K_c : Thermal conductivity of the core.

K_{mat} : Thermal conductivity of the mattress.

K_a : Thermal conductivity of the air.

V_{cb} : Blood volume.

bf : Blood flow rate parameter.

Nu : Nusselt number.

Re : Reynolds number.

h_{scv} : Heat transfer coefficient for infant skin.

h_{acv} : Heat transfer coefficient for forced convection.

h_{wa} : Heat transfer coefficient for water.

h_{al1}: Heat transfer coefficient for the exposed parts of aluminum block.

h_{al2}: Heat transfer coefficient for the submerged parts of aluminum block.

V_a : Air velocity.

D_{sph} : Approximated infant diameter.

μ_a : Dynamic (absolute) viscosity of air.

v : Kinematic viscosity of the air.

GA : Gestational age.

age : Postnatal age.

σ : Stefan-Boltzmann constant.

ε_s : Radiant emissivity of the skin.

ε_w : Radiant emissivity of the wall.

A_{wi} : Surface area of the incubator walls.

A_w : Normal surface area of the incubator.

A_{net} : Area of the mattress not covered by the infant.

A_{mat} : Total area of the mattress.

A_r : Surface area of the neonate's local segment normal to the incubator walls.

A_s : Surface area of skin in contact with the mattress.

A_{cv} : Surface area of skin exposed to the air.

A_c : Incubator area based on the direction of the air flow.

A_{al1} : Total surface area of the exposed parts of the finned-aluminum block.

A_{al2} : Total surface area of the submerged parts of the finned-aluminum block.

p : Incubator perimeter based on the direction of the air flow.

W_{con} : Width of the water container.

L_{con} : Length of the water container.

N_f : Number of fins of the aluminum block.

th_f : Fin thickness.

l_f : Fin length.

w_l : Height of the fin above water surface.

w_{lw} : Height of the fin inside water.

W_g : Width of the gap between the fins of the aluminum block.

n_g : Number of the gaps between the fins of the aluminum block.

ABSTRACT

Premature infant's birth is a worldwide problem. Their organs are not mature enough to allow normal postnatal survival relative to normal babies, consequently they will became hypothermic, which leads them to death. Premature neonates survive in a very narrow core temperature range (36.5-37.5ºC) and suitable relative humidity. As a result, some parameters have to be monitored and their accuracy remains an important matter. Infant incubators are complex medical devices, which are often used immediately after delivery and for the coming few months of their life depending on the infant's health condition. They use the convection of warm and humidified air to control the temperature of the infant. They have two modes of operation, either the incubator's air temperature is sensed and used to control the heat flow or infant's skin temperature is sensed and used in the feedback control system. Infant's skin temperature control only often leads to large fluctuations in the incubator's air temperature, similarly incubator's air temperature control only also leads to infant's skin temperature fluctuations.

This thesis presents the application of adaptive neuro fuzzy inference controller for ATOM V-850 model infant incubator system, in order to control the incubator's air temperature and the infant's skin temperature simultaneously. The corresponding fuzzy logic controller is designed for the same system, in order to work with structured knowledge in the form of rules in the FIS. However, there exists no formal framework for the choice of various design parameters and optimization of these parameters generally is done by trial and error technique. The combination of artificial neural networks and fuzzy logic systems offers the possibility of solving tuning problems and design difficulties of fuzzy logic system.

The performance comparison between the proposed ANFIS controller and FLC is analyzed through various conditions using MATLAB/Simulink® software. Simulation results show that the performance of the proposed ANFIS Controller, in tracking the desired incubator's air temperature and desired infant's skin temperature, improved to 0.39% and 0.2% error from 16.6% and 1.47% error in the FLC respectively. Results also show that, the ANFIS model on the closed loop infant incubator system provides best control performance over a wide range of operating conditions relative to FLC.

Key Words: Neonatal incubator, Preterm infant, ANFIS controller, ANN, FLC, MATLAB/Simulink®

CHAPTER 1

INTRODUCTION

1.1 Background

Every year, about 1 million infants in the developing world die due to prematurity complications [1]. Premature infants are babies born before 38-42 weeks of gestation or birth weight below 1000grams [2] and their organs are not mature enough to allow normal postnatal survival. Newborn babies with growth problems usually have a net body area greater than normal babies from the same age, this in turn makes their heat loss greater than normal babies. Moreover, their net mass is less than the normal babies and makes them unable to keep their body temperature to the required level, consequently the infants are at risk of developing hypoxia, hyperthermia, hypothermia and many other associated adverse improper thermoregulation conditions, as shown in Figure 1.1. The temperature inside the mother's womb is 38^{o}C (100.4^{o}F). Leaving the warmth of the mother womb at birth, the wet new born finds itself in a much colder environment and immediately starts losing heat. In the first 10-20 minutes the new born who is not thermally protected may lose enough heat and which will results their body temperature fall by 2-4^{o}C (3.6-7.2^{o}F), even greater falls happen in the following hours if proper care is not given [3][4]. If heat loss is not prevented and is allowed to continue, the baby will develop hypothermia and is at increased risk of developing health problems and finally death will happen. Therefore With regards to sick babies they usually could not control their body temperature without an external aid and they need special care and attention.

Commonly there are two type of heating devices which are used to help neonates in order to maintain their body temperature. These medical devices are incubators and radiant warmers, which are often used immediately after delivery and the coming few months of their life depending on the infants health condition. Infant incubators use the convection of warm and humidified air to control temperature of the infant, while radiant warmers uses infrared radiation [5] and both of these devices having a feedback system. The radiant warmers uses only skin servo control, while the incubator has two modes: skin and air servo control. The existence of these devices, has considerably reduce the rate of infant's mortality and morbidity.

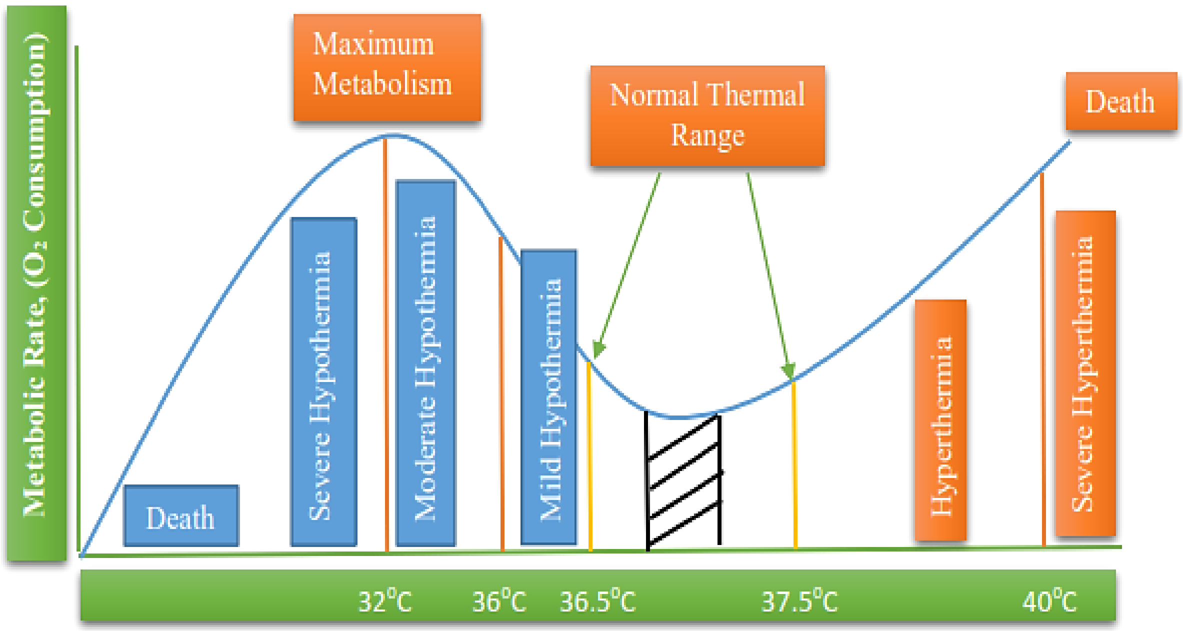

Figure 1.1: *Neutral thermal environment [18]*

1.2 Problem statement

Neonatal incubator is a very complex system including a number of subsystems with emphasized variables interdependency. It has the characteristics, multiple-input/multiple-output, nonlinearity, inaccessibility of some of the states for measurements and difficulties of establishing accurate mathematical model. Previous related research works investigated and analyzed the various physical dynamic processes of the neonatal incubators and they were carried out numerous numerical and experimental techniques. The major contribution of these research studies were the analysis of heat losses of the neonate, temperature distribution and control, air flow, humidity control and a better insight of the thermal interactions between the neonate and its surrounding environment, but due to the time-varying and non-linearity characteristics of the controlled parameters of the infant incubator systems together with thermal design complications of the system it is difficult to achieve an optimized performance of the system. Previous studies contributes their efforts to increase the performance and precise optimization of the controlled variables of the infant incubator system by developing an appropriate approximate mathematical models for the infant-incubator system and designing their own appropriate controller for infant-incubators, because as already discussed earlier premature neonates survive in a very narrow core temperature range (36.5-37.5°C) and suitable relative humidity depending up on individual infant's health status in a micro-environment. Different control system algorithms for neonatal incubator system have been studied and implemented so far, Some of them are simple on/off control, microcontroller based control, adaptive and predictive control, ANN based control and fuzzy logic based control. As a result, the optimization of the controlled parameters of the system and the precision of attaining the desired transient and steady state response characteristics of the system are critical scenarios and improvements are possible from time to time. Although the previous related research studies were successful and achieve their own objective, they have also their own limitations.In present day, many infant incubator systems having, incubator's air temperature control mode and infant's skin temperature control mode, which measures temperatures from the incubator's air surrounding and from the infant's skin layer, and used separately as a feedback for control action, but incubator's air temperature control only often leads to large fluctuations in the infant's skin temperature, similarly infant's skin temperature control only also leads to incubator's air temperature fluctuations [6][17].

Intelligent systems are an integration of biological structures with computing techniques. These systems are used to reach handling, robustness and low cost solutions with some degree of tolerance, imprecision, uncertainty and approximations. These characteristics make intelligent systems capable of solving problems which are not efficiently solved by conventional tools, classical control theory is based on the mathematical models that describe the physical dynamic system under consideration and this theories are not much more applicable to non-linear control systems [7].

Although fuzzy logic systems can encode expert knowledge directly using rules with linguistic labels, it usually takes a lot of time, in order to design and tune the membership functions which quantitatively define this linguistic labels. In opposite when we considering artificial neural networks the knowledge is automatically acquired by the back propagation algorithm but the analysis of the trained network is difficult to interpret or black box, it is impossible to extract structural knowledge from the trained neural network [33].

1.3 Objectives of the thesis

1.3.1 General objective

The main objective of this thesis is to design and simulate a neuro fuzzy based temperature controller for neonatal incubator.

1.3.2 Specific objectives

- Study the mathematical model of infant incubator systems in correspondence to the heat exchange mechanisms between the infants and the various components of the incubator.
- Model and develop the various compartments of the infant-incubator system and evaluate system performance using MATLAB/Simulink software.
- Collect training and checking data for the adaptive neuro fuzzy inference system based on the input/output parameters.
- Design, implement and simulate the ANFIS controller for the developed infant incubator system and analyze the performance of the closed loop system using MATLAB/Simulink software.
- Compare ANFIS control system with fuzzy logic control system, depending on their respective performance for selected conditions using MATLAB/Simulink software.

1.4 Significance of the thesis

In this thesis work we intend to show the hybridization of Fuzzy inference system together with artificial neural network methodology in controlling the skin temperature of the infant, which placed inside the incubator and the air temperature of the incubator simultaneously, in order to maintain normal thermal environment for the preterm infant. We believe that the enhancement on the performance of the Controller, will also improves the transient and steady state characteristics of the entire closed loop control system response, thereby showing that the controller will be able to reduce the effect of any disturbance on the temperature regulation of the system with more accurately and within a very short period of time.

In present time all medical institutions which were resides in our country import almost all medical equipment’s from other technologically developed countries. Neonatal incubator is one of the expensive medical equipment, which is import from the developed countries. In current condition the price of the infant incubators varies from $500 up to $9999 per pieces depending on the quality, functionality and efficiency of the infant incubator, which is very expensive to buy and import.

Recent technological research studies which were held in our country showed that microcontroller based neonatal incubator can be designed and developed in our country, which is a break through research work that motivates many researchers which are found in the same research study area for further research studies. We think that this thesis also contribute its effort in the advancement of an effective infant incubators control system.

1.5 Thesis layout

This thesis is organized in to six chapters including this chapter. Chapter 2 presents a review of the main theoretical backgrounds about premature infant physiology, neonatal incubator systems and summaries of the most important specialized research literatures on the modeling and control of infant incubator systems in the last couple of decades.

Chapter 3 focuses on the studies of fuzzy inference systems and artificial neural networks on the bases of their structural design and characteristics, finally we consider the various possible hybridization techniques of both systems in order to enhance the performance of the individual systems.

Chapter 4 presents the detail mathematical model of infant-incubator system and collecting the important data from the modelled system. Finally design of ANFIS and Fuzzy logic controller for the system on the bases of the collected data.

Chapter 5 focuses on the simulation results of both controllers on the control system and comparison between the performance of ANFIS controller and Fuzzy logic controller has been considered. Finally the results are discussed.

Chapter 6 present the conclusions from the work done in this thesis and indicates the direction for further future research works.

CHAPTER 2
LITERATURE SURVEY

In the previous Chapter we remarked that, the control of infant's body temperature in an infant incubator is not an easy task to carry out without solid background knowledge on the theme. Fortunately, this subject has attracted the attention of many researchers around the world in the last two decades. This chapter discusses the main theoretical backgrounds about premature infant physiology, neonatal incubator systems, summaries of the most important developments and accomplishments in the specialized research literatures on the modeling and control of infant incubator systems in the last couple of decades.

2.1 Premature infant physiology

Premature infants are babies born prior to the normal 36 or 37 weeks of gestation and their physiological systems are immature, consequently unable to regulate their body temperature and making the infant vulnerable to a number of health complications. Some of the common problems include jaundice caused by an immature liver, respiratory complications caused by fragile immature lungs, hypoglycemia, hypoxia, hypothermia and hyperthermia, which is finally death caused by an immature response of the nervous system to cold and over heat stress. The new born baby loses heat in four different ways as shown in the figure 2.1.

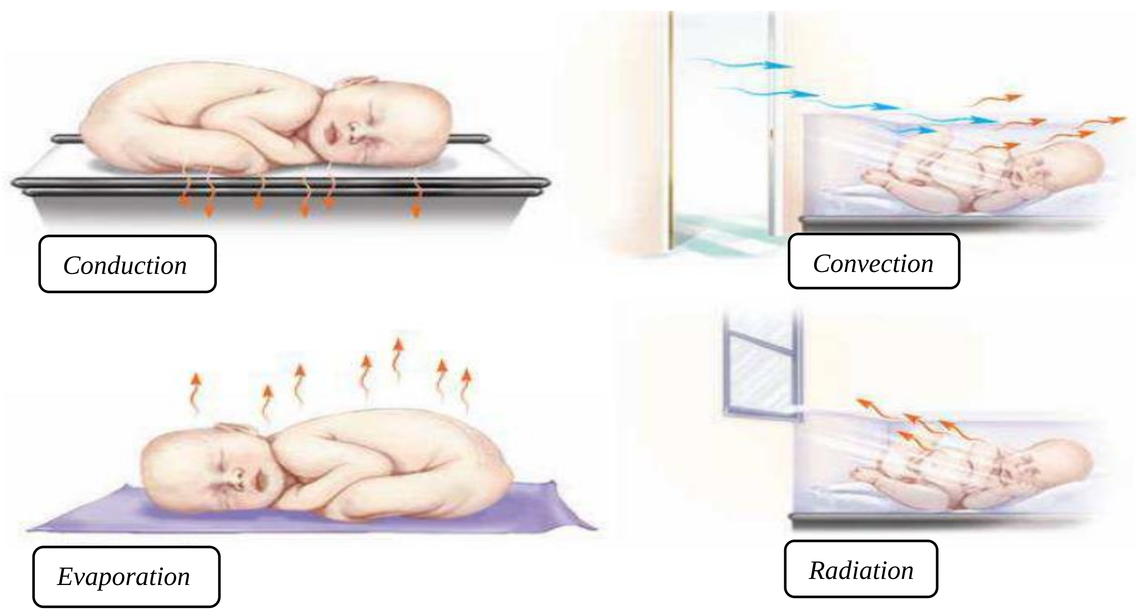

***Figure 2.1**: Ways of heat losses in new born infant [4]*

- ***Evaporation***: When amniotic fluid evaporates from the skin. Evaporative losses may be insensible (from skin and breathing) or sensible (sweating). Other factors that contribute to evaporative loss are the newborn's surface area, vapor pressure and air velocity. This is the greatest source of heat loss at birth.
- ***Conduction***: When the newborn is placed naked on a cooler surface, such as table, scale and cold bed. The transfer of heat between two solid objects that are touching, is influenced by the size of the surface area in contact and the temperature gradient between surfaces.
- ***Convection***: When the newborn is exposed to cool surrounding air or to a draft from open doors, windows and fans, the transfer of heat from the newborn to air or liquid is affected by the newborn's large surface area, air flow (drafts, ventilation systems) and temperature gradient.
- ***Radiation***: When the newborn is near cool objects, walls, tables and cabinets, without actually being in contact with them. The transfer of heat between solid surfaces that are not touching each other. Factors that affect heat change due to radiation are temperature gradient between the two surfaces, surface area of the solid surfaces and distance between solid surfaces. This is the greatest source of heat loss after birth.

Premature infants were lack of muscle mass, which allows adults to shiver and produce heat when necessary, they also have insufficient heat generating brown fat, which makes up about 5% of the body weight in preterm infants. This heat loss is enhanced by their large surface area to volume ratio (about four times the adult ratio). Furthermore, their immature skin allows for excessive water loss from the body causing a considerable evaporative heat loss and a potentially fatal imbalance of salts and acids in the infant's system. In evaporative heat loss moisture from the body diffuses across the epidermis (general outer layer of skin) after that it evaporates from the skin's surface, consequently cooling of the infant results. Premature infants have a thin immature stratum corneum or the rough outer layer of the epidermis which protects the skin from external disease causing agents. Evaporative heat losses make up a significant fraction of the total heat loss of a premature infant [8].

2.1.1 Hypothermia or Cold stress

Cold stress can be define based on the body temperature measurement of the preterm infant, if the body temperature measurement of the infant from the rectal area is below 36.5° C (97.6° F), then the infant is more likely hypothermic . The normal responses to cold stress for the adult are not adequately effective for the neonate. Full term neonates have a very limited ability to shiver to produce heat but preterm infants having nothing. In addition preterm neonates have unstable vasomotor responses to change in environment, therefore they cannot have vasoconstriction adequately to slow down heat losses and preterm infants have limited stores of brown fat, as a result inadequate production of heat metabolically.

While in the adults, control of body temperature is achieved by a complex system via negative feed-back, basically they creates a balance between heat production, heat gain and heat loss. The key of this system is a central controller located in the hypothalamus and limbic system which is based on information from central and peripheral thermo receptors (multiple-input) and controls the action of the so-called effectors: thermogenesis, the vasomotor system, sweat secretion and thermoregulatory behavior through the efficient nervous system. Body temperature therefore is the result of the combined action of the detectors, control system and the effectors. In new-born infants, especially preterm infant's, immaturity of the thermoregulatory system makes the infant more vulnerable to changes of environmental temperature. In the infant model the physiology of the response to cold stress is related to the oxidation of brown fat or brown adipose tissue. In full term newborn infants, non-shivering thermogenesis (oxidation of brown adipose tissue) is the major route of a rapid increase of heat production in response to cold surrounding air. Figure 2.2 represents the metabolic response to cold stress [9].

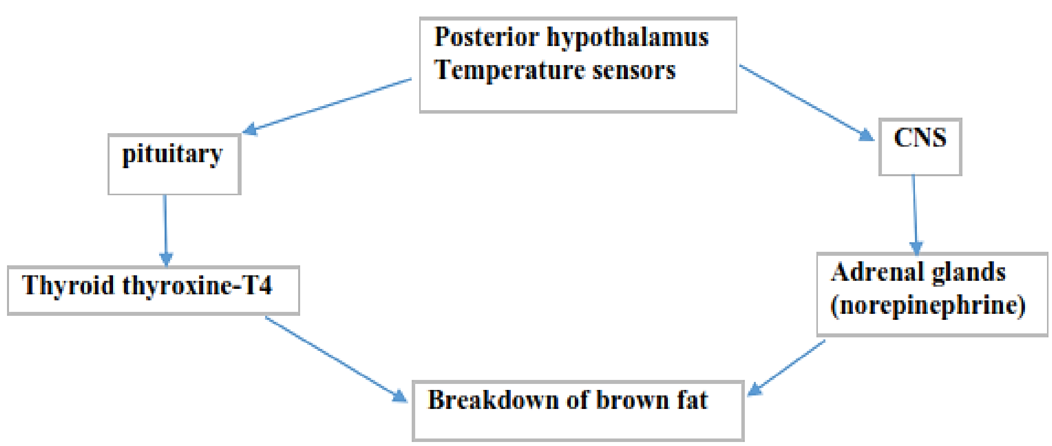

***Figure 2.2**: Metabolic response to cold stress [9]*

The consequences of cold stress can be quite severe. As the body temperature decreases the baby becomes less active, lethargic, hypotonic, sucks poorly, their cry becomes weaker, respiration becomes shallow and slow, the heart-beat decreases, sclerama hardening of skin develops mainly on the back and the limbs and the face may also become bright red. As the condition progresses it causes profound changes in body metabolism, resulting in impaired cardiac function, hemorrhage (especially pulmonary), jaundice and finally death [9].

2.1.2 Hyperthermia or Over heat stress

Hyperthermia can be defined as, the preterm infant's health problem due to which, the body temperature measurement of an infant become above 37.0°C (98.6°F). The determination of an external source of heat gain versus an actual febrile state can be made by observing the infant state of peripheral vasoconstriction, which is demonstrated by a higher rectal temperature versus a distal temperature of the foot. In the presence of overheating, the opposite would occur [9]. Hyperthermia shouldn't be confused with fever, which is a raised body temperature in response to infection with microorganisms or other sources of inflammation. However, it is important to distinguish between fever and hyperthermia by measuring the body temperature or by clinical signs. When the newborn has a raised temperature it is important to consider both causes. Infection should always be suspected first unless there are very obvious external reasons for the baby becoming overheated [9].Hyperthermia can cause increased metabolic demands for the neonate. The neonate may have increased oxygen requirements, apnea, dehydration, metabolic acidosis and in worse case scenarios heat stroke, brain damage, shock and finally death [9].

2.2 Thermal protection in new born

Thermal protection of the new born requires a series of measurements taken at birth and in the first days of life to ensure that the newborn does not become either too cold or overheated, in order to maintains a normal body temperature of 36.5-37.5°C (97.7-99.5°F). Since the consequences of an environment that is too cold or too warm are dangerous for the infant, it is important to know that, what is the optimal thermal conditions i.e. the most suitable thermal environment for the new born baby. This is the range of thermal conditions under which a new born baby can maintain normal body temperature. The range is narrow especially in low birth weight or sick babies. Basically the smaller and more premature the new born is the less it tolerates cold and heat. Thus there is no a single environmental temperature that is optimal for all infant sizes, gestational ages and various conditions of new born babies, The appropriate thermal condition for a healthy infant may be too cold for a preterm infant or the appropriate thermal condition for the preterm may be too hot for the healthy infant. The newborn preterm infant cannot regulate its body temperature as well as an adult. The smaller the new born, the greater the risk, but thermal stability improves gradually as the baby increases in weight. The basic principles are the same whether the baby is born at home or in health institution. Heat loss increases with air movement and the infant is in risk of getting cold even at a room temperature of 30°C (86°F) even if there is a draught. Most cooling of the new born occurs during the first minutes after birth. However, if heat loss is prevented the new born will stay warm and will have a much better chance of remaining healthy. In trying to keep babies warm, it is important to make sure they do not become overheated. The mechanisms described above may be acting in reverse way and cause hyperthermia. Although it is less common, it is dangerous as hypothermia [3][4].

2.2.1 Prevention and management of hypothermia

If newborn infants found to be hypothermic, they must be rewarmed as soon as possible. The temperature of the room where the rewarming takes place should be at least 25°C (77°F). Cold clothes should be removed and replaced with pre-warmed clothes and cap. The newborn should be quickly rewarmed, if a warming device is used its temperature should be checked frequently during the rewarming process. It is very important to continue feeding the baby to provide calories and fluid. Breast-feeding should resume as soon as possible, if the infant is too weak to breast feed, then breast milk can be given by nasogastric tube, spoon or cup. It is important to be aware that hypothermia can be a sign of infection, every hypothermic newborn should therefore be assessed for infection. In hospitals a diagnosis of hypothermia is confirmed by measuring the actual body temperature with a low-reading thermometer. The method used for rewarming depends on the severity of the hypothermia and the availability of medical staff and equipment. In cases of mild hypothermia (body temperature 36.0-36.4°C/96.8-97.5°F) the baby can be rewarmed by skin-to-skin contact in a warm room (at least 25°C/77°F). In cases of moderate hypothermia (body temperature 32-35.9°C/89.6-96.6°F) the clothed infant must be rewarmed:

- Under a radiant heater.
- In an incubator at 35-36°C (95-96.8°F).
- Using a heated water-filled mattress.

- In a warm room: the temperature of the room should be 32-34°C/89.6-93.2°F(more if the baby is small or sick).
- In a warm cot: if it is heated with a hot water bottle, these should be removed before the baby is put in to the cot.
- If nothing is available and the baby is clinically stable, skin-to-skin contact with the mother can be used in a warm room (at least 25°C/77°F).

The rewarming process should be continued until the baby's temperature reaches the normal range. The temperature should be checked every hour, and the temperature of the device being used or the room adjusted accordingly. The baby should continue to be fed. In cases of severe hypothermia (body temperature below 32°C/89.6°F) studies suggest that fast rewarming over a few hours is preferable than slow rewarming over several days [9]. Rapid rewarming can be achieved by using a thermostatically controlled heated mattress set at 37-38°C (98.6-100.4°F) or an air-heated incubator with the air temperature set at 35-36°C (95-96.8°F). Feeding should continue in order to provide calories and fluid and prevent the drop in the blood glucose level which is a common problem in hypothermic infants. Once the baby's temperature reaches 34°C (93.2°F) the rewarming process should be slowed down to avoid overheating. The temperature of the incubator and the baby's body temperature should be checked every hour [9].

2.2.2 Prevention and management of hyperthermia

If newborns found to be hyperthermic they should be moved away from the source of heat and undressed partially or fully if necessary. If the baby is in an incubator, the air temperature should be lowered. It is important that the infant should be breast-fed more frequently in order to replace fluids in their body. Every hyperthermic baby should be examined for infection. When hyperthermia is severe i.e. body temperature above 40°C (104°F°) the baby should be taken a bath and the water should be warm. If it is possible to measure the water temperature it should be about 2°C (3.6°F) lower than the baby's body temperature but using cooler or cold water is dangerous because it may not achieve the desired effect and the baby may be very quickly become hypothermic.

2.3 Measurement of infant body temperature

Obtaining infant body's temperature is the only reliable method available to evaluate thermal stability of the infant. Accepted normal body temperature ranges for the neonate are dependent upon the infant's body location from which the body temperature is measured.

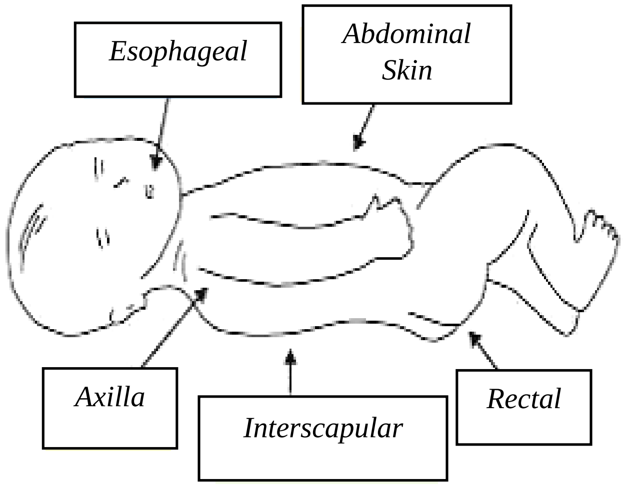

Figure 2.3: *Temperature measurement location [9]*

Rectal temperature

Traditionally the rectum area has been used as a measurement of the core temperature of the infant. However taking a rectal temperature is an invasive procedure and the measurement is not always reliable. The rectal temperature depends on the depth to which the probe is inserted, as shown in figure 2.4.

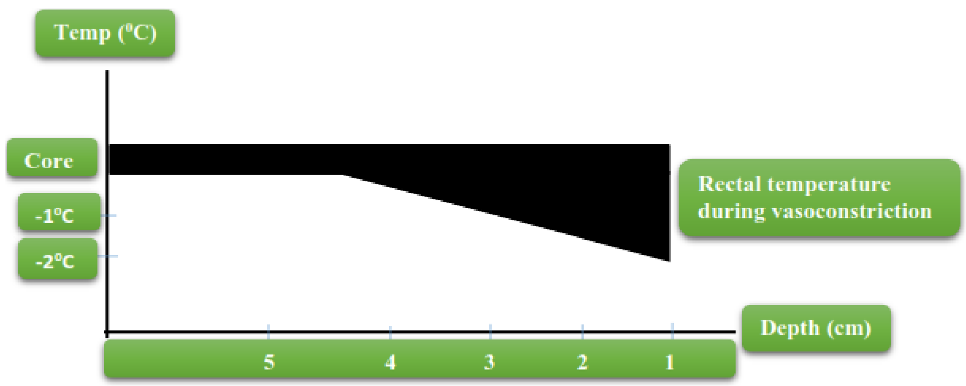

Figure 2.4*: Rectal temperature [9]*

From the practical point of view it is impossible to keep a rectal probe in the same position for any length of time, consequently this is not a suitable site for continuous temperature monitoring of the infant.

Axilla and abdominal skin temperatures

The Axilla and the abdomen (over the area of the liver) areas are alternative sites commonly used to represent central core temperature. In the newborn babies, these sites do not appear to react to lower temperatures with vasoconstriction. This means that, although the temperature measurements in the axilla or on the abdomen are slightly lower than the true central temperature, they will change in the same way as the central temperature. Monitoring the trends in the axilla or abdominal skin measurements will therefore give information on the way the central temperature is changing. The axilla is a perfect site for a probe, as it is not easily affected by changes in environmental temperature.

Interscapular temperature

If the baby is lying on a non-conducting mattress, the skin adjacent to the mattress will be unable to lose heat and will therefore warm up to the temperature of the body's core temperature. This is called the Zero heat flux temperature. When the infant is lying on its back on a non-conducting mattress, then the temperature can be measured by a probe placed in the interscapular region, it is important to use small and flat probes that will not cause pressure damage to the baby's skin.

Esophageal temperature

Esophageal temperature, with the probe positioned close to the heart of a baby is possibly the closest we can get to a true core temperature. This probe gives a measurement of the temperature of the blood in the great vessels. This is however an invasive procedure and there are currently no probes that can be used for long periods of time in the newborn baby. Zero heat flux temperature has been shown to be closely correlated with esophageal temperature.

2.3.1 Measurement devices

Temperature measurement is a commonly used assessment tool, used when caring for preterm infants. There are many different types of measurement devices, which are appearing frequently and are being utilized in neonatal units. These devices include mercury in glass, digital, electronic, chemical and infrared thermometers. Although the introduction of the digital thermometer has helped pave the way for a more rapid response axillary measurement in the neonate, but the most common is a thermistor probe attached to skin over upper abdomen in order to measure the skin temperature. Many new measurement devices are being compared with other better known or more commonly used devices to ascertain their accuracy, reliability and speed of the device.

2.4 Devices for thermal protection in NICU

LBW infants or sick newborns are at greater risk of developing hypothermia or hyperthermia. To keep low birth weight or sick newborn babies warm, the same principles apply like those of other newborns but these babies require extra warmth over a longer period of time. Moreover the baby's temperature and the temperature inside the device should be monitored frequently. No heating device can function efficiently in a cold room because heat loss by radiation to the cold environment may exceed heat generated by the device. All equipment should be used in room temperatures of at least 25°C (77°F).

The strategy used to keep the baby's temperature will depend on baby's weight, gestational age and health conditions, which can be taken care using medical devices such as:

- Radiant Warmers
- Infant Incubators

For LBW babies, who are stable, kangaroo-mother care is the most effective way of keeping babies warm without any cost, easy and applicable at home. Regular breast feedings and skin-to-skin contact are encouraged for all LBW babies who are prone for hypothermia [9].

2.4.1 Radiant warmer

This is an open bed system and the heating source is suspended from above, as shown in the figure 2.5. It allows immediate contact with the infant and provides skin servo controlled heating through radiation. For those infant lying in open bed, there is a large amount of humidity loss and the infant is more prone to infection. In addition the infant has a large amount of heat loss through convection and evaporation.

***Figure 2.5**: Radiant warmer*

2.4.2 Infant incubator

Due to the limitations of radiant warmers, eventually infants have to be transferred to incubators [10]. The infant incubator is considered as an air conditioned room with special specification which we can control it with respect to the health condition of the infant in the incubator, Incubators are designed to provide an optimal environment for newborn babies with growth problems or with illness problems. The incubator is an isolated environment with no dust, bacteria and has the ability to control temperature, relative humidity and oxygen concentration to remain them in acceptable levels such as (36.5°C-37.5°C) for temperature,(40%-90%) for relative humidity and (25%-60%) for oxygen concentration [6][11].

Thermo regulation inside the incubator depends on many factors. These factors may depend on infant related parameters or incubator related parameters [13]. Infant related parameters, include variables such as size, maturity level, gestational age, metabolic factor, maturity of skin and body development etc. Smaller size infants need different thermal care when compared to full term infants. The incubator related parameters include incubator size, geometry, thickness of walls, materials of the incubator, mattress, incubator heating type and control mechanisms. One of the most important of these entire incubator related parameters is the temperature control mechanism [14]. In addition, for various postnatal ages and birth weights there are also various operative neutral thermal environment [15][16].

Infant incubators are used mainly to keep a baby's core temperature stable at 37 degrees Celsius. The internal core temperature of the human body needs to be kept at a constant temperature of 37 degrees Celsius because, if the temperature goes too high or too low, then the organs can be damaged and death will happen . Premature infants have undeveloped nervous systems and also lack the energy to regulate their own temperature. We can only provide, for small babies a small amount of food for growing. We want them to use all of their energy for growth rather than wasting it on keeping their body temperature, so usually we use the incubator to help them growing faster.

2.4.2.1 Background of infant incubators

Stories differ regarding to the invention of the infant incubator, it seems that the Imperial Foundling Hospital in Moscow had been using a double-walled warming tank invented by Carl Credé 1874, while the first published account of a similar open double- walled tank came in 1857 from French pediatrician Denucé. This device is called a warmwännen consisted of a large metal tub into which was set a smaller metal tub. They were welded at the top edges, with an opening near the top to pour in warm water and a faucet near the bottom to drain it. By filling the space between the tubs with warm water, an infant placed in the inner tub could be kept warm.

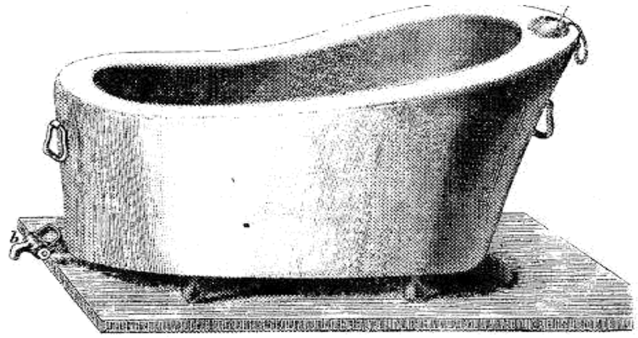

Figure 2.6*: Warmwännen [9]*

In 1883 Pierre-Victor-Adolph Auvard published another incubator, which was developed by Etienne Stéphane Tarnier for the use of the enormous Paris Maternité. Tarnier was visiting a poultry exhibit at the Paris zoo, when struck with the idea to have a poultry incubator built with the purpose of warming premature infants. In Tarnier device, the couveuse consisted of a double-walled wooden box, the space between the walls filled with sawdust for insulation to prevent fumes from a gas or alcohol heater reaching the infant, Tarnier used a thermosiphon with a gas burner to heat a reservoir of water in the lower compartment of the box. The infant was placed in the upper compartment and air would enter the box at the bottom which is warmed by the reservoir then pass upwards through vents to reach the baby at the above compartment. It would then pass out through the top of the incubator vents in the double thick glass lid. A thermometer placed next to the baby allowed the caretakers to monitor the incubator temperature without opening the box.

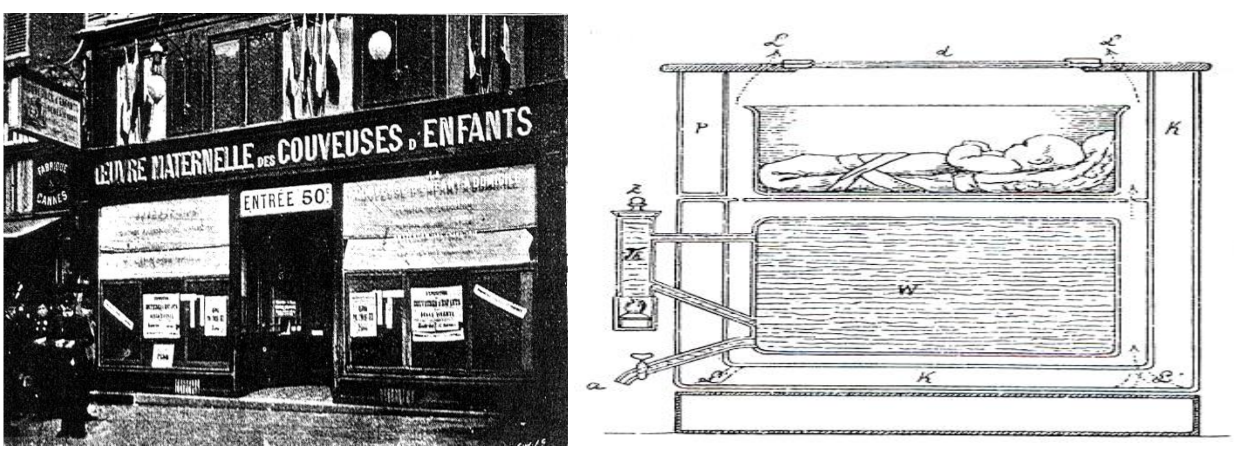

Figure 2.7*: The couveuse [9]*

However this device was large, expensive and conducting heat excessively, so that it may risking infants to cold stress. Two solutions were proposed to solve these problems. The first One designed by Tarnier student Budin, incorporated a mercury thermostat and a battery operated alarm to alert caretakers, if the temperature raise too high or dropped too low and the second one is more popular design which was nurses began periodically filling the reservoir with hot water two or three times daily. Tarnier and his intern Auvard developed a low-tech version of the incubator, a two-tiered sawdust-insulated box heated by removable clay hot water bottles. It was the device that produced on a large scale and it was the most popular model until the late 1890s.

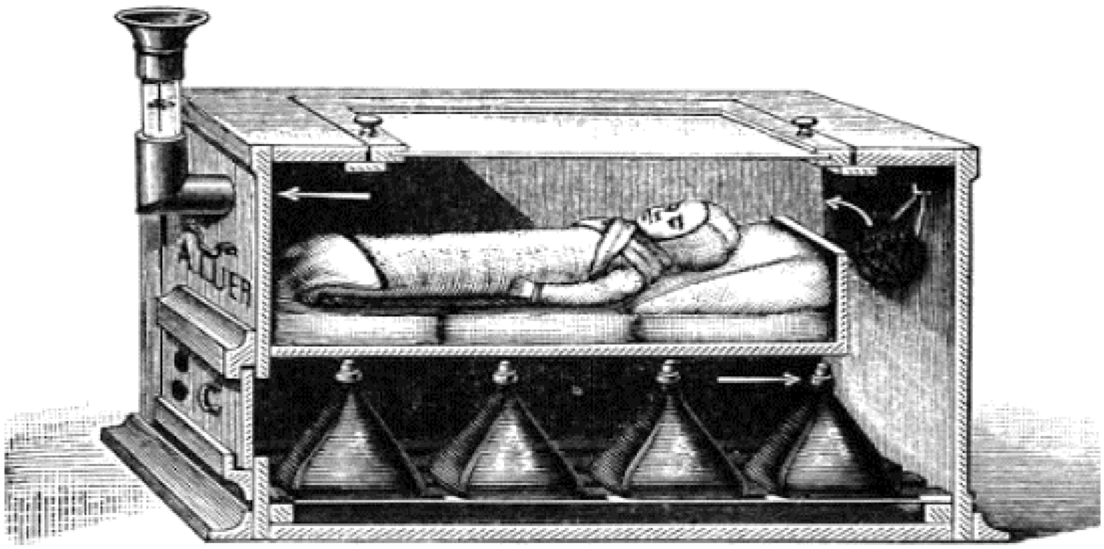

Figure 2.8*: Two-tiered sawdust-insulated box [9]*

The first report on the use of an incubator presented by the American journal in 1887 and it was reported to the Chicago Medical Society, John Bartlett a Professor and physician of diseases related to Women and Children at the Chicago Policlinic developed incubator which were made of inset metal tubs like the warmwännen and it is also used a boiler attached to the sides like Tarnier original couveuse plan with a complicated thermosiphon arrangement intended to keep the water at a regular temperature throughout the process. The incubator had no provisions for ventilation but it does not have no solid top, Bartlett recommended that a blanket big enough to cover the device and draped over the top of the incubator except around the face of the infant. In 1891 reports reviles that a new incubator design developed in France which is designed by Alexander Lion of Nice. The Lion incubator were made of iron with glass doors in the front and hot water circulating through a spiral pipe in the bottom, warming the air with in the incubator, which were ventilated by pipes which drew air from the outside environment and filtering the air before delivering it to the base of the incubator and the fan at the top of the incubator determines the rate of air circulation. The infant was placed on a mattress in a basket which was suspended from the sides of the apparatus by springs. The boiler which is placed to the side of the device could be heated with gas, oil, electricity, methylated spirits or any other fuel and temperature was automatically regulated via a thermostat. The device were large, expensive, complex and requires installation in to the insides of the building in order to use [9].

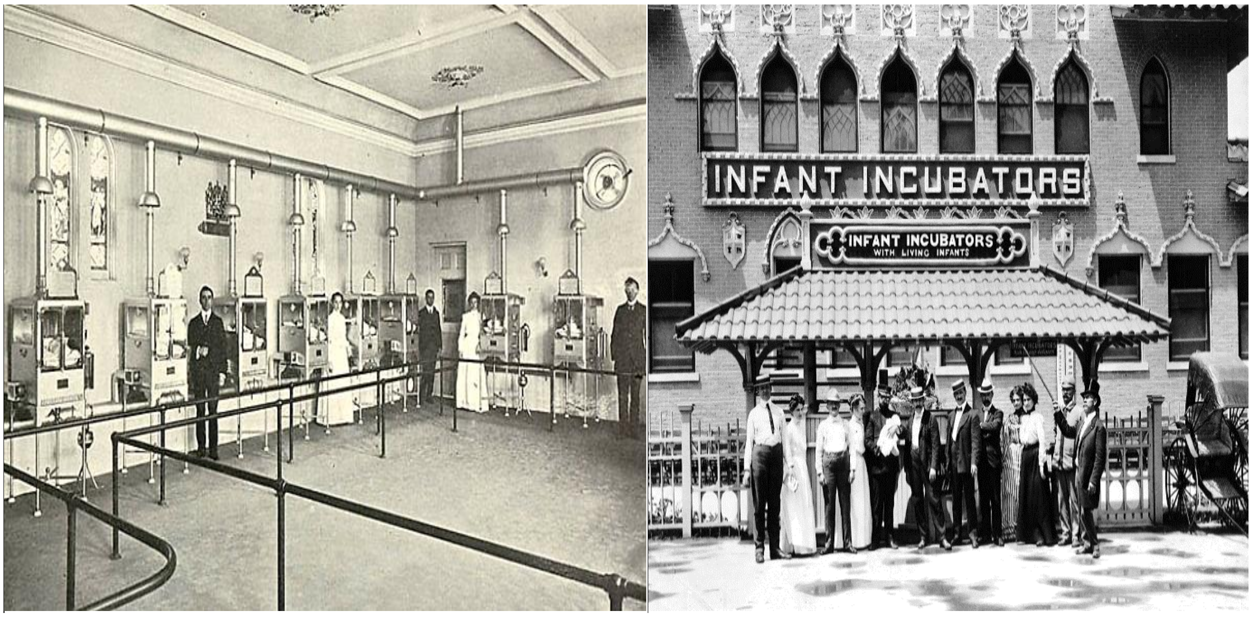

Figure 2.9*: Lion incubator [9]*

Hess's model were a double-jacket warming tub, after Credé's model was introduced with little enthusiasm in the year 1915. Julius Hess's pioneering oxygen therapy incubators were introduced in the year 1934. Since then technologically incubators has been frequently updated but the parameters being controlled were the same such as temperature, humidity and oxygen in the neonatal incubator.

2.4.2.2 Principles of operation

The premature neonate lies on a mattress inside the incubator compartment, which is enclosed by a clear transparent plastic hood. Most incubators have hand access ports with doors that permit the infant to be handled while limiting the introduction of the cold room air. The clinician can raise or remove the plastic hood in order to gain greater access to the infant. Most incubators warm the infant by a forced or natural flow of heated air in to the incubator compartment. Heating and humidification systems are located beneath the incubator compartment, which is shown in Figure 2.10-(a) and (b).

Most incubators are equipped with proportional heating controls that provide electrical power to the heating coil in response to the difference between the actual temperature and the desired temperature. Modern incubators are fitted with various sensors for measuring the actual values of the controlled parameters, controlling/monitoring screens, safety standards, voice and light alarm indictors in case of emergency.

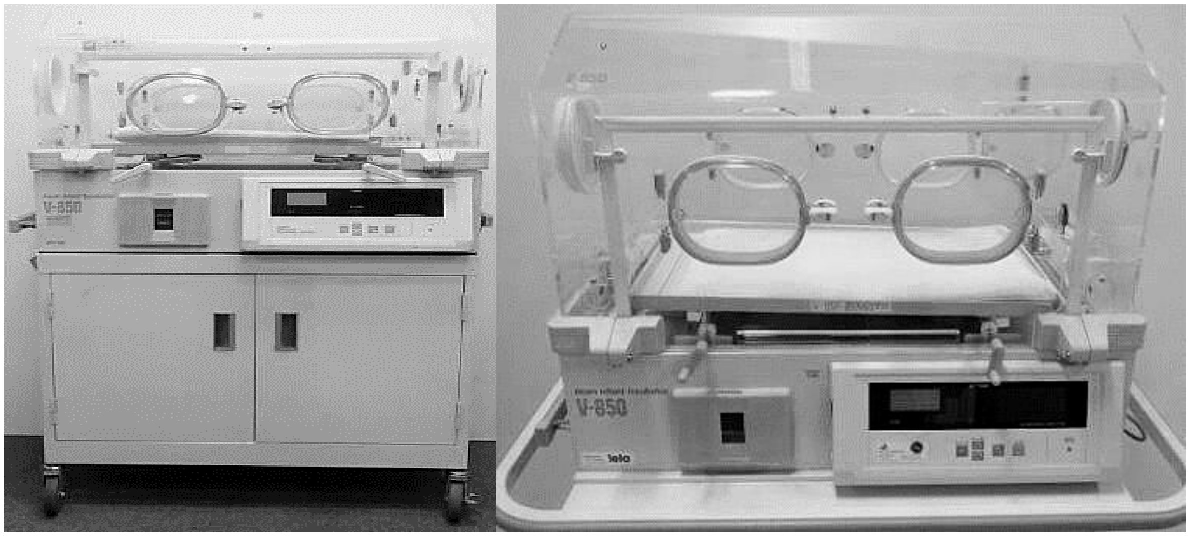

***Figure 2.10**: (a) ATOM V-850 neonatal incubator [18]*

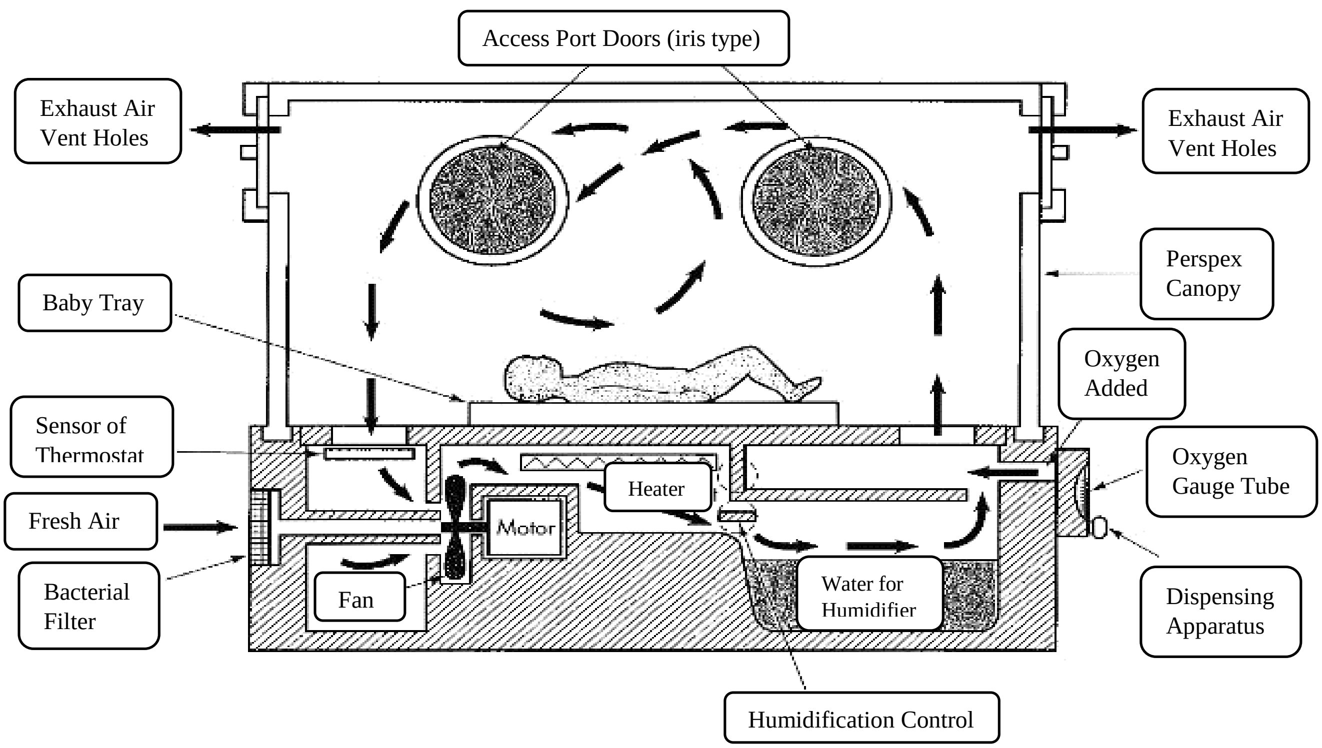

***Figure 2.10**: (b) Detail structure of neonatal incubator [5]*

- **Fan**: The fan takes the filtered room air and blows it over or through the heating element and the humidifier. Without the fan the heat cannot be conducted away from the heating element.

- **Filter**: Simple incubators are equipped with washable foam filters, after washing and drying they can be reused. Modern incubators however usually have disposable bacterial filters, they cannot be cleaned and renewed.
- **Heater**: A heating element made from coiled resistance wire as known from hair dryers or the tube type as seen in autoclaves are used to heat up the air. But unlike in autoclaves, the heater has much less power and thus does not get so hot. The power rating is between 100W up to 900W.
- **Temperature control**: Simple incubators are controlled by a thermostat which consists of a sensor and pressure can. The sensor is a thin capillary tube which leads into the pressure can (expansion chamber), this chamber has a movable metal lid or diaphragm. This closed system consists a liquid or gas which expands when getting warmer, then the lid moves and activates a connected electrical switch.

  Generally most of neonatal intensive care units have two modes of temperature controlling mechanism:

  I. ***Air temperature control***: In air-temperature (manual) control mode, the operator sets the temperature of the air in the incubator; changes in infant body temperature are usually measured periodically with a thermometer and adjustments in air temperature are made accordingly.

  II. ***Skin temperature control***: In skin temperature (automatic or servo) control mode, a sensor is taped to the infant’s skin and the heater responds to changes in the sensor to keep the skin temperature at the pre-set level.

- **Humidity control**: The heated air flows over the water in the water reservoir used to humidify the air (if desired) into the incubator compartment. The humidity can be regulated by closing and opening a deflector plate over the container, some other incubators have a water heater which creates more humidity. The humidity should be adjustable between 40% - 90% and the humidity measured by a hygrometer, which is either a digital or a traditional dial instrument. The humidifier should be filled up only with distilled water in order to avoid corrosive damage to the incubator and most NICU allow the user to vary relative humidity from either a built-in reservoir or an outside source (a humidifier that attaches to one of the inlet ports). Although increasing the relative humidity in an incubator can reduce evaporative heat loss, many clinicians avoid supplemental humidification because of concern that infectious organisms may proliferate in the water reservoir.

- **Oxygen control**: Most incubators have one or two oxygen inlet ports and can be equipped with optional oxygen controllers. These incubators can also provide support and protection for oxygen cylinders when oxygen must be delivered to the infant in the incubator, consequently the warmed and moistened air gets also enriched with the oxygen. Alternatively the baby can get the additional oxygen directly via a nasal cannula.

Based on their functionality, from the various compartmental components of the infant incubator system, the most vital and crucial component of the infant incubator is the control unit which controls the controlled parameters (temperature, relative humidity and oxygen concentration) of the infant incubator environment, in order to provide a sustainable congenial environment for the premature neonate depending on the conditions of the premature infant.

As mentioned in the previous section infant incubators having a rich background, which lids to advance developments in this technological sector. Neonatal incubators categorized into three categories, these are manually controlled incubators, servo controlled incubators and transport incubators [9].

2.5 Related research studies

Research studies which were done regarding on the modeling and control system design strategies for neonatal incubators have been published by different scholars.

1. **Barry N. Simon Jr., Narender P. Reddy and Anand Kantak**, [17] A spatially lumped mathematical model were proposed and designed for a computer simulation of infant incubator system for parametric analysis of the factors that influence neonatal thermo-regulation. The simulation examined the effects of the following parameters; (1) Size of the infant, (2) Respiratory rate, (3) Metabolic rate, (4) Heart rate, (5) Thermal properties of the mattress, (6) Specific heat capacity of the incubator wall, (7) Air flow rate and (8) Heater controlling mechanisms. Heat loss in newborns occurs by conduction, radiation, convection and evaporation. The model utilized a single wall rectangular incubator with forced convection heating and three control mechanisms; infant skin, incubator air and infant core temperature. For the purpose of the spatially lumped modeling, the infant-incubator system was partitioned into five distinct homogeneous compartments: The

infant core, the infant skin, incubator air space, incubator wall and mattress as shown in figure 2.11.

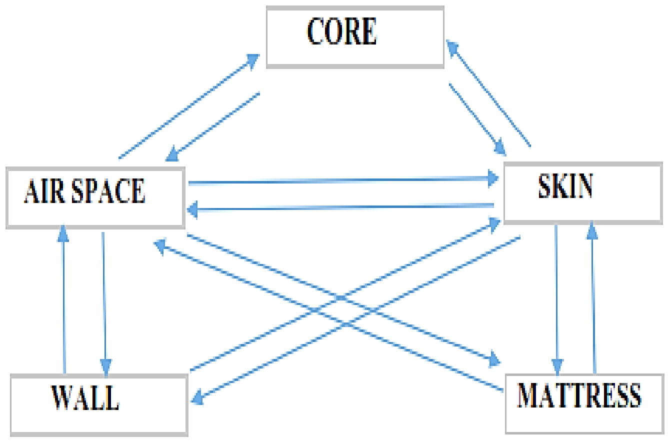

Figure 2.11*: The five distinct homogeneous compartments of an infant-incubator system [17]*

Several assumptions were made in the development of the model. Each compartment was assumed to be homogeneous in all properties throughout its substance, all airflow fields in the incubator were assumed to be uniform, the baseline metabolic rate for each size infant was assumed to be that which enabled the infant to maintain his own body temperature while in a nonfunctional incubator and the conduction of heat from the mattress to the incubator '*Qmat*' was assumed to be negligible. Model equations were developed to describe the rate of change of temperature over time in each of these compartments. The model equations based upon the law of conservation of energy, were:

$dTc/dt= (Qm - Qc- Qbl- Qbs- Qbe)/(Cpc* m_a)$

$dTs/dt= (Qc+Qbl-Qcd-Qr-Qcv-Qe)/(CPs*m_s)$

$dTa/dt= (Qcv+ Qbs+ Qbe+ Qh- Qci- Qmat)/(CPa * m_a)$

$dTw/dt= (Qci+Qr-Qri-Qcvi)/(Cpw*m_{wi})$

$dTm/dt= (Qmat+ Qcd- Qmc)/(Cp* m_m)$

The initial conditions were chosen to simulate the typical conditions existing for an infant after delivery and the standard examination that follows. T_c is assumed to be 34°C and still falling from an intrauterine temperature of 38°C up to 39°C. T_s is assumed to be 36°C and it is still falling from 38°C. The incubator has been cleaned and moved into the neonatal intensive care unit which is slightly warmer than storage area but the incubator has not been started prior to placing the baby inside the incubator.

T_e the room temperature in the neonatal intensive care unit, is assumed to be 23°C. T_a is assumed to be 25°C as that of T_m due to cleaning and preparation by the medical staff. T_w is assumed to be 20°C, the temperature in the storage room. The values for the parameters, which were obtained from several sources and the set of equations developed to describe the infant-incubator system was simulated on a digital computer. An explicit trapezoidal predictor-corrector method was used to integrate the set of differential equations. The computer simulation of the infant incubator system provided the plot of the five compartment temperatures versus time. The simulation of the dynamic behavior of the infant-incubator system almost always reached a steady-state condition with in a one hour of simulation time.

2. **Yasser Amer Al-Taweel and Ahmed Al-jumaily**, [18] proposed a comprehensive simulation model for the infant-incubator system in order to investigate all heat exchange relationships, variables and factors that have an influence on the overall thermo-neutrality of the environment. The infant was modelled as one lump with two layers: the core layer and skin layer. The infant shape was approximated to a cylinder. The model incorporated all compartments of the infant-incubator system including: The infant core, the infant skin, incubator air space, mattress, incubator wall, air circulating fan, heating element, added oxygen (for resuscitation purpose) and humidification chamber, which was not previously considered. The result of the simulation were in terms of the temperature variation over time for the various compartments of the system. The simulation model is a closed loop system with a PID controller for each mode; air servo controlled and skin servo controlled. The controller parameters were virtually estimated by Zeigler-Nichols methods and the overall stability of the whole system had been achieved by applying a step input, which was verified by root locus method. The result with added relative humidity showed that the body temperature of a 900gm infant with an initial body temperature of 35.5^{0}C did not reach the thermo-neutral range 36.5^{0}C - 37.5 ^{0}C in two hours on air mode whereas on skin mode both the core and skin temperature reached to 36.87^{0}C and 36.5^{0}C respectively in two hours, thus a thermo-neutral environment was reached.

   While PID controllers are applicable to many control problems and often perform satisfactorily without any improvements or only coarse tuning, they can perform poorly in some applications and do not in general provide optimal control. The fundamental difficulty with PID control is that, when there no direct knowledge of the process and the other problem faced with PID controllers is that they are linear and in particular symmetric, thus the performance of PID controllers in non-linear systems (such as HVAC systems) is variable. For example, in temperature control, a common use case is active heating (via heating element) and passive cooling. The overshoot can only be corrected slowly, in this case the PID should be tuned to be overdamped, in order to prevent overshoot, though this reduces the performance (it increases settling time).

This thesis paper based on Yasser Amer Al-Taweel's simulation model for the infant-incubator system, regarding to the discussed advantages of the system model in order to implement the proposed controller for the infant-incubator system. We will discuss this model of the infant incubator system, in detail on the coming chapters.

3. **Garima Mathur and Narender P. Reddy**, [7] Proposed a fuzzy logic control which incorporate both incubator air temperature and infants skin temperature in the control action in order to address the case, skin temperature control only often leads to large fluctuations in the incubator air temperature and similarly incubator air temperature control only, also leads to skin temperature fluctuation. The temperature space was divided in to a number of sub-domains, the crisp values of skin and air temperature were first fuzzified to obtain membership values which were input to the rule-base in order to obtain the output and then the output was defuzzified in order to obtain a crisp value for the heat flow parameter. The fuzzy logic control system was evaluated using a mathematical model of the infant incubator system (Simon, Reddy and Kantak – 1994), simulation results revealed that fuzzy logic system incorporate both skin and air temperatures provides a better and smooth control when compared to on-off air servo control, on-off skin servo control and proportional control for different selected conditions but system tuning was done according to the set values of skin temperature and incubator air temperature, then the corresponding fuzzy rule gives the required amount of flow of hot air in order to maintain the core temperature in the desired range 36.5-37.5^{0}C. So that look up table was changed several times in order to get the desired combination of rules and different membership functions were investigated in order to get the desired shape and range because fuzzy logic controls are incapable of generality .

This trial and error tuning mechanism of the fuzzy rules and membership functions will be time consuming and inhibit the performance of the process. The design and development of a systematic tuning mechanism for the fuzzy rules and membership functions is the main concern of this thesis paper.

4. **Ghada M. Amer and Kasim M. Al-Aubidy,** [19] In this paper a novel technique by using artificial neural network is used in order to simulate the premature infant incubator control system by implementing the back propagation method. Sensors are used to indicate temperature, humidity and oxygen concentration of the incubator internal environment, sensors output are entering to the ANN. The proposed ANN with 12 neurons organized in three layers having one input layer, one hidden layer and one output layer is used in premature incubator control system and discriminate between any condition that occur in the incubator and provide alarms or lights for the situations in case of any condition occur. The number of neurons in the input and hidden layers are decided empirically and the input variables have to be normalized in order to reach the ANN input level from 0 to 2, which identify the corresponding case and decide the suitable reaction upon previous training. The training patterns should contain the necessary information to generalize the problem, this would enable the network to grasp and absorb the essence of the problem but the analysis of the trained network is difficult to interpret or black box, it is impossible to extract structural knowledge (rule) from the trained neural network. Although the proposed ANN based control of the premature infant incubator system was tested with a set of different conditions including very extreme cases, the % errors of the system is ranged between 1.6e-2 to 4.6e-2 in controlling the temperature, 0.1 to 0.12 in controlling the humidity and 0.12 to 1.3 in controlling the oxygen concentration.

The above reviewed research studies clearly indicates us, fuzzy logic systems and artificial neural networks are equivalent, in that they are convertible. Hybrid intelligent systems combining fuzzy logic, neural networks, genetic algorithm and expert systems are proving their effectiveness in a wide variety of real-world problems. Every adaptive intelligent technique has a particular computational properties that make them suited for particular problems and not for others. For example, while neural networks are good at recognizing patterns but they are not good at explaining how they reach their decisions. Although fuzzy logic systems, can reason out with imprecise information and they are good at explaining their decisions, but cannot automatically acquire the rules they use to make those decisions. These limitations have been a central driving force behind the creation of intelligent hybrid systems where two or more techniques are combined in a manner that overcomes the limitations of individual techniques.

Hybrid systems are also important when we considering model uncertainty and varied nature of application domains. Many complex domains have many different component problems, each of which may require different types of processing. The use of intelligent hybrid systems is growing rapidly with successful applications in many areas: process control, financial trading, credit evaluation, medical diagnosis, etc. Different scholars implement hybrid control systems for specific process [20].

CHAPTER 3
METHODOLOGY

3.1 Introduction

The main idea of fuzzy logic control is to build a model of a human control expert which is capable of controlling the plant without thinking in terms of a mathematical model. The control expert specifies his control actions in the form of linguistic rules. These control rules are translated into the framework of fuzzy set theory providing a calculus which can simulate the behavior of the control expert. The specification of good linguistic rules depends on the knowledge of the control expert, but the translation of these rules into fuzzy set theory framework is not formalized and arbitrary choices concerning. The quality of FLC can be drastically affected by the choice of membership functions. Thus, methods for tuning fuzzy logic controllers are necessary. Neural networks offer the possibility of solving the problem of tuning. Although a neural network is able to learn from the given data, the trained neural network is generally understood as a black box. Neither it is possible to extract structural information from the trained neural network nor integrate special information into the neural network in order to simplify the learning procedure. On the other hand, a fuzzy logic controller is designed to work with the structured knowledge in the form of rules and nearly everything in the fuzzy system remains highly transparent and easily interpretable. However, there exists no formal framework for the choice of various design parameters and optimization of these parameters generally is done by trial and error. The combination of neural networks and fuzzy logic offers the possibility of solving tuning problems and design difficulties of fuzzy logic. The resulting network will be more transparent and can be easily recognized in the form of fuzzy logic control rules or semantics. This approach combines the well-established advantages of both methods and avoids the drawbacks of both methods.

3.2 Fuzzy logic control scheme

Humans, when making decision tends to work with vague or imprecision concepts which can often be expressed linguistically. One of the ways of modelling this decision making process has been proposed by Zadeh [21] and is based on the theory of approximate reasoning which enables certain classes of linguistic statements to be treated mathematically. He was the first to introduce the fuzzy set theory in the field of control. He proposed that all problems in which the data, the objectives and the constraints are too complex or too ill-define to admit a precise mathematical analysis have to be treated by approximate (fuzzy) solution. Fuzzy control has received a lot of attention since it was applied for the first time by Mamdani and Assilian [21].

3.2.1 Linguistic variables and Membership functions

Linguistic variable is a general data type (such as strings) that represent process states and control variables, such as temperature, rate of change, distance, speed, angle etc. We can use fuzzy sets to represent the variables, the concept of the fuzzy set is only an extension of the concept of a classical or crisp set. The fuzzy set is actually a broader set compared with the classical or crisp set. The classical set only considers a limited number of degrees of membership such as '0' or '1' or a range of data with limited degrees of membership. Every fuzzy set can be represented by its membership function, a membership function defines the degree of membership of all crisp values in the fuzzy set. If the referential set is a finite set, we can represent these values defined in the range between '0' and '1'. If the referential set is an infinite set, we can represent these values as a continuous membership function. In general, the shape of the membership functions depends on application can be monotonous, triangular, trapezoidal or bell-shaped as shown in the figure 3.1.

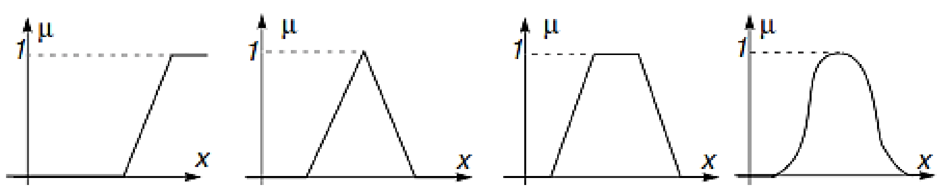

Figure 3.1*: Different shapes of membership function: monotonous, triangular, trapezoidal and bell-shaped [21]*

One of the first steps in every fuzzy application is to define the universe of discourse (dynamic range) for every linguistic variable. Every fuzzy set on a universe of discourse represent one linguistic value or label.

3.2.2 Notation of linguistic rule

As mentioned in the previous section, the principal idea of fuzzy logic system is to express human knowledge in the form of linguistic if-then rules. Every rule has two parts:

- The antecedent part, expressed by ***if***...............
- The consequent part, expressed by ***then***...........

The antecedent part is the description of the state of the system which should turn on the rule, and the consequent is the action that the operator who controls the system must take. There are several forms of if-then rules. The general one is:

If a set of conditions is satisfied ***then*** a set of consequents can be inferred

Zadeh was the first to introduce a notation of fuzzy rule of the form: $\Re_1$: *If x* is *A*, *then y* is *B*. *A* and *B* are linguistic values characterized by appropriate membership function of fuzzy sets defined on the universe of discourse of the linguistic variables *x* and *y* respectively.

Takagi and Sugeno proposed a form which has fuzzy sets only in the premise part of the rule, and the consequent part is described by a non-fuzzy equation of the input variables:

$\Re_2$: *If x* is *A*, *then y* is *f(x)*, like in Zadeh's rule, *A* is the linguistic label. When *f(x)* is a first order polynomial then the resulting fuzzy inference system is called first-order Sugeno fuzzy model. When *f* is a constant, we then have a zero-order Sugeno fuzzy model, which can be viewed as a special case of Mamdani inference system, in which each rule's consequent is specified by a fuzzy singleton (pre-defuzzified consequent).

3.2.3 Procedure for fuzzy reasoning

A fuzzy logic system contains sets used to categories input data (fuzzification), decision rules that are applied to each set and a way of generating an output (defuzzification). Inference unit is the core of the fuzzy controller. It determines the degree to which each measured valued is a member of a given labeled group and generates fuzzy control actions using the rules in the knowledge base to the current process state. The structure of fuzzy controller is shown in Figure 3.2.

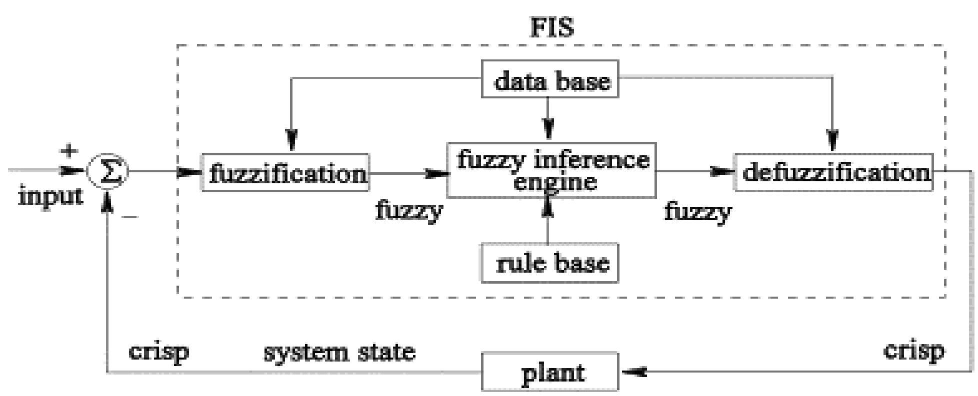

Figure 3.2*: General structure of fuzzy inference system*

Crisp value: A crisp value is an explicitly defined value in the set of real numbers. Crisp input values typically generated from sensors or instruments.

Fuzzification: Transform crisp inputs into fuzzy subsets. Given crisp inputs x_i, $i = 1, \ldots, n$ fuzzification is to construct the same number for fuzzy sets A^i, $A^i = fuzz(x_i)$. Fuzzification is determined according to the defined membership functions.

Fuzzy inference process: Combine membership functions according to the control rules in order derive the fuzzy output. Every control rule is implemented by a fuzzy implication (fuzzy relation) and is defined as $\mu_{R1} = \mu_{A \to B}(x, y) = \mu_A(x) \to \mu_B(y)$, where $\mu_{R1} = \mu_{A \to B}(x, y)$ is the truth value for the statement R_1, μ_A and μ_B are the levels of membership of the variables *x* and *y* in the fuzzy sets *A* and *B* respectively. The generalization of a control rule which has two condition in the antecedent part has the following form: $\Re_3$: *If x* is *A and y* is *B, then z* is *C*. Then the truth value of the statement is:

$\mu_{R3} = \mu_{A \text{ and } B \to C}(x, y, z) = [\mu_A(x) \text{ and } \mu_B(y)] \to \mu_C(z)$, *A*, *B* and *C* are fuzzy sets defined on the universe of discourse of the linguistic variables *x*, *y* and *z* respectively. μ_A, μ_B and μ_C are the levels of membership of the variables *x*, *y* and *z* in the fuzzy sets *A*, *B* and *C* respectively.

For the fuzzy intersection (*and operator/ T-norms*) Zadeh suggested *min operator* and for the fuzzy union (*or operator/ T-conorm*) suggested *max operator*. There are many ways in which the fuzzy inference may be defined, the most commons are.

1. **Mamdani fuzzy model**: The final output membership function is the union of fuzzy sets assigned to the output in a conclusion after cutting their degree of membership values at the degree of membership for the corresponding premise. The crisp value of the output is, most usually, the center of gravity of the resulting fuzzy set.

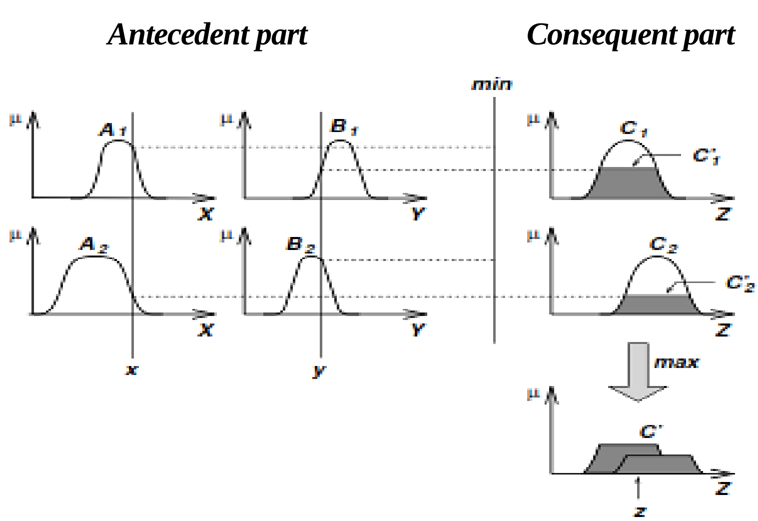

Figure 3.3*: Mamdani fuzzy inference system using min and max for fuzzy AND and OR [21]*

2. **Takagi and Sugeno (T-S) fuzzy model**: Each rule's output is a linear combination of input variables. The crisp output is the weighing average of each rule's output.

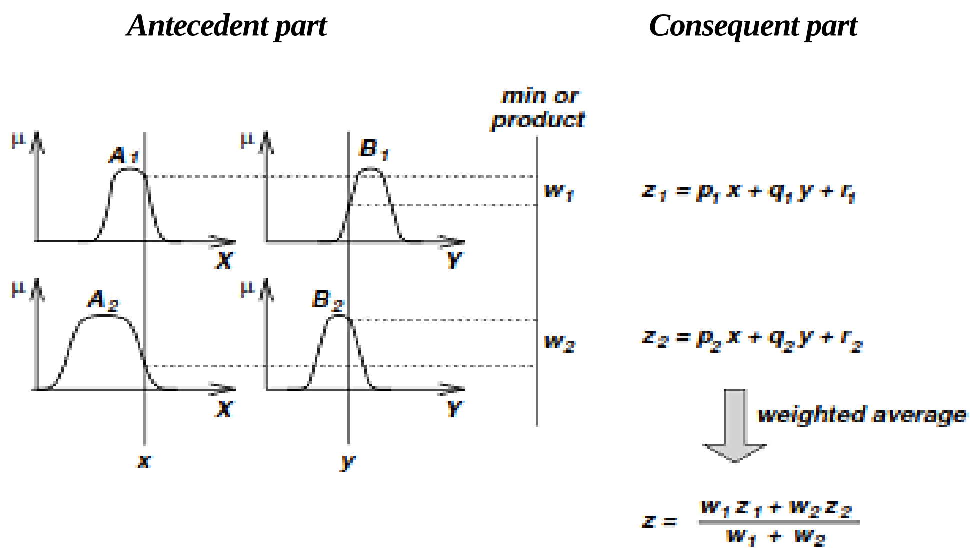

***Figure 3.4**: Takagi and Sugeno fuzzy model [21]*

The aggregator and defuzzifier block in the previous model replaced by the operation of weighted average, thus avoiding the time consuming procedure of defuzzification.

Defuzzification: Is an operation with the aim to produce a non-fuzzy control action. It transforms a union of output fuzzy sets into crisp value. There are several methods are available for the method of defuzzification, the most common is the center of gravity (centroid of area) method, which is given by:

$COG = \dfrac{\int zC(z)dz}{\int C(z)dz}$, Where $C(z)$ the aggregate output membership function.

Essentially, this procedures makes possible the use of fuzzy categories in the representation of words and abstract ideas of the human being in the description of the decision making process. There are a lot of advantages of fuzzy logic inference systems, some of them are:

- Capacity to represent inherent uncertainties and impressions of the human knowledge with linguistic variables.
- Convenient user interface and easier end-user interpretation, when the final user is not a control engineer.
- Easy computation due to widely available toolboxes and dedicated integrated circuits.

- FLC can incorporate a conventional design (PID, State-feedback) and fine-tune it to certain plant nonlinearities due to universal approximation capabilities.

But they have also some drawbacks:

- In capable to generalize, it only responds to what is written in its rule base and they are not robust in relation to topological changes of the system, such changes would demand alterations in the rule base.
- Depends on the existence of an expert in order to determine the inference logic rules.

3.3 Artificial neural networks

The aim of artificial neural networks is to model networks of biological neurons in the brain. From the neuroscientist's point of view, these models are extremely simplified. However, we use them because we hope that they give some insights into the principle of biological computation. ANN models have many names in the literatures like: connectionist model, parallel distributed processing models, neuromorphic systems, associative networks, etc. Their structure is based on our present understanding of biological nervous system. In fact, they are parallel structures composed of many computational elements connected by links with variable weights.

3.3.1 Biological Neuron

There are about 10^{11} neurons of different type found in a brain. The main components are: cell body or soma, dendrites and axon, which are shown in Figure 3.5. The cell nucleus is located in soma, while dendrites are fiber connected to it. The axon is one long fiber that is the extension of the cell body, it braches into strands and sub-strands, at the end of these strands there are synapses to other neurons. One axon makes typically a few thousands of excitatory or inhibitory synapse with other neurons.

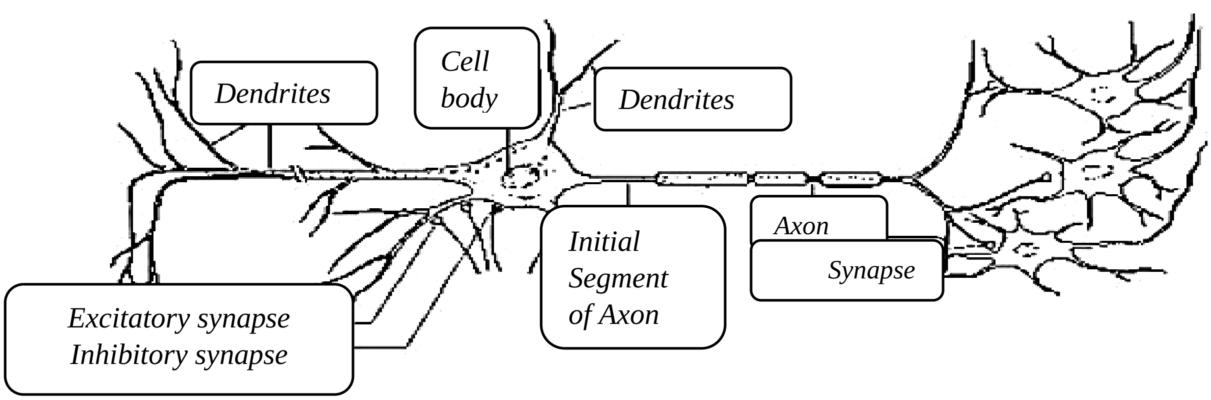

Figure 3.5*: Biological neuron [21]*

The process of transmitting a signal from one neuron to another is chemically complex and is beyond the scope of this paper. Generally, the receiving cell's electrical potential raises or lowers depending on the incoming signal. When this potential reaches a threshold, an action potential of fixed strength and duration sent through the axon to other cells.

3.3.2 Model of artificial neuron

The first wave of interest in neural networks emerged after the introduction of simplified neurons by McCulloch and Pitts in 1943.These neurons were presented as models of biological neurons and as conceptual components for circuits that could perform computational tasks.The complexity of real neurons is highly abstracted when modelling artificial neurons. These basically consist of inputs (like synapses), which are multiplied by weights (strength of the respective signals) and then computed by a mathematical function which determines the activation of the neuron. Another function (which may be the identity) computes the output of the artificial neuron (sometimes depend on a certain threshold). ANNs combine artificial neurons in order to process information.

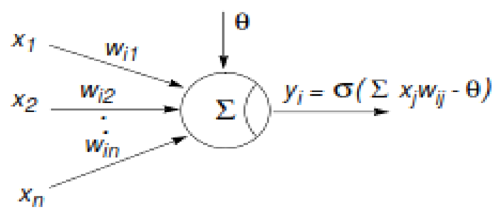

Figure 3.6*: Artificial neuron [22]*

In the figure 3.6, x_j is the input stimuli that can be either 1 or 0 representing the state of neuron *j* as firing and non-firing respectively. The synaptic weight w_{ij} can be positive (excitatory) or negative (inhibitory) and represent the strength of synapse that connects the neuron *j* to the neuron *i*, θ is a threshold or a bias. This neuron sums *n* weighted inputs and passes the result through an activation function. The node is characterized by an internal threshold θ and by the type of activation function (nonlinearity). Figure 3.7 illustrate some common types of nonlinearities.

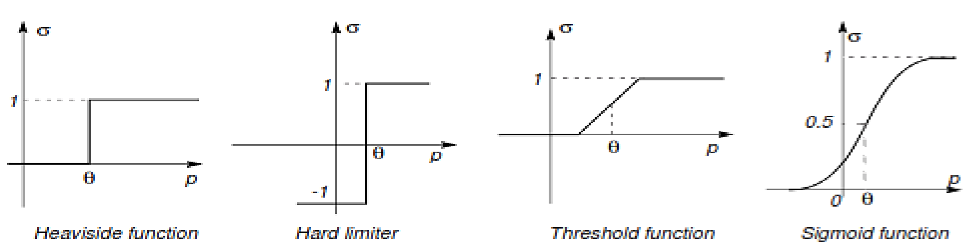

Figure 3.7*: Nonlinearities in the model of artificial neuron [21]*

The most employed function is a sigmoid function, because it is considered to be very close to the input/output function of a real biological neuron [21]. It is obvious that this model does not imitate the biological neuron, then why this all excitement about neural networks? The most important reason is their ability to learn and to generalize to new situations. Once a neural network has been trained for a set of data, it can interpolate and produce answers for the cases not present in the training set. Neural networks are specified by their topology, node characteristics and training or learning rules.

3.3.2.1 Network topology

In the previous section we discussed the properties of the basic processing units in an artificial neural network. This section focuses on the pattern of connections between the units and the propagation of data. For this pattern of connections, the main distinction we can make is between:

- **Feed-forward neural networks**: Networks where the data flow from input to output units is strictly feed-forward. The data processing can extend from single to multiple layers, but there is no feedback connections are present, that is, connections extending from output units to input units and units in the same layer or previous layers. Classical examples of FNN are the Perceptron and Adaline.
- **Recurrent neural networks**: Networks that do contain feedback connections. Contrary to feed-forward networks, the dynamical properties of the network are important, in some cases, the activation values of the units undergo a relaxation process such that the network will evolve to a stable state in which these activations do not change anymore. In other applications, the change of the activation values of the output neurons are significant, such that the dynamical behavior constitutes the output of the network. Examples of RNN have been presented by Anderson, Kohonen and Hopfield.

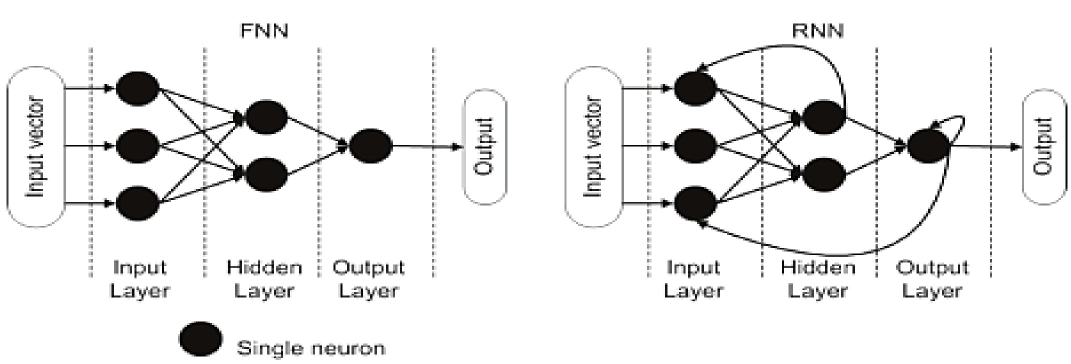

***Figure 3.8**: Feed-Forward and Recurrent topology of artificial neural network*

3.3.2.2 Training of artificial neural networks

Artificial neural networks have to be configured in such a way that the application of a set of inputs produces the desired set of outputs. There are various methods are available in order to set the strengths of the connections exist in ANNs. Generally, the learning process in ANNs categorized into two sets:

- **Unsupervised learning**: This method is used when the learning goal is not defined at all in terms of specific correct examples. The only available information is in the correlation of the input data. The network has to create categories from these correlations and produce output signals corresponding to the input category.
- **Supervised learning:** The weights are adjusted on the basis of comparison of the outputs of the network with the desired outputs. It means that we "teach" the network by using known input/output patterns, in order to perform a desired computation.

Both learning paradigms discussed above result in an adjustment of the weights of the connections between units, according to some modification rule. Virtually all learning rules for models of this type can be considered as a variant of the Hebbian learning rule suggested by Hebb in his classic book "Organization of Behavior". The basic idea is that if two units *j* and *k* are active simultaneously, their interconnection must be strengthened. If *j* receives input from *k*, the simplest version of Hebbian learning prescribes to modify the weight w_{jk} with:

$$\Delta w_{jk} = \gamma y_j y_k \tag{3.1}$$

Where γ is a positive constant of proportionality representing the learning rate. Another common rule, which is not use the actual activation of unit *k* but the difference between the actual and desired activation for adjusting the weights.

$$\Delta w_{jk} = \gamma y_j (d_k - y_k) \tag{3.2}$$

In which d_k is the desired activation provided by a teacher. This is often called the Widrow-Hoff rule or the delta rule. For a single layer network with an output unit with a linear activation function the output is simply given by

$$y = \sum_j w_j x_j + \theta \tag{3.3}$$

Such a simple network is able to represent a linear relationship between the value of the output unit and the value of the input units. By thresholding the output value, a classifier can be constructed, but here we focus on the linear relationship and use the network for a function approximation task. In high dimensional input spaces the network represents a hyper-plane and it will be clear that also multiple output units may be defined.

Suppose we want to train the network such that a hyper-plane is fitted as well as possible to a set of training samples consisting of input values x^p and desired (or target) output values d^p. For every given input sample, the output of the network differs from the target value d^p by $(d^p - y^p)$, where y^p is the actual output for this pattern. The delta-rule now uses a cost or error-function based on these differences to adjust the weights. The error function, as indicated by the name least mean square, is the summed squared error. That is, the total error E is defined to be

$$E = \sum_p E^p = \frac{1}{2}\sum_p (d^p - y^p)^2 \tag{3.4}$$

where the index p ranges over the set of input patterns and E^p represents the error on pattern p. The LMS procedure finds the values of all the weights that minimize the error function by a method called gradient descent. The idea is to make a change in the weight proportional to the negative of the derivative of the error as measured on the current pattern with respect to each weight:

$$\Delta_p w_j = -\gamma \frac{\partial E^p}{\partial w_j} \tag{3.5}$$

where γ is a constant of proportionality. The partial derivative

$$\frac{\partial E^p}{\partial w_j} = \frac{\partial E^p}{\partial y^p}\frac{\partial y^p}{\partial w_j} \tag{3.6}$$

Because of the linear units (equation (3.3))

$$\frac{\partial y^p}{\partial w_j} = x_j$$
$$\frac{\partial E^p}{\partial y^p} = -(d^p - y^p) \tag{3.7}$$

Such that

$$\Delta_p w_j = \gamma \delta^p x_j \tag{3.8}$$

where $\delta^p = d^p - y^p$ is the difference between the target output and the actual output for pattern p. The delta rule modifies weight appropriately for target and actual outputs of either polarity and for both continuous and binary input and output units, but one of Minsky and Papert's most discouraging results shows that a single layer perceptron cannot represent a simple exclusive-or function. For the specific XOR problem, by introducing hidden units extending the network to a multi-layer perceptron, then the problem can be solved, but did not present a solution to the problem of how to adjust the weights from input to hidden units. This was presented by Rumelhart, Hinton and Williams in 1986, The central idea behind this solution is that the errors for the units of the hidden layer are determined by back-propagating the errors of the units of the output layer. For this reason the method is often called the back-propagation learning rule. Back-propagation can also be considered as a generalization of the delta rule for non-linear activation functions and multi-layer networks.

Back-Propagation Algorithm

Since we are now using units with nonlinear activation functions. we have to generalize the delta rule which was presented in the previous section for linear functions to the set of non-linear activation functions.

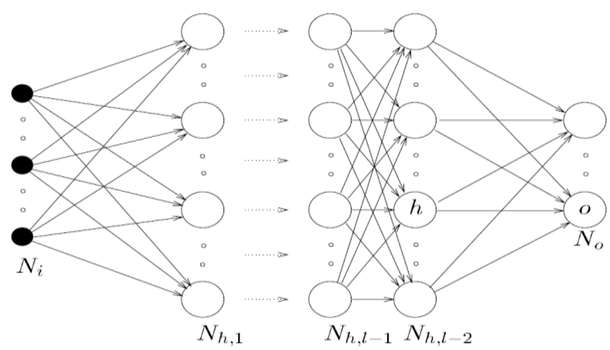

Figure 3.9*: A multi-layer network with l layers of units [22]*

The activation is a differentiable function of the total input, which is given by:

$$y_k^p = \mathcal{F}(s_k^p) \tag{3.9}$$

Where

$$s_k^p = \sum_j w_{jk} y_j^p + \theta_k \tag{3.10}$$

In order to get the correct generalization of the delta rule as presented in the previous section, we set

$$\Delta_p w_{jk} = -\gamma \frac{\partial E^p}{\partial w_{jk}} \tag{3.11}$$

The error measure E^p is defined as the total quadratic error for pattern *p* at the output units, which is given by:

$$E^p = \frac{1}{2} \sum_{o=1}^{N_o} (d_o^p - y_o^p)^2 \tag{3.12}$$

Where d_0^p is the desired output for unit o when pattern p is clamped. We further set $E = \sum_P E^p$ as a summed squared error. We can also write

$$\frac{\partial E^p}{\partial w_{jk}} = \frac{\partial E^p}{\partial s_k^p} \frac{\partial s_k^p}{\partial w_{jk}} \tag{3.13}$$

From equation (3.10) we see that, the second factor is computed as:

$$\frac{\partial s_k^p}{\partial w_{jk}} = y_j^p \tag{3.14}$$

When we define

$$\delta_k^p = -\frac{\partial E^p}{\partial s_k^p} \tag{3.15}$$

we will get an update rule which is equivalent to the delta rule, which is described in the previous section, resulting in a gradient descent on the error surface if we make the weight changes according to

$$\Delta_p w_{jk} = \gamma \delta_k^p y_j^p \tag{3.16}$$

The trick is to figure out what δ_k^p should be for each unit *k* in the network. The interesting result, which we now derive, is that there is a simple recursive computation of these δ'*s* which can be implemented by propagating error signals backward through the network. To compute δ_k^p we have to apply the chain rule, in order to write this partial derivative as the product of two factors, one factor reflecting the change in error as a function of the output of the unit and the other reflecting the change in the output as a function of changes in the input. Thus, we have

$$\delta_k^p = -\frac{\partial E^p}{\partial s_k^p} = -\frac{\partial E^p}{\partial y_k^p} \frac{\partial y_k^p}{\partial s_k^p} \tag{3.17}$$

Using equation (3.9), we can obtain that

$$\frac{\partial y_k^p}{\partial s_k^p} = \mathcal{F}'(s_k^p) \tag{3.18}$$

which is simply the derivative of the squashing function $\mathcal{F}$ for the k^{th} unit, evaluated at the net input s_k^p to the unit. To compute the first factor of equation (3.17), we consider two cases. First case, assume that unit *k* is an output unit *k*=o of the network. In this case, it follows from the definition of E^p that

$$\frac{\partial E^p}{\partial y_o^p} = -(d_o^p - y_o^p) \tag{3.19}$$

which is the same result as we obtained with the standard delta rule. Substituting equation (3.18) and

(3.19) into equation (3.17), we get

$$\delta_o^p = (d_o^p - y_o^p)\,\mathcal{F}_o{}'(s_o^p) \tag{3.20}$$

for any output unit o. Second case, if k is not an output unit but a hidden unit $k = h$, we do not readily know the contribution of the unit to the output error of the network. However, the error measure can be written as a function of the net inputs from hidden to output layer: $E^p = E^p\ (s_1^p, s_2^p, \ldots\ , s_j^p, \ldots)$ and we use the chain rule to write:

$$\frac{\partial E^p}{\partial y_h^p} = \sum_{o=1}^{N_o} \frac{\partial E^p}{\partial s_o^p}\frac{\partial s_o^p}{\partial y_h^p} = \sum_{o=1}^{N_o} \frac{\partial E^p}{\partial s_o^p}\frac{\partial}{\partial y_h^p}\sum_{j=1}^{N_h} w_{ko} y_j^p = \sum_{o=1}^{N_o} \frac{\partial E^p}{\partial s_o^p} w_{ho} = -\sum_{o=1}^{N_o} \delta_o^p w_{ho} \tag{3.21}$$

Substituting the above equation into equation (3.17) yields

$$\delta_h^p = \mathcal{F}'(s_h^p)\sum_{o=1}^{N_o} \delta_o^p w_{ho} \tag{3.22}$$

Equations (3.20) and (3.22) give a recursive procedure for computing the δ's for all units in the network, which, are then used to compute the weight changes according to equation (3.16). This procedure constitutes the generalized delta rule for a feed-forward network of non-linear units [22]. Sometimes the error surface of a complex network is full of hills and valleys, because of the gradient descent, the network can get trapped in a local minimum when there is a much deeper minimum nearby. Probabilistic methods can help to avoid this trap, but they tend to be slow. Another suggested possibility is to increase the number of hidden units. Although this will work because of the higher dimensionality of the error space, the chance to get trapped is smaller, it appears that there is some upper limit of the number of hidden units. When the number of hidden units exceeded the limit, which also results in the system being trapped in local minima. From the previous discussions we can specify a lot of advantages of artificial neural network systems, some of them are:

- Artificial neural Networks are powerful computational systems consisting of many simple processing elements connected together to perform tasks analogously to biological brains.
- They are massively parallel, which makes artificial neural networks efficient, robust, fault tolerant and noise tolerant.
- They can learn from training data and generalize to new situations.
- They are useful for brain modelling and real world applications involving pattern recognition, function approximation and prediction.

But they have also some drawbacks.

- In artificial neural nets, both knowledge extraction and knowledge representation are difficult.
- They are prone to over fitting.

3.4 Neuro-Fuzzy control scheme

Neuro-Fuzzy computing is a popular framework for solving complex problems. If we have knowledge expressed in linguistic rules, we can build a FIS, and if we have data, or can learn from a simulation (training) then we can use ANNs. For building a FIS, we have to specify the fuzzy sets, fuzzy operators and the knowledge base. Similarly for constructing an ANN for an application the user needs to specify the architecture and learning algorithm. An analysis reveals that the drawbacks pertaining to these approaches seem complementary and therefore it is natural to consider building an integrated system combining the concepts. While the learning capability is an advantage from the viewpoint of FIS, the formation of linguistic rule base will be advantage from the viewpoint of ANN.

3.4.1 Types of Neuro-Fuzzy systems

In general, all the combinations of techniques based on neural networks and fuzzy logic can be called neuro-fuzzy systems. The different combinations of these techniques can be divided in the following classes.

Cooperative Neuro-Fuzzy system: In a cooperative system the neural networks are only used in an initial phase. In this case, the neural networks determines sub-blocks (Fuzzy sets and Fuzzy rules) of the fuzzy system using training data, after this, the neural networks are removed and only the fuzzy system is executed. In the cooperative neuro-fuzzy systems, the structure is not totally interpretable, which can be considered as a disadvantage [23].

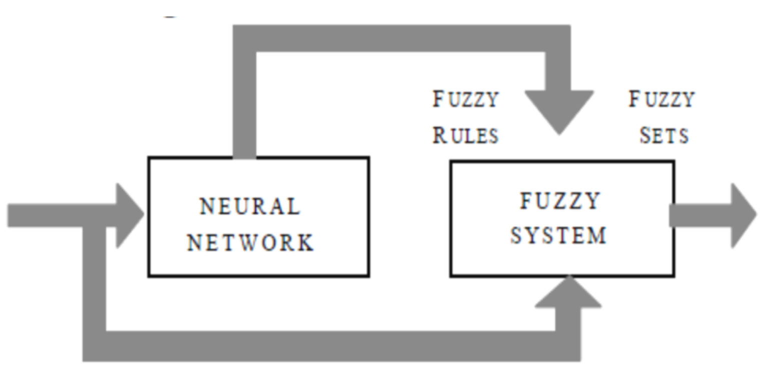

Figure 3.10*: Cooperative Neuro-Fuzzy system [23]*

Concurrent Neuro-Fuzzy system: A concurrent system is not a neuro-fuzzy system in the strict sense, because the neural network works together with the fuzzy system. This means that the inputs enters in the fuzzy system, are pre-processed and then the neural network processes the outputs of the concurrent system or in the reverse way. In the concurrent neuro-fuzzy systems, the results are not completely interpretable, which can be considered as a disadvantage [23].

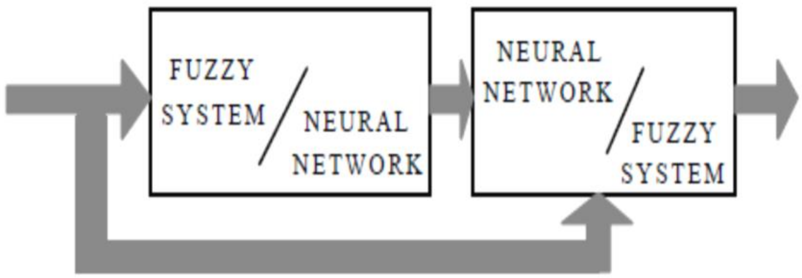

Figure 3.11*: Concurrent Neuro-Fuzzy system [23]*

Hybrid Neuro-Fuzzy system: In Nauck [24] definition: "A hybrid neuro-fuzzy system is a fuzzy system that uses a learning algorithm based on gradients or inspired by the neural networks theory (heuristical learning strategies) to determine its parameters (fuzzy sets and fuzzy rules) through the patterns processing (input and output)". A neuro-fuzzy system can be interpreted as a set of fuzzy rules. This system can be totally created from input/output data or initialized with the à priori knowledge in the same way of fuzzy rules. The resultant system by fusing fuzzy systems and neural networks has as advantages of learning through patterns and the easy interpretation of its functionality. There are several different ways to develop hybrid neuro-fuzzy systems, therefore, being as a recent research subject, each researcher has defined its own particular models. These models are similar in its essence, but they present basic differences. Some of the major woks in this area are GARIC [25], FALCON [26], ANFIS [27], NEFCON [28], FUN [29], SONFIN [30], FINEST [31], EFuNN [32] and many others.

3.4.1.1 Adaptive Neuro Fuzzy Inference System (ANFIS) model

The architecture of the ANFIS model is a graphical representation of the TS-FLC model. The general ANFIS control structure for the control of any plant is presented in this section. The functions of the various layers are given in the form of an algorithm as described below. The structure contains the same components as FIS, except for the ANN block. The network structure is composed of a set of units arranged into five interconnected network layers [33], as shown in the Figure 3.12.

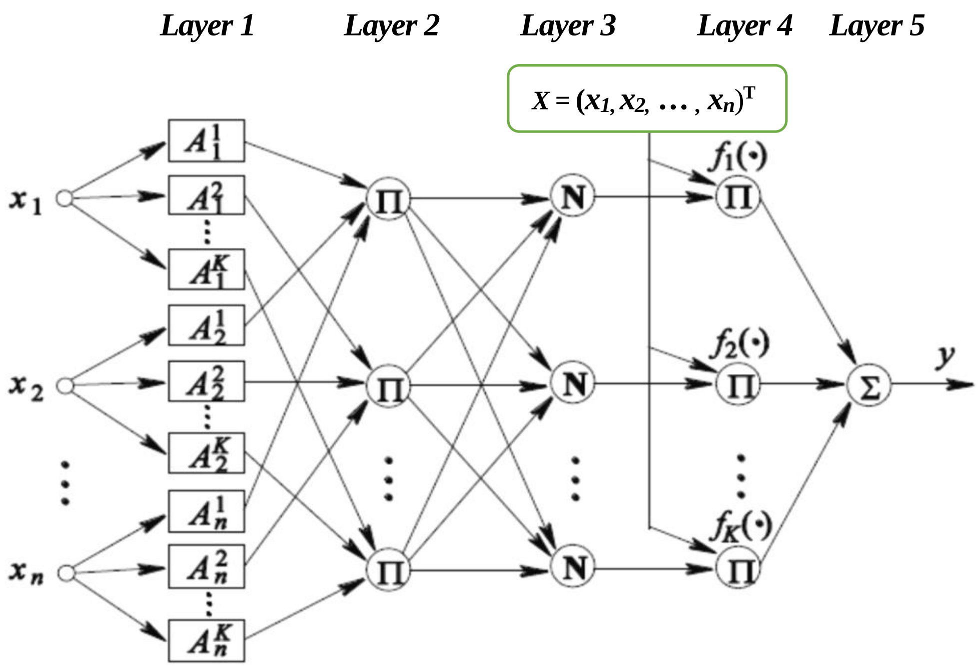

Figure 3.12: *ANFIS architecture [20]*

Layer 1: This layer is the input layer with n nodes. The weights between the first two layers, $w_{ij}=\mu_{A_i^j}(xi)$, $i=1,\ldots,n$ and $j=1,\ldots,k$, denotes membership values of the *i-th* input (antecedent) of the *j-th* rule, where A_i^j corresponds to a partition of the space of xi, and $\mu_{A_i^j}(xi)$ is typically selected as a Generalized bell Membership Function, which is given by

$$\mu_{A_i^j}(xi) = \frac{1}{1+\left|\frac{xi - c_i^j}{a_i^j}\right|^{2b_i^j}} \tag{3.23}$$

Where c_i^j, a_i^j and b_i^j are referred to as premise parameters.

Layer 2: This layer has K fuzzy neurons with the product T-norm as the aggregation operator. Each node corresponds to a rule, and the output of the *j-th* neuron determines the degree of fulfillment of the *j-th* rule.

$$O_j^{(2)}=\prod_{i=1}^{n}\mu_{A_i^j}(xi) \tag{3.24}$$

Layer 3: Each neuron in this layer performs normalization, the *j-th* node calculates the ratio of the *j-th* rule's firing strength to the sum of all rule's firing strengths and the outputs are called normalized firing strengths.

$$O_j^{(3)} = \frac{O_j^{(2)}}{\sum_{m=1}^{K} O_m^{(2)}} \tag{3.25}$$

Layer 4: The output of each node in this layer is an adaptive node with a node function defined by

$$O_j^{(4)} = O_j^{(3)} f_i(\boldsymbol{X}) \tag{3.26}$$

and the parameters in $f_i(\boldsymbol{X})$ are referred to as consequent parameters.

Layer 5: The outputs of layer 4 are summed and the output of the network gives the Takagi and Sugeno model.

$$O_j^{(5)} = \sum_{j=1}^{K} O_j^{(4)} \tag{3.27}$$

In the ANFIS model, functions used at all the nodes are differentiable, thus the Back-Propagation algorithm can be used to learn the premise parameters by using a sample sets. The effectiveness of the model is dependent on the Membership Functions used. The TS fuzzy rules are employed in the ANFIS model. After the rule base is specified, the ANFIS adjusts only the MFs of the antecedents and the consequent parameters. The BP algorithm can be used to train both the premise and consequent parameters. A more efficient procedure is to learn the premise parameters by the BP, but to learn the linear consequent parameters by the Least Square Estimate method [33]. The learning rate γ can be adaptively adjusted by some heuristics. It is reported in [33] that this hybrid learning method provides better results than trained by the BP method. However, the ANFIS is computationally expensive due to the curse-of-dimensionality problem arising from grid partitioning. Tree or scattering partitioning can resolve the curse of dimensionality, but leads to a reduction in the interpretability of the generated rules. Thus, the ANFIS model is suitable for applications, where performance is more important than interpretation.

CHAPTER 4

SYSTEM MODELING AND CONTROLLER DESIGN

4.1 Introduction

This chapter basically focuses on the design and development of a neuro-fuzzy based controller for neonatal incubator. As we have discussed in the literature review, neuro-fuzzy controllers are one of the recent controllers, which combining the advantages of fuzzy inference systems and artificial neural networks, they are advantageous for model uncertainties and non-linear complex systems. This chapter starts by discussing the development of the selected mathematical model of convective infant incubator system, in accordance to the heat and mass conservation law, then finally design the neuro-fuzzy controller on the basis of the input/output data sets, which are collected from the developed system model.

4.2 Mathematical model of neonatal incubator

An incubator system comprises of an infant and incubator compartments. The model is intended to develop the heat exchange relationships between the infant, incubator compartments and the environment. In this section, mathematical model of an infant-incubator system will be developed with all heat exchange routes incorporated. These include conduction, convection, evaporation, radiation and heat generation from the infant in terms of metabolic rates. The model targets preterm infants, as they are more susceptible to illnesses than full-term infants.

Although other simplified models are available in this regard [17][34][35], the present model provides better accuracy and more comprehensiveness than the previous simplified models. It also considers the fan-heater/humidification system which is not available in other models. Figure 4.1 illustrates all interactions within the infant-incubator system including the baby's core and skin layers, mattress, incubator air space, incubator's walls, and the fan-heater/ humidification section.

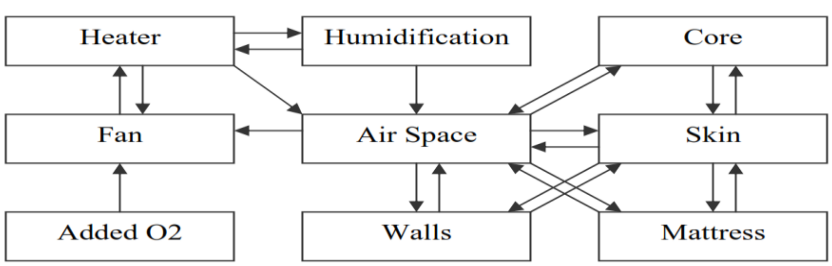

***Figure 4.1**: Interaction between compartments of infant-incubator system [18]*

The incubator used for modelling is an ATOM V-850 manufactured in Japan in 1985 by ATOM Medical. The incubator is single-walled with a slanted front and is convectively heated using a fan and a heating element. It also has a humidification system that maintains the required humidity level inside the incubator at all times and pure oxygen is supplied to the incubator for resuscitation purposes via a bottle connected to a throttle valve placed at the back of the incubator. Finally the moist air enters the incubator air space, as shown in the figure 4.2.

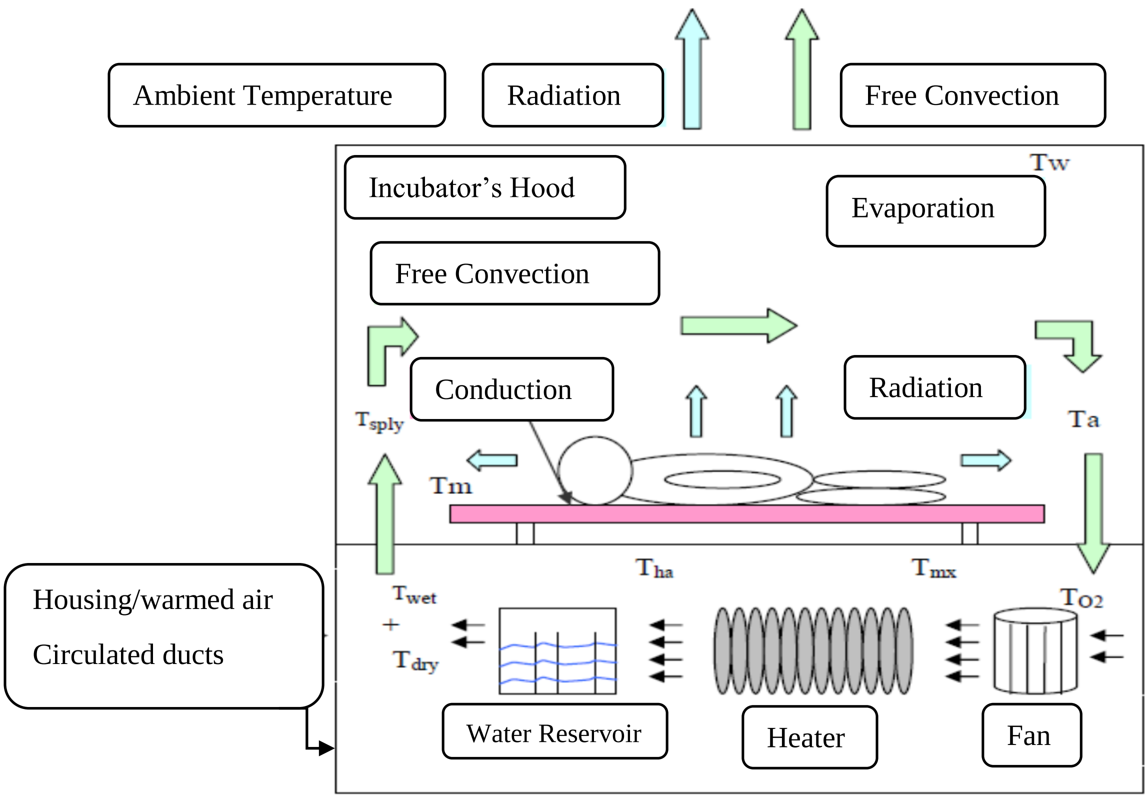

Figure 4.2: *Heat flow diagram [18]*

The modelling of each compartments, which were shown in the Figure 4.1 will be developed in the following sections.

4.2.1 Infant modeling

There are several methods available for modelling infants. An infant can be modelled as a one-lumped mass [18] or as a four-lumped mass representing the head, trunk, upper limbs and lower limbs [34]. The latter model has the advantage in demonstrating that, there is a temperature difference between the infant segments, and that this temperature gradient is attributed to the allocation of heat production and heat losses for each segment. Rojas, however showed that this temperature difference is usually not significant [34]. The one lumped model consider the infant with two layers: core and skin layers. Figure 4.3 (a) and (b) illustrate the heat exchange between the core and skin layers within an infant's body.

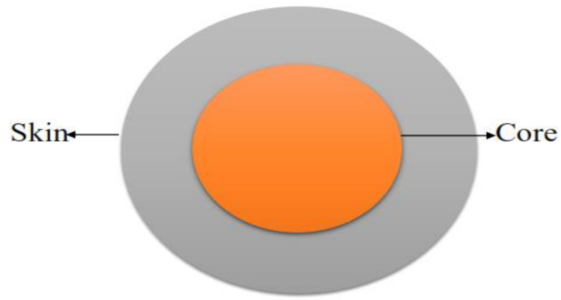

Figure 4.3: *(a) One lump infant model [18]*

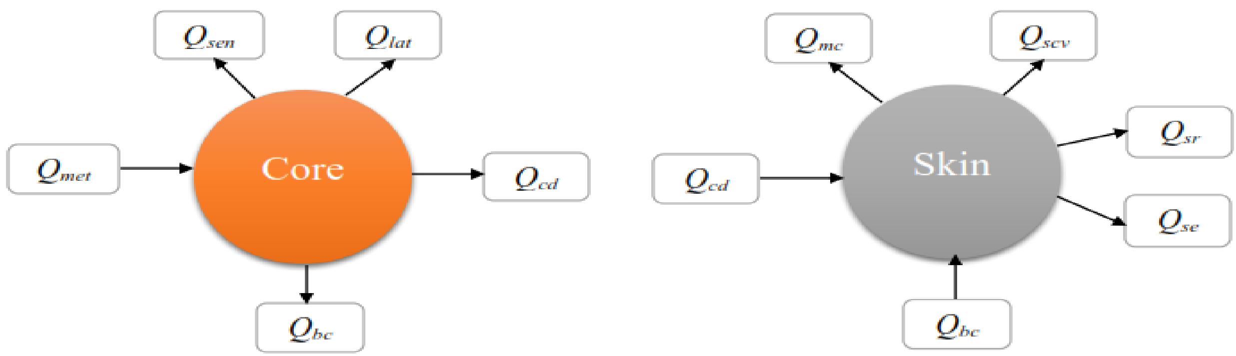

Figure 4.3: *(b) Heat exchange block diagram for infant's core and skin compartment [18]*

One lumped model is based on Rojas's model [34]. From Figure 4.3 (b) the core of an infant gains heat via:

- Metabolic rate, Q_{met}.

While the core of an infant losses heat via:

- Convection with the blood, Q_{bc}.
- Respiration (i.e. sensible heat, Q_{sen} and latent heat, Q_{lat}).
- Conduction with the adjacent skin layer, Q_{cd}.

Similarly the infant skin layer gains heat via:

- Conduction with the adjacent skin layer, Q_{cd}.
- Convection with the blood, Q_{bc}.

And the skin of an infant losses heat via:

- Conduction with the mattress, Q_{mc}.
- Convection with incubator air space, Q_{scv}.

- Radiation losses to the incubator walls, Q_{sr}.
- Evaporation losses through the skin, Q_{se}.

In order to simplify the infant-incubator model the following assumptions are made:

1. Single-walled rectangular incubator with one slanted front wall, forced convection heating and a humidification system [18].
2. The material of each compartment has homogenous properties [18].
3. Uniform airflow throughout the system.
4. Consider the required metabolic rate for self-thermoregulatory of the infant is the resting metabolic rate, M_{rst} [18].
5. For modeling purposes, the infant is considered as a black colored cylinder.
6. The self-thermoregulatory systems of the infant are not included in the model (i.e. sweating and shivering) [18].
7. The conductive heat between the mattress and the incubator, Q_{ic}, is neglected (Simon [17] and Rojas [34] models).
8. The only perturbation occurs to the model via port doors and/or front panel for care giving purposes [18].
9. The infant incubator is placed in a thermo-regulated room and the velocity of air currents is minimal. Thus, only external free convection is permissible [18].

Each compartment of the model is subjected to the first law of thermodynamics (law of energy conservation) and each of the model equations describes the temperature variation of each compartment over time (i.e. instantaneous temperature).

Core layer

Consider a one-lumped mass model for the infant as shown in Figure 4.3. In a period of time dt, the heat balance of the core layer can be written as:

$$[Q_{met} - Q_{sen} - Q_{lat} - Q_{cd} - Q_{bc}]dt = M_c C_{p_c} dT_c \tag{4.1}$$

Therefore, the instantaneous temperature of the core can be written as:

$$\frac{dT_c}{dt} = \frac{Q_{met} - Q_{sen} - Q_{lat} - Q_{cd} - Q_{bc}}{m_c C_{p_c}} \tag{4.2}$$

Equation (4.2) describes all heat flow rates, which manipulate the heat transfer relationships associated with the infant body. Each one of the terms in this equation determined as follows:

Heat production of infant core

The heat production of the core of the infant body can be written as:

$$Q_{met} = M_{rst} \times S_a \tag{4.3}$$

Where M_{rst} is the resting metabolic rate and S_a is the surface area of the infant. This is a function of infant weight and can be determined using an empirical formula that will be shown later in this section. It is necessary to use the resting metabolic rate because the basal metabolic rate can only be measured after overnight fasting and this is ethically unacceptable for neonates [18]. The estimated value for M_{rst} is 24.80 W/m^2 [15]. This is determined at the thermo-neutral zone during the first week of life.

Heat losses of infant core

The infant core loses heat during breathing process in the form of convective heat which takes the form of Q_{sen} due to warming the inhaled air and Q_{lat} caused by the difference between water-vapour pressure of the inhaled and exhaled air, in terms of respiratory rate and tidal volume. The equations for respiration losses can be determined by [17].

$$Q_{sen} = rr \times C_{p_a} \times v_t \times \rho_a \times (T_{ex} - T_a) \tag{4.4}$$

$$Q_{lat} = hfg \times rr \times \rho_a \times v_t \times (W_{ex} - W_a)$$

Equations (4.4) will be modified in terms of inspired minute volume (*IMV*) of 200 mL/kg of infant mass [36]. This value represents the total volume of the air inhaled and exhaled in one minute per kilogram mass of infant. Equation (4.4) can be re-written as:

$$Q_{sen} = IV \times m \times C_{p_a} \times \rho_a \times (T_{ex} - T_a) \tag{4.5}$$

$$Q_{lat} = IV \times m \times hfg \times \rho_a \times (W_{ex} - W_a)$$

Where, the inspired air volume, *IV*, equals to 3.333 mL/kg/sec [18].

Equations (4.5) written in terms of infant's mass *m* or mass of the body local segment and inspired air volume (*IV)*. They are more reliable in comparison with Simon's equations [17], since the respiratory rate and tidal volume of infant is not well-documented. In this paper, equations (4.5) will be employed. For more precise results, T_{ex} is assumed to be equal to T_c [18].

The humidity ratio of the exhaled air is determined by [18], which is given by:

$$W_{ex} = 0.622 \frac{P_{H_2O}}{P_t - P_{H_2O}} \tag{4.6}$$

and the inhaled air also given by:

$$W_a = 0.622 \frac{P_{H_2O}}{P_t - P_{H_2O}} \tag{4.7}$$

The partial pressure of water-vapour P_{H_2O} at T_a and T_{ex} is determined by [18]:

$$P_{H_2O} = P_{sat.} \times RH\% \tag{4.8}$$

P_t is the atmospheric pressure and $P_{sat.}$ is the saturation pressure for air which can be found from data, which is available in most heat transfer books (Stoecker or Cengel) [37]. $P_{sat.}$ is a function of air temperature and for simulation purposes, exponential formula can be developed from Figure 4.4[18] [37]:

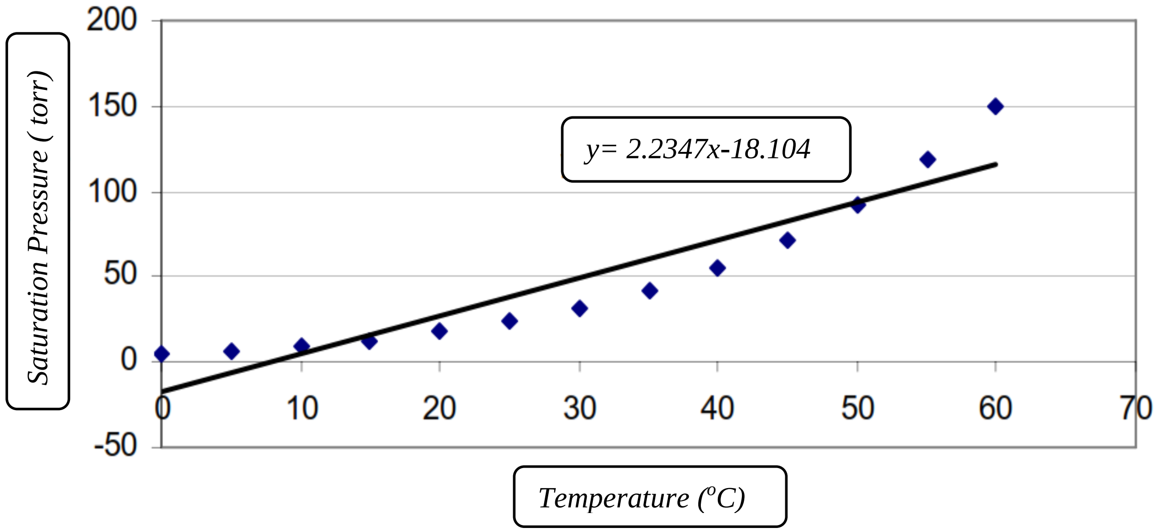

***Figure 4.4**: Pressure-Temperature curve [18][37]*

Thus, the relationship between $P_{sat.}$ and T can be written as:

$$P_{sat.} = 2.2347T - 18.104 \tag{4.9}$$

This is calculated for a temperature range of 0.01-60 °C and is used to estimate the saturation pressure at any given temperature within that range. The relative humidity of the exhaled air *RH%* at 37 °C body core temperature is also assumed to be 100% [18].

The infant core also loses heat via conduction through the skin layer. Thus, the rate of conduction can be determined by [18]:

$$Q_{cd} = \frac{(T_c - T_s) \times K_c \times S_a}{(m/\rho_c \times S_a)} \tag{4.10}$$

The core blood constitutes a medium for convective heat losses, which can be determined by [18]:

$$Q_{bc} = (T_c - T_s) \times \rho_{bl} \times bf \times C_{p_b} \times V_{cb} \tag{4.11}$$

The blood volume V_{cb} in equation (4.11) is directly determined from the mass of the infant body using [18]:

$$V_{cb}(mL) = 80(\frac{mL}{kg}) \times m(kg) \tag{4.12}$$

The blood flow rate parameter *bf* in per second for the infant body is derived as follows [18]:

$$bf = \rho_{bl} \times q_c \tag{4.13}$$

where q_c is the cardiac output of the infant (3.333 mL/kg.sec) [18] and ρ_{bl} is 1.06×10^{-3} kg/mL [18]. Using these values in equation (4.13), results in a blood flow parameter value of 0.00353 (1/sec).

The mass of the infant core m_c can be determined as follows [18]:

$$m_c = m \times m_s \tag{4.14}$$

where m_s is the mass of the infant skin and determined using [18]:

$$m_s = th_s \times \rho_s \times S_a \tag{4.15}$$

The total surface area of the infant body S_a can be calculated using the empirical formula [18]

$$S_a = mass^{0.75}/10.80 \tag{4.16}$$

where S_a is in m^2 and mass is in kilograms.

Skin layer

Consider the skin layer shown in Figure 4.3. In a period of time *dt*, the heat balance equation for the skin layer can be written as follows:

$$[Q_{cd} + Q_{bc} - Q_{scv} - Q_{mc} - Q_{se} - Q_{sr}]dt = m_s C_{p_s} dT_s \tag{4.17}$$

Therefore, the instantaneous temperature of the skin can be written as:

$$\frac{dT_s}{dt} = \frac{Q_{cd} + Q_{bc} - Q_{mc} - Q_{scv} - Q_{se} - Q_{sr}}{m_s C_{p_s}} \tag{4.18}$$

where Q_{cd}, Q_{bc} and m_s are given in equations (4.10), (4.11) and (4.15) respectively, while the rate of conductive heat loss from the skin in contact with the mattress Q_{mc} can be determined by [18]:

$$Q_{mc} = A_s \times K_{mat} \times (T_s - T_m)/th_m \tag{4.19}$$

the average mattress temperature is taken in the middle of the given thickness of the mattress [18]. Thus the mattress thickness, th_m is halved. The surface area of the skin in contact with the mattress for either infant local segment or infant body A_s is estimated to be 10% of the total infant surface area (m^2) [18]. Thus,

$$A_s = 0.1 \times S_a \tag{4.20}$$

In addition, the skin undergoes convective heat losses due to the difference in temperature between skin and air space. This can be determined by [18]:

$$Q_{scv} = h_{scv} \times A_{cv} \times (T_s - T_a) \quad (4.21)$$

Since the surface area in contact with the mattress is 10% of the total surface area, the surface area exposed to the air is 90%. A_{cv} can then be written as:

$$A_{cv} = 0.9 \times S_a \quad (4.22)$$

In equation (4.21) the convective heat transfer coefficient for forced convection h_{scv} depends on the geometry of the infant and is a function of the Nusselt and Reynolds numbers. The Nusselt number is defined as [18]:

$$Nu_{sph} = \frac{h_{scv} D_{sph}}{K_a} \quad (4.23)$$

and Reynolds number given by [18]:

$$\mathrm{Re}_D = \frac{\rho_a V_a D_{sph}}{\mu_a} \quad (4.24)$$

The shape of the infant body is not uniform and is difficult to model. The direction of the air flow parallel to the infant body longitudinal axis creates another complexity in choosing appropriate empirical formulas for Nusselt number. Therefore, in this work the infant body is approximated as a cylinder with air flows parallel to its axis, as shown in figure 4.5.

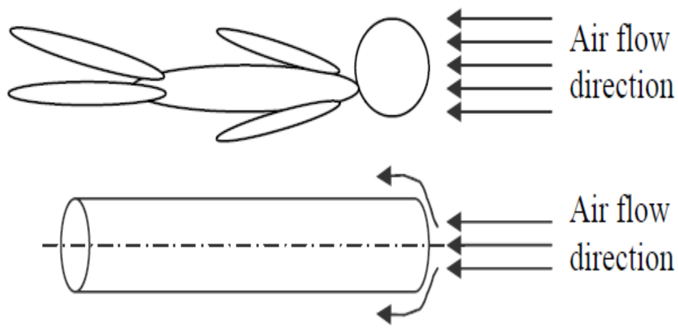

Figure 4.5*: Infant shape approximation [18]*

Since the cross-section area for the cylinder with regard to the direction of air flow is as for a sphere. Thus, the Nusselt number for this situation can then be approximated as [18]:

$$Nu_{sph} = \frac{h_{scv} D_{sph}}{K_a} = 2 + \left[0.4\,\mathrm{Re}^{1/2} + 0.06\,\mathrm{Re}^{2/3}\right]\mathrm{Pr}^{0.4}\left(\frac{\mu_a}{\mu_s}\right) \quad (4.25)$$

where the Prandtl number is defined by [18]:

$$\Pr = \frac{\mu_a C_{p_a}}{K_a} \tag{4.26}$$

The air properties in equations (4.24-4.26) are evaluated at T_a, except for μ_s which is evaluated at skin temperature, T_s.

The water loss from the skin to the air space through evaporation is inversely proportional to the ambient partial pressure of water vapour [18][38]. The evaporation heat rate Q_{se} (in watts) can be determined by [18]:

$$Q_{se} = \frac{hfg \times m \times Evap. \times \rho_{h_2o}}{86400} \tag{4.27}$$

Where *Evap.* is the evaporation loss from the skin of the infant to the environment (mL/kg/day), which is a function of gestational age (*GA*) and postnatal age (*age*), which can be determined from the equation developed by LeBlanc[18][38] as follows:

$$Evap. = \left[6.5\exp\left(168/\left(age+11.8\right)\right)\times\exp\left(-5.2GA/\left(age+12.2\right)\right)+4.8\right]*\left[2-\left(\frac{P_{H_2O}}{23}\right)\right] \tag{4.28}$$

where P_{H_2O} is determined by equation (4.8).

The skin of an infant also loses heat to the walls of the incubator by radiation. Thus, the rate of radiant heat losses can be determined by [18]:

$$Q_{sr} = A_r \times \sigma \times \varepsilon_s \times [(T_s + 273.15)^4 - (Tw + 273.15)^4] \tag{4.29}$$

The surface area of the neonate body normal to the walls of the incubator, A_r, is a fraction of the infant surface area exposed to air, A_{cv} and for various parts of the infant body is defined as [17]:

1. 30% of total surface area is given to the objects directly above a reclining infant.
2. 17% of total surface area is given to the sides.
3. 8.5% of total surface area for above the head or below the feet.

Equations (4.1 – 4.29) describe the heat exchange of the infant model as a one lump.

4.2.2 Incubator modeling

The incubator comprises of the following compartments:

1. Air Space
2. Walls (Hood)
3. Mattress

Air space modeling

The incubator air space exchanges heat with all compartments of the infant-incubator system, mainly due to convection, but also due to heat and mass transfer via respiration and evaporation. Figure 4.6 illustrates all heat gains and losses within the air space compartment.

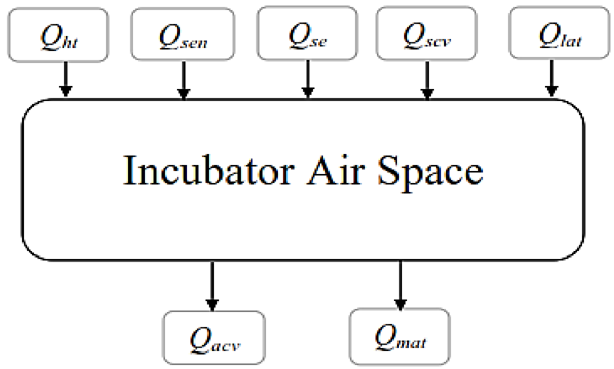

***Figure 4.6**: Block diagram for heat exchange within the incubator air space*

In a period of *dt*, the heat balance equation for the incubator air space can be written as follows:

$$[Q_{scv} + Q_{se} + Q_{ht} + Q_{sen.} + Q_{lat.} - Q_{acv} - Q_{mat}]dt = M_a C_{p_a} dT_a \tag{4.30}$$

Thus, the instantaneous temperature of the air space:

$$\frac{dT_a}{dt} = \frac{[Q_{scv} + Q_{se} + Q_{ht} + Q_{sen.} + Q_{lat.} - Q_{acv} - Q_{mat}]}{M_a C_{p_a}} \tag{4.31}$$

The incubator air space gains heat by convection from the infant skin, Q_{scv} , which can be determined using equation (4.21), and from the heating/humidification compartment, Q_{ht} , which will be defined during the modeling of the humidification compartment. An estimation of the incubator air space mass, M_a , will be derived in the modeling of the circulated-air fan. Also, the water losses from the skin occur via evaporation into the air space and this vaporized energy is defined by Q_{se} , and can be determined using equation (4.27).

In addition, there is a heat and mass transfer associated with infant's respiration. The heat transfer is in the form of sensible heat, $Q_{sen.}$, due to warming the inhaled air, which can be determined by equation (4.5). The mass transfer is in the form of latent heat, $Q_{lat.}$, which is due to the difference in partial pressure of water-vapour between the inhaled and exhaled air, can be determined by equation (4.5).

In contrast, the air space compartment loses some of its heat to the walls of the incubator by convection, Q_{acv} , which can be determined [18], as follows:

$$Q_{acv} = h_{acv} A_{wi} (T_a - Tw) \tag{4.32}$$

The convective heat transfer coefficient, h_{acv} , depends on the geometry of the incubator hood and the regime of the air flow inside the hood. It is also a function of the Nusselt and Reynolds numbers according to equations (4.23) and (4.24).

Since the given air velocity inside the hood is not high (approximately 10 cm/sec, supplied by the manufacturer [18]) the Reynolds number for such a velocity is 4970.6. Therefore the pattern of the airflow regime is turbulent to transitional flow [18][37]. This calculation was done by assuming the shape of the hood is rectangular rather than with a slanted front, as follows:

The equivalent hydraulic diameter of the incubator, D_h , can be determined using [18]:

$$D_h = \frac{4A_c}{p} \tag{4.33}$$

The Nusselt number for this regime of flow in the incubator can be determined by [18]:

$$Nu_1 = \frac{h_{acv} D_h}{K_a} = \frac{(f/8)(\mathrm{Re} - 1000)\mathrm{Pr}}{1 + 12.7(f/8)^{0.5}(\mathrm{Pr}^{2/3} - 1)} \tag{4.34}$$

The friction factor, f , in equation (4.34) is then determined by [18]:

$$\frac{1}{\sqrt{f}} = -2.0 \log\left(\frac{\varepsilon/D_h}{3.7} + \frac{2.51}{\mathrm{Re}\sqrt{f}}\right) \tag{4.35}$$

Since the roughness, ε , of the hood material (plexiglass) is zero, the friction factor is around 0.0119 [18].

Likewise, the mattress is convectively heated by the air. Not all of the area of the mattress is convectively heated, however only the area which is not covered by the infant, can be determined [18], as follows:

$$Q_{mat} = h_{acv} A_{net} (T_a - T_m) \tag{4.36}$$

In equation (4.36), the convective heat transfer coefficient, h_{acv}, can be determined using equation (4.34). While the net area of the mattress not covered by the infant, A_{net}, can easily be determined using [18]:

$$A_{net} = A_{mat} - A_s \tag{4.37}$$

Where A_s is defined by equation (4.20).

Wall (Hood) modeling

The compartment of the incubator walls 'hood' is made of transparent plexiglass and has 6 port doors plus a front panel for care giving purposes. One of the front sides also has a slanted surface. The incubator wall is considered as a single one-lump of 6mm thickness. Thus, the temperature gradient within such thickness is not significant and the conduction resistance of the wall is negligible [18].

The following assumptions are made to simplify the modeling:

1. The material of the wall is homogenous and uniform [18].
2. There is a uniform temperature distribution across the internal and external surfaces of the wall [18].

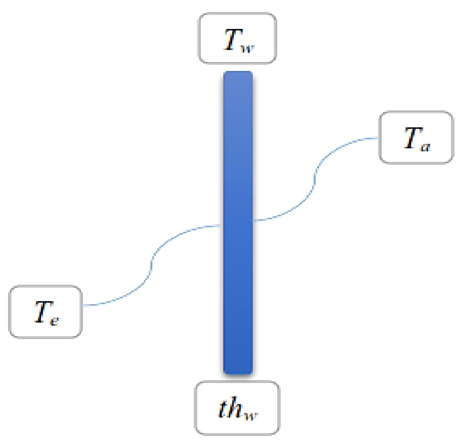

Figure 4.7: *Temperature difference across the wall [18]*

Figure 4.7 shows the anticipated temperature gradient between the inside of the incubator (*Ta*) and the outside environment (*Te*). Since air is the only medium crossing the inner and outer surfaces, heat losses are therefore in forms of convection and radiation, as shown in Figure 4.8.

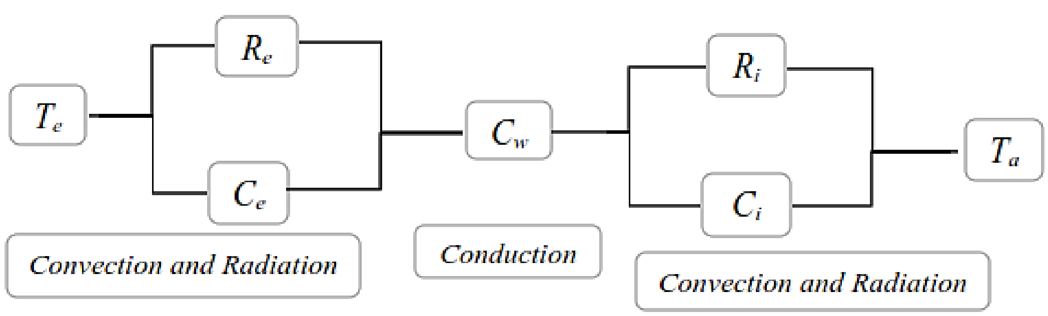

Figure 4.8: *Heat transfer diagram across the wall [18]*

In the above figure, C_i and R_i represent the convective and radiative heat gains to the internal surface of the walls respectively. Likewise, C_e and R_e represent the heat losses from the external walls to the environment by convection and radiation respectively. C_w represents the heat transfer by conduction between the inner and outer surfaces of the wall, which in this case is considered negligible. Figure 4.9 illustrates the rates of heat transfer within the wall compartment.

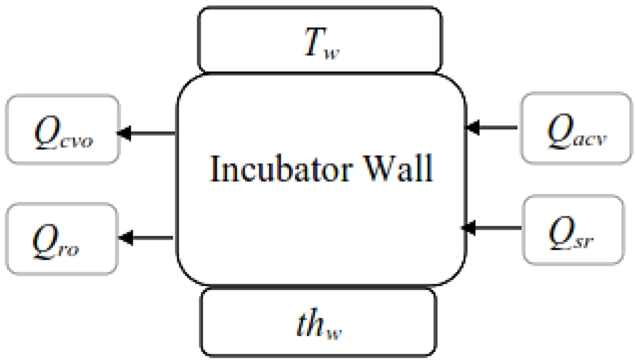

Figure 4.9*: Block diagram for heat exchange across the wall*

From Figure 4.9, in a period of *dt* the heat balance equations for the incubator walls can be written as [18]:

$$[Q_{acv} + Q_{sr} - Q_{cvo} - Q_{ro}]dt = M_w C_{pw} dTw \tag{4.38}$$

Therefore, the instantaneous temperature of the wall can be written as:

$$\frac{dTw}{dt} = \frac{[Q_{acv} + Q_{sr} - Q_{cvo} - Q_{ro}]}{M_w C_{pw}} \tag{4.39}$$

The inner surface of the incubator wall gains heat by convection from the incubator air space, Q_{acv}, which is determined using equation (4.32). The wall also gains heat from the skin of the infant by radiation, the rate of radiative heat transfer, Q_{sr}, being determined by equation (4.29). Due to the temperature gradient between the incubator air space and outside environment, the wall of the incubator loses heat to the environment (room) in the form of radiation and convection. For free (natural) convection occurs from the incubator walls to the outside environment. Thus, convective heat loss is a function of the Nusselt and Prandtl numbers, which can be determined by [18][37]:

$$Nu_{inc} = \frac{h_{cvo} L_c}{K_a} = C\left(Gr_L \Pr\right)^n = CRa_L^n \tag{4.40}$$

Where Gr_L is the Grashof number and Ra_L is the Rayleigh number, defined by [18][37]:

$$Gr_L = \frac{g\beta(Tw - Te)L_c^3}{v^2} \tag{4.41}$$

$$Ra_L = Gr_L \Pr = \frac{g\beta(Tw - Te)L_c^3}{v^2}\Pr$$

The fluid properties related to the above equations are evaluated at the average temperature of the inner wall's temperature and room temperature as follows [18][37]:

$$T_{avg} = \frac{1}{2}(Tw + Te) \tag{4.42}$$

Since the incubator hood has approximately horizontal and vertical surfaces, the Nusselt number will be determined as follows [18][37]. For the horizontal (upper) surface of the incubator:

$$Nu_{hzt} = 0.27 Ra_L^{1/4} \tag{4.43}$$

For the four vertical-sides, the Nusselt number is given by [18][37]:

$$Nu_{vrt} = \left\{ 0.825 + \frac{0.387 Ra_L^{1/6}}{\left[1 + (0.492/\Pr)^{9/16}\right]^{8/27}} \right\}^2 \tag{4.44}$$

For the Grashof number in equation (4.41), L_c is given by [18]:

$$L_c = \frac{A_c}{p} \tag{4.45}$$

Based on equations (4.43) and (4.44), two different values of convective heat transfer coefficients are determined for each surface. Using these coefficients, the rate of convective heat transfer is determined by:

$$Q_{cvo} = h_{cvo} A_{wi} (Tw - Te) \tag{4.46}$$

The total convective heat losses from the horizontal-side and the four vertical-sides of the incubator, Q_{cvt} (i.e. two long sides and two short sides) are added together to give:

$$Q_{cvt} = Q_{c_{hzt}} + 2\left[Q_{c_{vrt}}\right]_{long} + 2\left[Q_{c_{vrt}}\right]_{short} \tag{4.47}$$

For the radiation loss, the rate of radiant heat transfer from the walls to the environment is determined as [18][37]:

$$Q_{ro} = A_w \times \sigma \times \varepsilon_w \times [(Tw + 273.15)^4 - (Te + 273.15)^4] \quad (4.48)$$

The mass of the incubator walls, M_w, is determined using:

$$M_w = \rho_w th_w A_{wi} \quad (4.49)$$

Where ρ_w, th_w and A_{wi} are the wall material density (kg/m^3), wall thickness (m) and the surface area of the incubator walls (m^2) respectively.

Mattress modeling

The mattress gains heat by conduction with the skin of the infant, and is convectively heated by the incubator air space. Since the two thin support plates carry the mattress and the contacted area is considered small, the conductive heat transfer from the mattress to the incubator, Q_{ic}, is not significant and can be ignored [18].

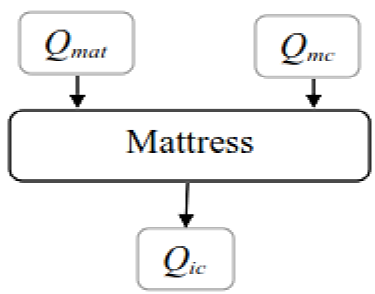

***Figure 4.10**: Block diagram for heat exchange across the mattress*

From Figure 4.10, in a period of dt, the heat balance equation for the mattress can be written as follows:

$$[Q_{mc} + Q_{mat} - Q_{ic}]dt = M_m C_{p_m} dT_m \quad (4.50)$$

Thus, the instantaneous mattress temperature can be written as:

$$\frac{dT_m}{dt} = \frac{[Q_{mc} + Q_{mat} - Q_{ic}]}{M_m C_{p_m}} \quad (4.51)$$

Both Q_{mc} and Q_{mat} can be determined using equations (4.19) and (4.36) respectively.

4.2.3 Heating-Fan system modeling

Figure 4.11 illustrates the parts of the heating compartment. Several assumptions are made to simplify the modeling of this compartment:

1. The material of the heater is assumed to be homogenous with constant characteristics such as the specific heat, C_P, cross-sectional area of the coil and the gaps between the coils [18].
2. The distribution of the temperature is uniform [18].
3. The specific heat of the mixed heated air, C_{Pm}, is the same as for normal air [18].

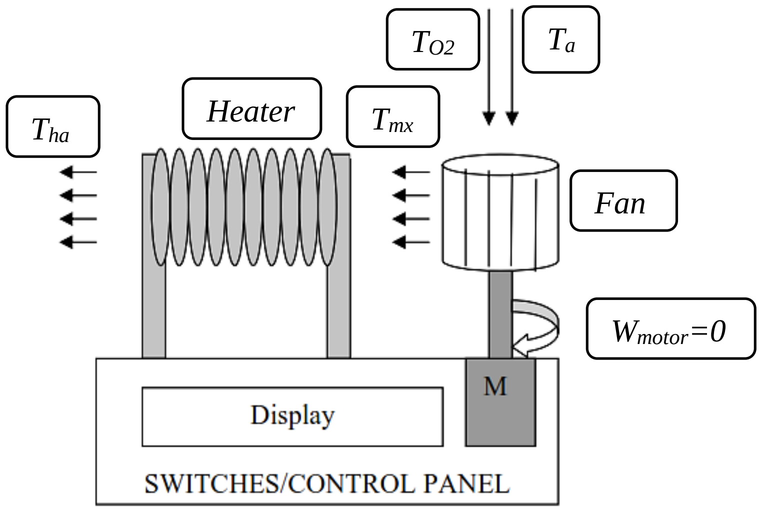

***Figure 4.11**: Schematic diagram for heater/fan compartment [18]*

The oxygen flow rate to the incubator depends on the required concentration level of O_2 (i.e. O_2 %) and is given by the manufacturer [18], which is listed in Table 4.1:

***Table 4.1**: Oxygen flow rates and concentrations [18]*

Oxygen flow rate (l/min)	2	3	4
Concentration %	28-31	32-36	37-40

This concentration level is reached within 20-30 min. The above scheme for oxygen concentration illustrates that the air space inside the incubator comprises of at least 28% oxygen and 72% nitrogen. Therefore, this air can consider as an ambient air which normally has concentrations of 21% oxygen and 79% nitrogen [18].

Neglecting the work done by the fan motor (*i.e.* $W_{motor}=0$) and considering the process to be adiabatic, the heat balance equation for the fan can be written as [18]:

$$\dot{m}_a C_{p_a} T_a + \dot{m}_{O_2} C_{p_{O2}} T_{O_2} = \dot{m}_{mx} C_{p_{mx}} T_{mx} \tag{4.52}$$

This is illustrated in Figure 4.11.

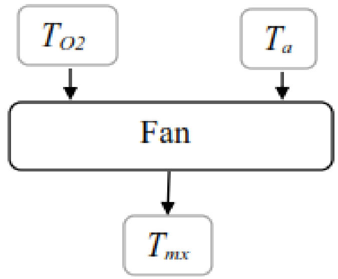

Figure 4.12*: Block diagram for heat exchange across the fan*

Using equation (4.52), the mixed air temperature is given by:

$$T_{mx} = \frac{\dot{m}_a C_{p_a} T_a + \dot{m}_{O_2} C_{p_{O2}} T_{O_2}}{\dot{m}_{mx} C_{P_{mx}}} \tag{4.53}$$

The mass flow rate of the mixed air, $\dot{m}_{mx}$, is the summation of the returned air plus the mass flow rate of the added oxygen. In terms of the volumetric air and oxygen flow rates, equation (4.53) can be re-written as [18]:

$$T_{mx} = \frac{q_{air}\rho_a C_{p_a} T_a + q_{O_2}\rho_{O_2} C_{p_{O2}} T_{O_2}}{\left(q_{air}\rho_a + q_{O_2}\rho_{O_2}\right) C_{P_{mx}}} \tag{4.54}$$

Since the variation range of the incubator air temperature is between 25 - 40°C, the specific heat of the mixed air, C_{Pmx}, is assumed the same as C_{Pa} , and thus C_{Pa} = 1007 J/kg.°C [18][37].

The mass flow rate of the mixed air, $\dot{m}_{mx}$, depends on the final density of the air inside the incubator, which depends on the concentration of the oxygen added to the incubator air as well as the variation of the returned air temperature T_a [18][35].

The incubator air is assumed to be a perfect gas, and the mixed mass, $\dot{m}_{mx}$, can be determined [18] and the final density of the incubator air is estimated on the basis of the final concentration of the both nitrogen and oxygen gases. Since the incubator air is assumed to comprise of 21% oxygen and 79% nitrogen, the final concentration of the both gases is easily determined [18].

For nitrogen:

$$Y_{N_2\%} = 0.79 - O_2\% \tag{4.55}$$

And for oxygen:

$$Y_{O_2\%} = 0.21 + O_2\% \tag{4.56}$$

The density of each of oxygen and nitrogen is calculated on a per mole basis and using the perfect gas law [18][37]:

$$P_t V_{inc} = N_t R_u T_a \tag{4.57}$$

where N_t is the total number of the moles, R_u is the molar gas constant (8.31447 kJ/kmol.K), V_{inc} is the volume of the incubator air space and P_t is the atmospheric pressure.

Since the air is assumed to be an ideal gas, equation (4.57) can be written in terms of the percentage of the concentration of each gas $Y_{gas\%}$ [18]:

$$\frac{P_{gas}}{P_t} = \frac{N_{gas} R_u T_a / V_{inc}}{N_t R_u T_a / V_{inc}} = \frac{N_{gas}}{N_t} = Y_{gas\%} \tag{4.58}$$

Therefore, the molar concentration, C, for each gas (in kmol per unit volume) can be determined using [18][37]:

$$C = \frac{N_{gas}}{V_{inc}} \tag{4.59}$$

Finally, the density of each gas in terms of molar weight M and concentration C can be written as [18]:

$$\rho = C \times M \tag{4.60}$$

The molar weights for oxygen and nitrogen are 32 and 28 kg/kmol respectively.

Equation (4.58) is employed to estimate the mass of the incubator air space, M_a, mentioned earlier in section 4.2.2 as follows:

Using the general form of the ideal gas law for each gas (N_2 and O_2) [18][37].

$$P_{gas} V_{inc} = M_a R_{gas} T_a \tag{4.61}$$

Where R_{gas} is the gas constant which equals to 0.2968 kJ/kg.K and 0.2598 kJ/kg.K for N_2 and O_2 respectively and T_a is the temperature in Kelvin. P_{gas} can be defined from equation (4.58) as:

$$P_{gas} = Y_{gas\%} \times P_t \tag{4.62}$$

Thus, $Y_{gas\%}$ for N_2 and O_2 can be determined using equations (4.55) and (4.56) respectively, then, the mass of the incubator air, M_a, can be determined using [18][37]:

$$M_a = \left[\left(\frac{Y_{N_2\%}P_t}{R_{N_2}}\right) + \left(\frac{Y_{O_2\%}P_t}{R_{O_2}}\right)\right] \times \frac{V_{inv}}{T_a} \tag{4.63}$$

For the heater modelling, assuming adiabatic processes (i.e. no heat losses) and that all of the heat generated is absorbed by the air, then the heat balance equation for the heater can be derived as follows [18]:

$$\dot{m}_a C_{P_a} T_{mx} + Q_{heater} = \dot{m}_a C_{P_a} T_{ha} \tag{4.64}$$

This is illustrated in figure 4.13

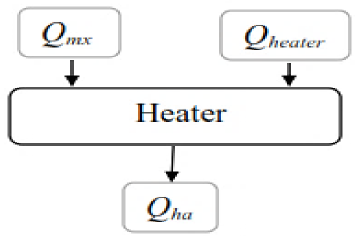

Figure 4.13*: Block diagram for heat exchange across the heater*

Using equation (4.64), the heated air temperature can be written as:

$$T_{ha} = T_{mx} + \frac{Q_{heater}}{\dot{m}_a C_{P_a}} \tag{4.65}$$

Where $\dot{m}_a$ is mass flow rate of the incubator air, kg/sec.

4.2.4 Humidification system modeling

The humidification system is the last compartment in the infant-incubator system, where system water vapor is added to the air from the humidifier. The system comprises of a plastic container and a finned-aluminum block that is placed inside the container as shown in figure 4.14 and figure 4.15. The water level is specified by the manufacturer [18].

Heated air enters the water chamber via an opening in the lid of the chamber, which is also placed at the end of the duct of the heated air. The moist air leaves the water chamber from an opening at the far side of the chamber and past the aluminum block. Both openings are 80×50 mm wide [18]. Therefore, the volumetric air flow rate, Q_{ah}, undergoing heat exchange with the water surface is a function of both air velocity and the size of the openings (in and out) on the lid, can be determined as follows [18]:

$$Q_{ah} = A_{op} \times V_a \tag{4.66}$$

where V_a is equal to 0.1 m/sec [18] and A_{op} is equal to 0.004 m^2. Thus, the volumetric air flow rate from equation (4.66) is calculated to be 0.0004 m^3/sec.

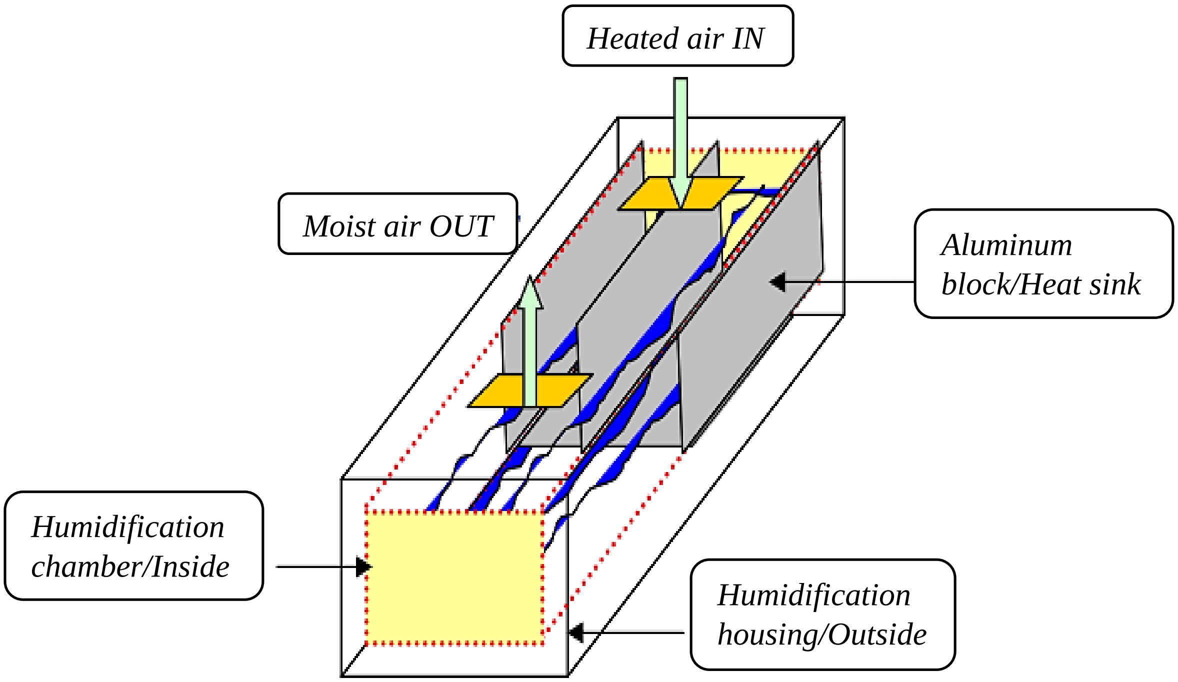

Figure 4.14: *Schematic diagram for humidification system [18]*

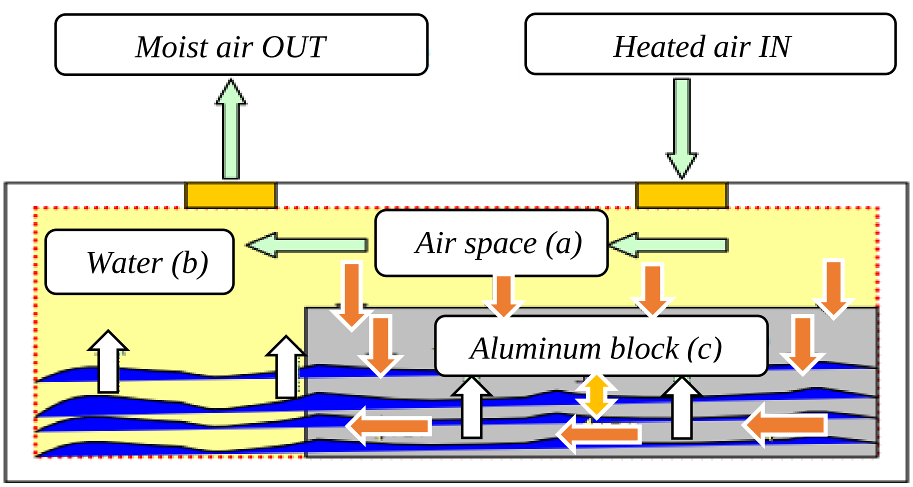

Figure 4.15: *Water chamber heat exchange cross-sectional view [18]*

The purpose of the finned-aluminum block is to store heat and exchange it with the water and air. The finned-aluminum block is half-immersed in water, and the exposed parts of it exchange heat with the heated air by convection. There is also heat transfer within the aluminum block by conduction between the exposed and the immersed parts. This heat exchange occurs rapidly between the submerged parts and vice versa with a high efficiency, estimated around 99.5% [18]. Therefore, it is reasonable to assume that the temperature gradient between the exposed parts of the aluminum block and the submerged parts is zero (i.e. $T_{al1}=T_{al2}=T_{al}$) [18], and the finned-aluminum block acts as a heat sink. As a result, the heat energy of the heated air is accumulated in the aluminum block and within the mass of the water accordingly. For this reason, the water in the container will constantly be warmed as the heated air continues entering the water chamber, and this will cause a mass flow of water vapor to the air in form of latent heat via evaporation.

Several assumptions are made in order to simplify the modelling of this system:

1. Uniform temperature distribution all over the control system [18].
2. Water, air and aluminum blocks have a constant thermal characteristics [18].
3. Conduction between the exposed and immersed parts of the finned-aluminum block is negligible. This is due to the high efficiency of the heat transfer between these parts, estimated around 99.5% [18][37].
4. Heat losses by convection or conduction from the water container to the humidification housing and to the environment are considered to be negligible [18].
5. Since the base of the aluminum block is fully contacted with the plastic water container, the heat flow along the bottom surface of the base is negligible [18].
6. The entire heat exchange process is about heat and mass transfer under forced convection for the parts exposed to the heated air and natural convection for the immersed parts [18].
7. The water chamber comprises of 3 parts: air space, water and aluminum block, and heat exchange between these three parts are correlated [18].

From figure 4.15, the air space gains heat from the heated air that enters the chamber. Since there is a temperature difference between the heated air and the wetted surface, some of the heat energy of this heated air will be dissipated in the form of sensible heat into the water surface and the exposed part of the aluminum block via convection. Due to the temperature difference, there will also be a difference in the saturation pressure and the partial pressure of water vapor. Thus, some mass of water will evaporate from the water surface and the vaporization energy needed for this process is in form of latent heat [18]. The moist air that leaves the water chamber at T_{wet} will directly enter to the hood without any further heating processes.

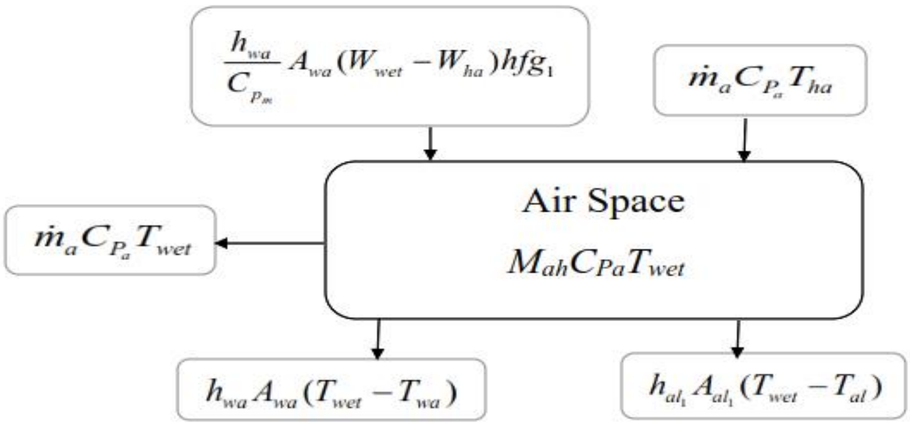

Figure 4.16*: Block diagram for heat exchange across the air space (above the water surface)*

Thus, in a period of dt, the heat balance equation for the air space inside the water chamber can be written as:

$$\left[\dot{m}_a C_{P_a} T_{ha}\right]dt + \left[\frac{h_{wa}}{C_{P_m}} A_{wa}(W_{wet} - W_{ha})hfg_1\right]dt - \left[h_{wa} A_{wa}(T_{wet} - T_{wa})\right]dt - \left[h_{al_1} A_{al_1}(T_{wet} - T_{al})\right]dt - \left[\dot{m}_a C_{P_a} T_{wet}\right]dt = M_{ah} C_{P_a} dT_{wet} \tag{4.67}$$

Therefore, the instantaneous temperature of the air inside the water chamber can be determined by:

$$\frac{dT_{wet}}{dt} = \frac{\left[\dot{m}_a C_{P_a} T_{ha}\right] + \left[\frac{h_{wa}}{C_{P_m}} A_{wa}(W_{wet} - W_{ha})hfg_1\right] - \left[h_{wa} A_{wa}(T_{wet} - T_{wa})\right] - \left[h_{al_1} A_{al_1}(T_{wet} - T_{al})\right] - \left[\dot{m}_a C_{P_a} T_{wet}\right]}{M_{ah} C_{P_a}} \tag{4.68}$$

where W_{wet} and W_{ha} are the humidity ratios of the wetted surface and heated air respectively, and can be determined from equations (4.6), (4.7) and (4.8).

$\dot{m}_a$ can be estimated using [18]:

$$\dot{m}_a = A_{in/out} V_a \rho_{ha} \tag{4.69}$$

where $A_{in/out}$ is the opening area where the heated air enters and leaves the water chamber and is estimated to be around 0.004 m^2 [18], V_a is the incubator air velocity which equals to 0.1 m/sec [18] and ρ_{ha}, density of the heated air is determined using the same technique described in equations (4.55) to (4.60).

Experimentally, in an empty incubator, the heated air T_{ha} enters to the water chamber is around 53.5°C and leaves T_{wet} around 46.5°C, while the water temperature T_{wa} is approximately 30°C [18]. The heated and wetted air properties could also be evaluated at the film temperature (which gives an average temperature of 50°C and 40°C respectively for the heated air in and out the water chamber). However, equation (4.9) is again employed to determine the precise air properties inside the water chamber as the temperature of the heated air varies over time.

The area of the water surface A_{wa} is determined using the equation [18]:

$$A_{wa} = L_{con} W_{con} - N_f \left(th_f \times l_f \right) \tag{4.70}$$

while the area of the exposed parts of the aluminum block, A_{al_1}, is calculated as [18]:

$$A_{al_1} = 2 N_f l_f w_l \tag{4.71}$$

The mass of the air in the water chamber M_{ah} can be estimated using:

$$M_{ah} = \rho_{wet} w_l L_{con} W_{con} \tag{4.72}$$

and the specific heat of the moist air C_{Pm} is determined by [18]:

$$C_{P_m} = C_P + W_{wet} C_{ps} \tag{4.73}$$

Since the flow regime of the air, inside the water chamber is laminar (due to a Reynolds number of around 1112.6 for the aluminum and 1863.6 for the water surface), the Nusselt number for the aluminum and water can be determined using equation [18][37]:

$$Nu = 0.664 \, \mathrm{Re}_L^{0.5} \, \mathrm{Pr}^{1/3} \tag{4.74}$$

Therefore, h_{wa} and h_{al_1} can be determined by the general form of Nusselt equation [18][37]:

$$Nu = \frac{h L_c}{K_a} \tag{4.75}$$

Both the Reynolds and Prandtl numbers in equation (4.74) are defined as [18][37]:

$$\mathrm{Re} = \frac{\rho_a V_a L_c}{\mu_a} \qquad \mathrm{Pr} = \frac{\mu_a C_{P_a}}{K_a} \tag{4.76}$$

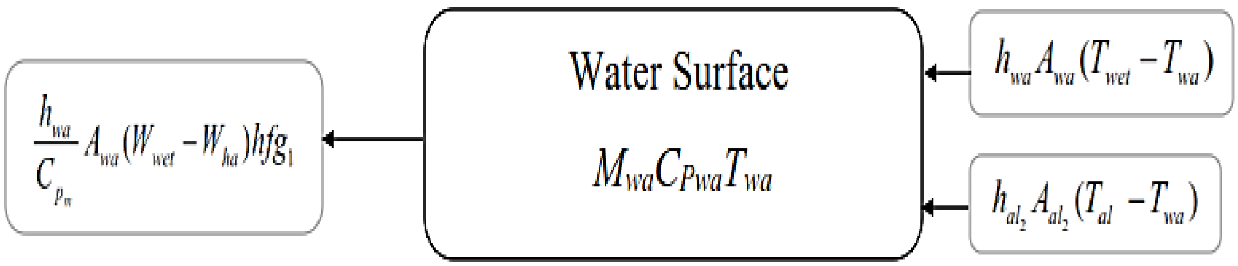

Figure 4.17*: Block diagram for heat exchange across the water surface*

Similarly, in a period of *dt*, the heat balance equation for the mass of the water in the chamber can be written as follows:

$$\left[h_{wa} A_{wa} \left(T_{wet} - T_{wa}\right)\right] dt + \left[h_{al_2} A_{al_2} \left(T_{al} - T_{wa}\right)\right] dt - \left[\frac{h_{wa}}{C_{P_m}} A_{wa} \left(W_{wet} - W_{ha}\right) hfg_1\right] dt = M_{wa} C_{P_{wa}} dT_{wa} \tag{4.77}$$

$$\frac{dT_{wa}}{dt} = \frac{\left[h_{wa} A_{wa} \left(T_{wet} - T_{wa}\right)\right] + \left[h_{al_2} A_{al_2} \left(T_{al} - T_{wa}\right)\right] - \left[\frac{h_{wa}}{C_{P_m}} A_{wa} \left(W_{wet} - W_{ha}\right) hfg_1\right]}{M_{wa} C_{P_{wa}}} \tag{4.78}$$

where A_{al_2} is determined as follows [18]:

$$A_{al_2} = 2 N_f l_f w_{lw} + n_g W_g l_f \tag{4.79}$$

Since no agitator or stirrer is used in the water chamber, the mechanism of heat transfer that occurs between the submerged parts of the aluminum block and the water is natural convection. Therefore, the temperature difference between the water and the aluminum is the buoyancy force that drives the convective heat exchange. The convection heat transfer coefficient h_{al_2} depends on the geometry of the submerged parts of the aluminum block and can be determined using equation [18][37]:

$$h_{al_2} = \frac{Nu \times k_{wa}}{S} \tag{4.80}$$

where k_{wa} the thermal conductivity of water and S is the spacing between adjacent fins (21.63 mm) [18]. The Nusselt number, Nu, is a function of Raleigh number, R_a, and can be expressed as follows [18][37]:

$$Nu = \left[\frac{576}{\left(Ra_S S/L\right)^2} + \frac{2.873}{\left(Ra_S S/L\right)^{0.5}} \right]^{-0.5} \tag{4.81}$$

and Ra_s is determined by [18][37];

$$Ra_S = \frac{g\beta\left(T_s - T_\infty\right)S^3}{v^2}\Pr \tag{4.82}$$

The propertie of the water is evaluated at a film temperature T_f equal to 40 °C and L the height of the fin (200 mm). This yields h_{al_2} equal to 433.80 W/m^2*°C [18].

Likewise, the two partitions of the aluminum block are convectively heated by both the air space and water. The conduction between the exposed and immersed parts is considered to be negligible [18][37].

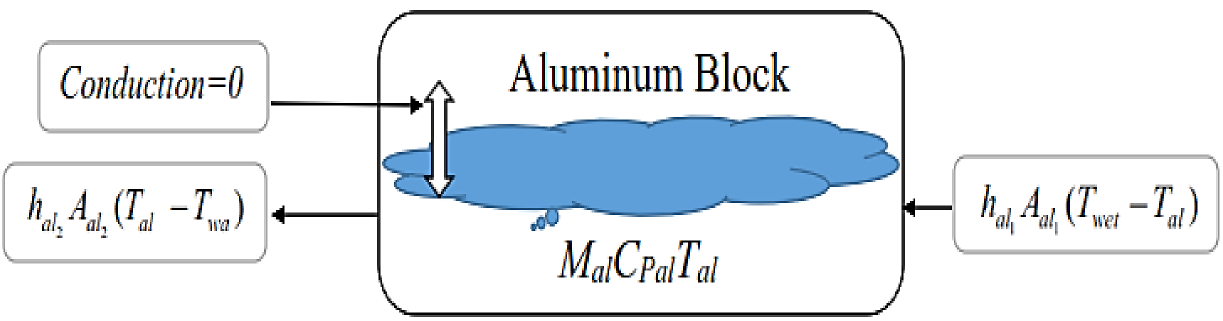

Figure 4.18*: Block diagram for heat exchange across the finned-aluminum block*

From figure 4.18, the heat balance equation for the aluminum block can be written as:

$$\left[h_{al_1} A_{al_1} (T_{wet} - T_{al})\right]dt - \left[h_{al_2} A_{al_2} (T_{al} - T_{wa})\right]dt = M_{al} C_{P_{al}} dT_{al} \tag{4.83}$$

The instantaneous temperature of the aluminum block can be determined using:

$$\frac{dT_{al}}{dt} = \frac{\left[h_{al_1} A_{al_1} (T_{wet} - T_{al})\right] - \left[h_{al_2} A_{al_2} (T_{al} - T_{wa})\right]}{M_{al} C_{P_{al}}} \tag{4.84}$$

where A_{al_1}, h_{al_1}, A_{al_2} and h_{al_2} can be determined by equations (4.71), (4.75), (4.79) and (4.80) respectively.

The amount of the heated air as well as the moist air that enter the hood is adjusted by a mechanical lever (manually), which slides over the two side openings (i.e. one for the moistened air and the other for the heated air) at the end of the heated air duct, which is shown in figure 4.19. The setup position of the slider lever is based upon the required level of humidity inside the hood, and is graded from 20-99% in steps of 10% [18].

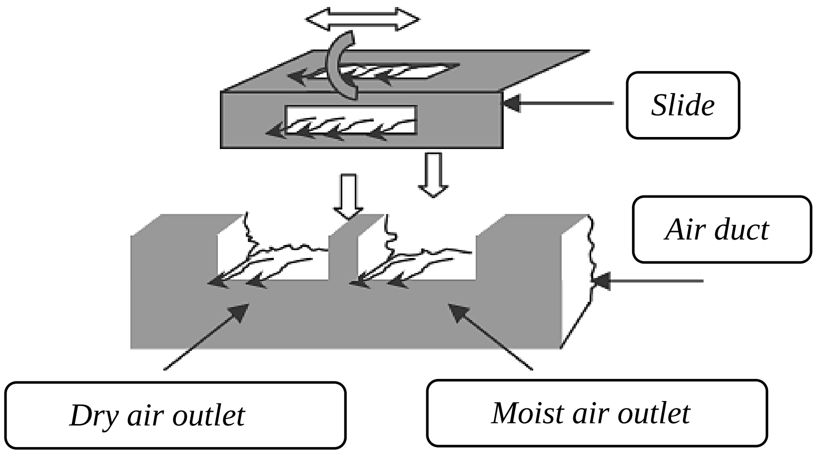

Figure 4.19*: Slider/Air outlets assembly [18]*

The amount of wetted and heated air is proportional to the area of the openings they flow through, which is accordingly a function of the relative humidity *RH %*. This is experimentally evaluated against each level of *RH%* and the best fit equations for the areas of the moist air outlet and the dry air outlet [18], are shown in Figure 4.20.

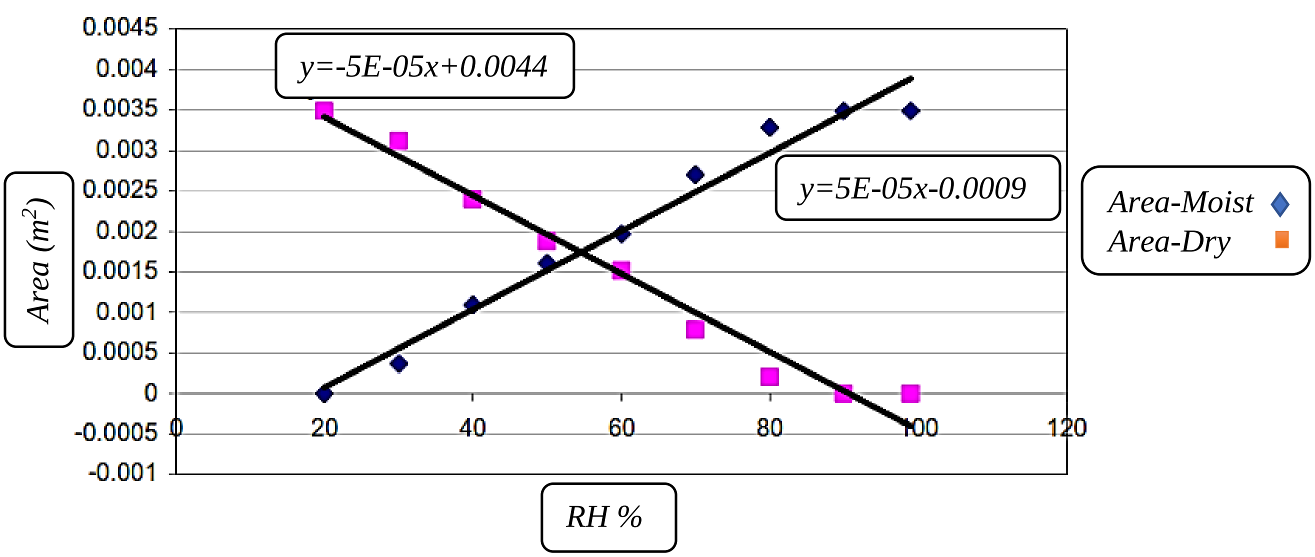

Figure 4.20*: Area Vs Relative Humidity Approximate plot [18]*

From figure 4.20 the area of the moist air can be written as:

$$A_{wet} = 5\times10^{-5}\left(RH\%\right) - 0.0009 \tag{4.85}$$

and for the dry air:

$$A_{dry} = 0.0044 - 5\times10^{-5}\left(RH\%\right) \tag{4.86}$$

Thus, the supplied air temperature to the hood can be evaluated using the following equation [18]:

$$\dot{m}_{wet}C_{P_a}T_{wet} + \dot{m}_{dry}C_{P_a}T_{ha} = \left(\dot{m}_{wet} + \dot{m}_{dry}\right)C_{P_a}T_{sply} \tag{4.87}$$

Since the heat capacity C_{Pa} is same for wetted air and heated air (1007 J/kg*°C), equation (4.87) can be re-written as:

$$T_{sply} = \frac{\dot{m}_{wet}T_{wet} + \dot{m}_{dry}T_{ha}}{\left(\dot{m}_{wet} + \dot{m}_{dry}\right)} \tag{4.88}$$

where $\dot{m}_{wet}$ and $\dot{m}_{dry}$ estimated as follows [18]:

$$\dot{m}_{wet} = \rho_{wet}A_{wet}V_a \tag{4.89}$$

$$\dot{m}_{dry} = \rho_{ha}A_{dry}V_a \tag{4.90}$$

The variables ρ_{wet} and ρ_{ha} are evaluated at T_{wet} and T_{ha} respectively. The convective heat energy supplied to the hood Q_{ht} (i.e. incubator's air space) can be determined by the equation [18]:

$$Q_{ht} = \dot{m}_a C_{P_a}\left(T_{sply} - T_a\right) \tag{4.91}$$

Equation (4.91) is associated with section 4.2.2. As a result, equations (4.1)-(4.91) describe a comprehensive detailed model of the infant-incubator system, with the infant described as a one lump with 2 layers.

4.2.5 Development of Simulink model

A computer simulation for the various compartment of the infant-incubator system, which was mathematically modelled in the previous sections will be developed. As shown in the figure 4.21, the system model is being developed in MATLAB®/Simulink environment for each compartments of the system. Individual Simulink models are then interlocked via internal loops (called iterations) in one block, which is the Plant. In other words, the output of one compartment is the input to another compartment. The subsystem in figure 4.22 has only two inputs: the heater power, Q_{heater} (Watts), which varies upon the variation in the feedback signals (i.e. both controlled temperatures, skin and air mode) and incubator air relative humidity, *RH%*, which is considered to be a constant parameter during simulation. The outputs are all final temperatures of the system compartments. All the parameters and initial conditions related to the system model are already being identified in a separate *m-file* given in appendix (B).

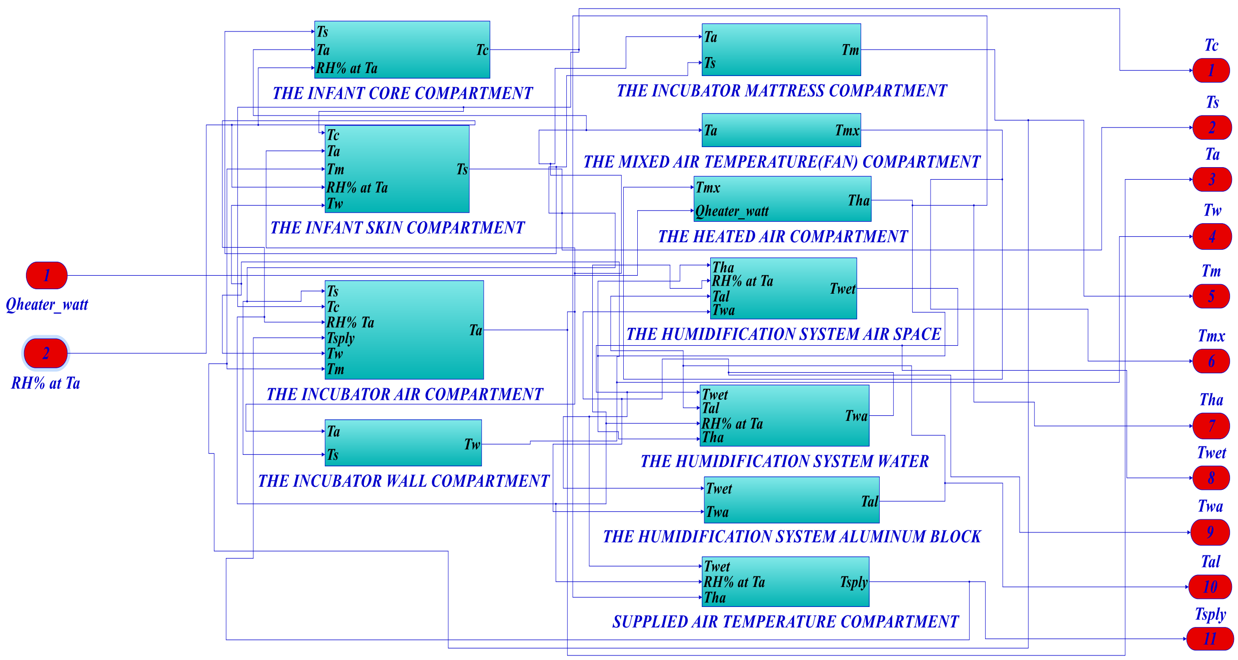

***Figure 4.21**: Combined system compartments*

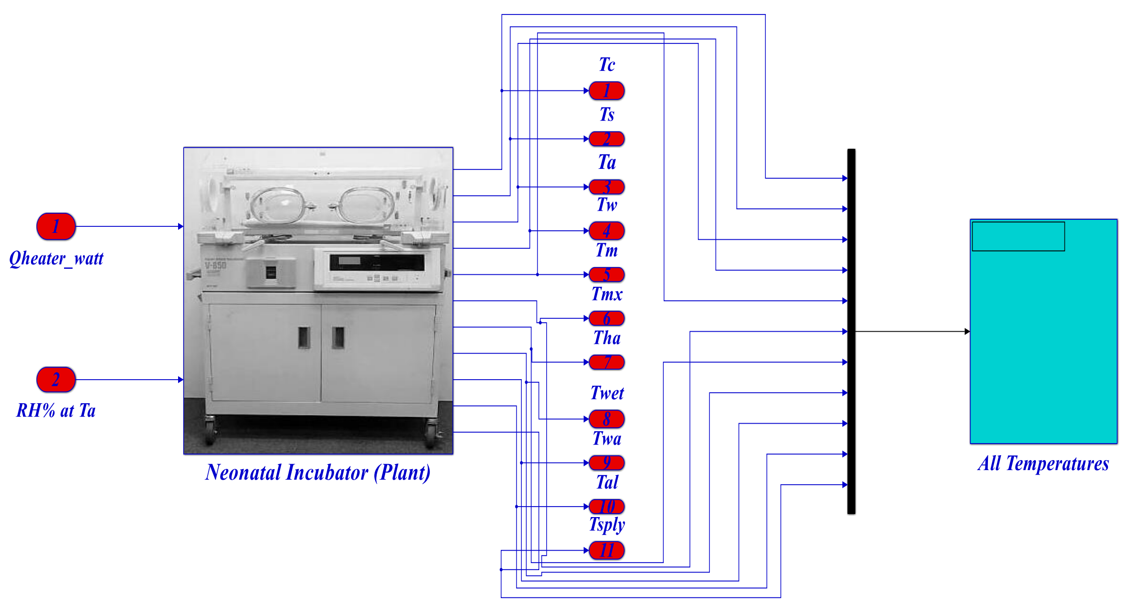

***Figure 4.22**: Open loop sub-system*

System stability

The system model stability is verified using the Matlab function called Single Input–Single Output Tool (*Sisotool*). An open-loop Simulink model is developed for each mode (skin and air), as shown in figure 4-23 and figure 4.24 respectively. This developed model includes all 11 compartments of the infant-incubator system as mentioned in the previous sections, but the relative humidity is set as a constant 0.5 and with only a single input and single output.

Figure 4.23: *Simulink model-Skin mode*

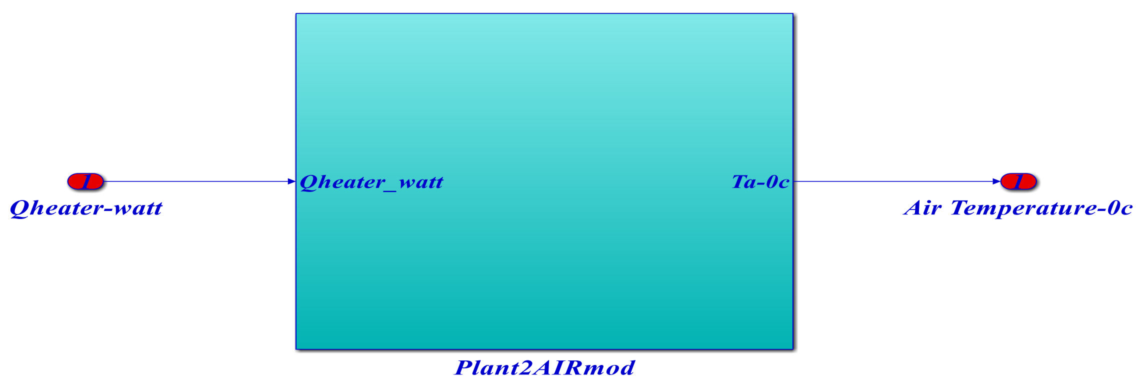

Figure 4.24: *Simulink model-Air mode*

Code was written (Appendix (C)) for each mode (skin and air) in order to linearize the Simulink model and convert into a state-space model. The open-loop Simulink model for each mode is compiled within the *Sisotool* and the results displayed in the SISO window. The displayed results are analyzed using a root locus editor and open-loop bode editor as shown in figures 4.25 and 4.26 for the skin and air modes respectively.

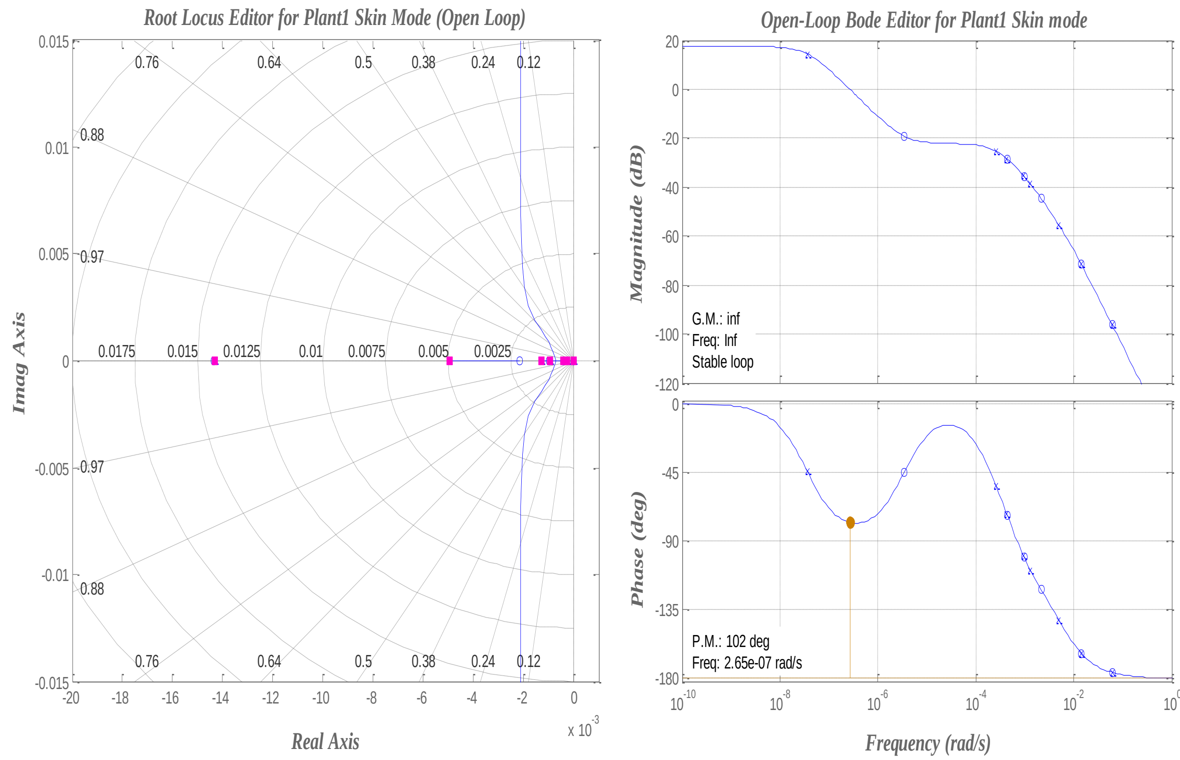

***Figure 4.25**: SISO window-Skin mode/open loop*

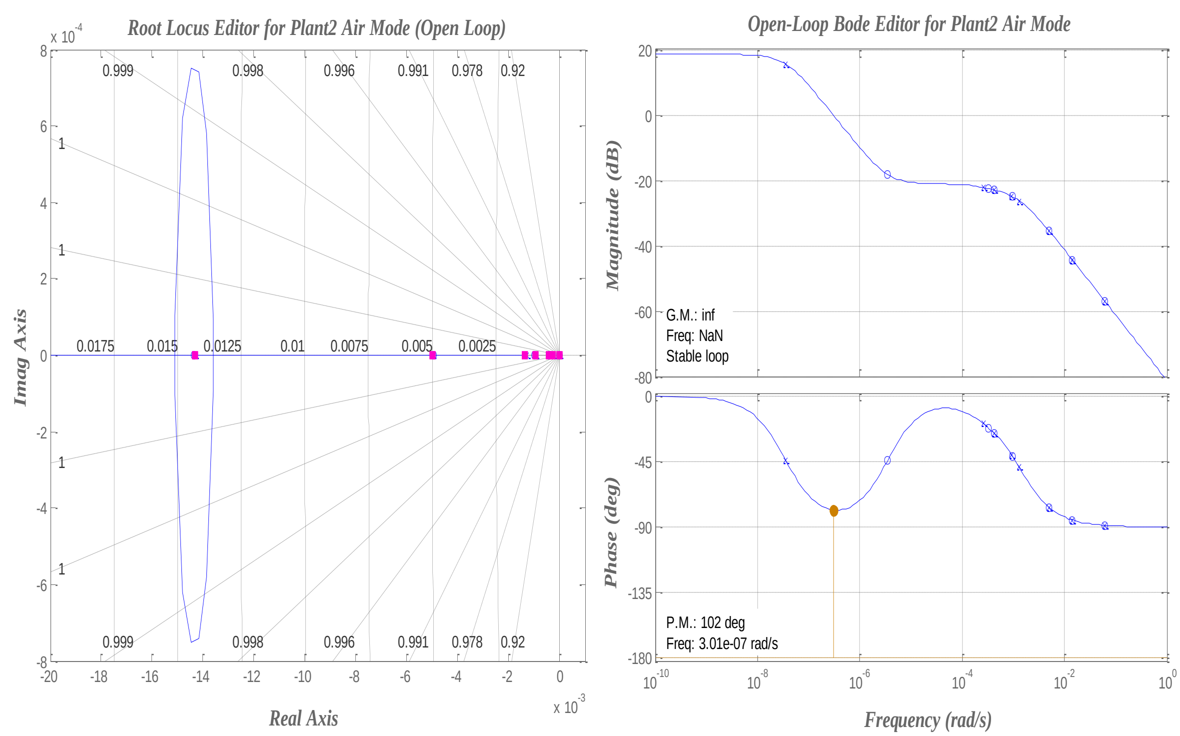

***Figure 4.26**: SISO window-Air mode/open loop*

Using the available features in the Sisotool, the transfer function of the open-loop model for skin mode can be generated based on the state-space parameters. The skin mode have proven to be continuous-time model and the transfer function is given as in Gain/Zero/Pole format.

5.6556e-08(s+0.0611)(s+0.014355)(s+0.002156)(s+0.0009846)(s+3.4317e-06)(s+0.0004346)

(s+0.0611)(s+0.0143)(s+0.00497)(s+0.001299)(s+0.0009385)(s+0.0004286)(s+0.000259151)(s+3.5778e-08)

Similarly, the transfer function corresponding to the air mode is given as:

8.69e-05(s+0.0611)(s+0.014355)(s+3.432e-06)(s+0.495157)(s+0.0009721)(s+0.0004310176)(s+0.000326788)

(s+0.0611)(s+0.01431)(s+0.004968)(s+0.00129925)(s+0.0009385)(s+3.57778e-08)(s+0.00026)(s+0.0004287)

The open-loop system stability for both skin and air modes are verified. At this stage, either the compensator or reference input can be considered.

4.3 Design of ANFIS based neonatal incubator controller

This section mainly describes the design of the proposed ANFIS controller for infant-incubator system. Figure 4.27 exhibits the block diagram of complete infant-incubator system integrated with ANFIS Controller.

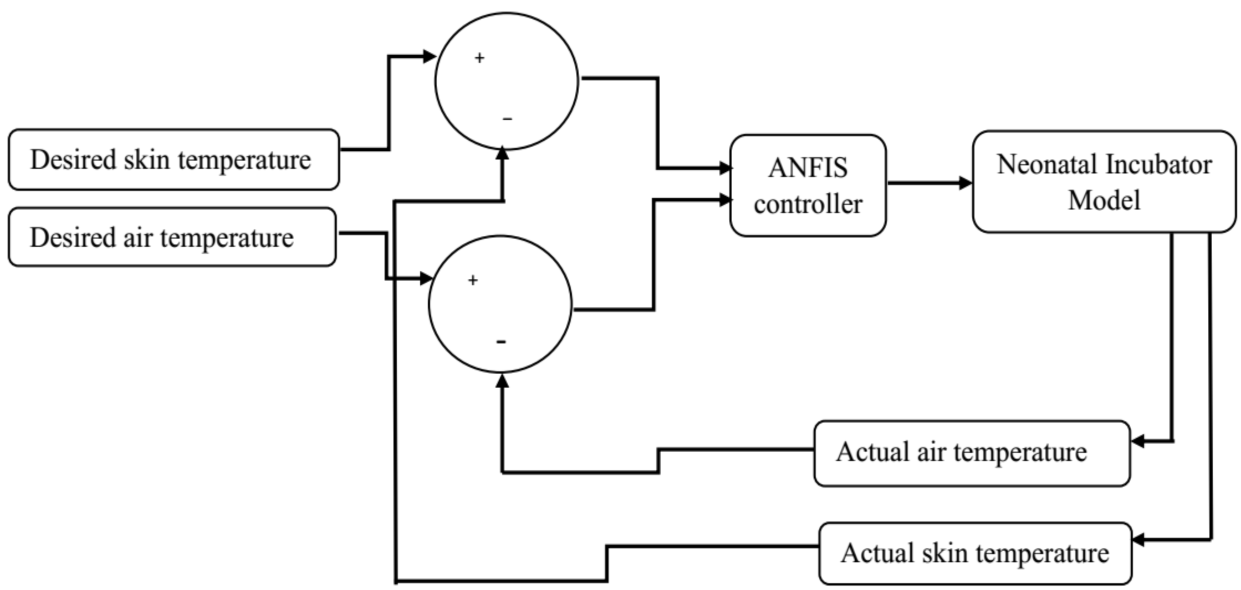

***Figure 4.27**: Block diagram of infant-incubator control system*

Desired incubator air and infant skin temperatures

The incubator air and infant skin temperature settings should be individually assessed for each infant according to weight, gestational age and the temperature recordings during the admission process. These desired values corresponding to weight and gestational age are given in table 4.2.

Table 4.2*: Suggested incubator air and abdominal infant skin temperatures [Princess Margaret Hospitals and Rutter, 2008]*

Incubator air Temperature for infants day 1-5				
Age	**1000 - 1200g +/- 0.5⁰C**	**1201 - 1500g +/- 0.5⁰C**	**1501 - 2500g +/- 1.0⁰C**	**>2500g and >36wk**
0 – 12 Hours	35.0	34.0	33.3	32.8
12 - 24 Hours	34.5	33.8	32.8	32.4
24 - 96 Hours	34.5	33.5	32.3	32.0

Incubator air Temperature for infants > 5 days of age			
Age	**<1500g**	**1501 - 2500g**	**>2500g and > 36 wk**
5 - 14 Days	33.5	32.1	32.0
2 - 3 Weeks	33.1	31.7	30.0
3 - 4 Weeks	32.6	31.4	
4 – 5 Weeks	32.0	30.9	
5 - 6 Weeks	31.4	30.4	

Weight (g)	Abdominal skin Temperature (°C)
< 1000g	36.7
1000-1500g	36.6
1500-2000g	36.4
2000-2500g	36.2
>2500g	36.0

- In a single-walled incubator, the environmental temperature needs to be increased by 1°C for every 7°C difference between room and incubator temperature
- VLBW infants (< 1000g) need higher air temperature and a humidified incubator in the first week.

ANFIS Controller

The flow-diagram of ANFIS procedure is shown in figure 4.28. ANFIS distinguish itself from normal fuzzy logic systems by the adaptive parameters, which is both the premise and consequent parameters are adjustable.

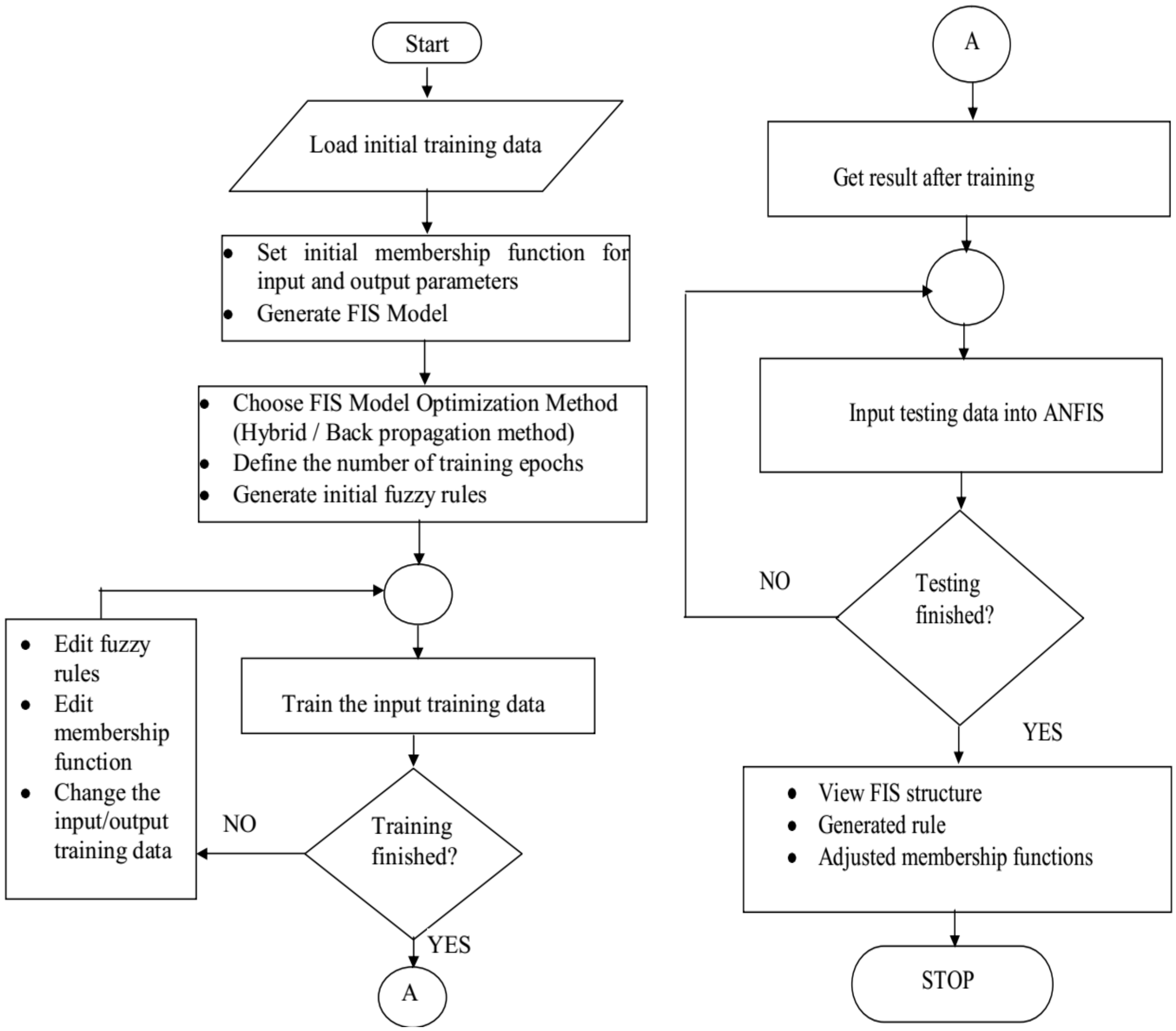

***Figure 4.28**: Flow diagram of computations in ANFIS*

The data sets are generated after simulation of the system model, which can be used to train the ANFIS controller. A total of 239 data sets were collected (208 data sets for training and 31 data sets for checking), also 4 and 5 generalized bell inputs MFs were used for *Error (Ta)* and *Error (Ts)* respectively, as a result a total of 20 rules for training. Though we can apply the gradient method to identify the parameters in an adaptive network, the method is generally slow and likely to become trapped in local minima. In this paper the training is done using Hybrid learning algorithm, which is a combination of Back-propagation and least square method [32].

***Table 4.3**: Two passes in the hybrid learning algorithm for ANFIS [33]*

	Forward Pass	Backward pass
Premise Parameters	Fixed	Gradient Descent
Consequent parameters	Least-squares estimator	Fixed
Signals	Node Outputs	Error Signals

The Grid partition method [34] was further used for building an initial FIS structure. The rules which are obtained from the clustering or the grid partition based method are updated by neural network which uses back propagation learning method with gradient descent algorithm. This updating leads to the optimization of the premise parameters of the fuzzy membership functions to give the final fuzzy model. The values of error tolerance and epochs were set to 0 and 100 respectively. We will discuss this section in detail in the next chapter.

The ANFIS controller generate a change in the heater power (Q_{heater}) of the system based on the inputs, incubator air temperature error (*Error (Ta)*) and infant skin temperature error (*Error (Ts)*), which defined as:

$$Error(Ta) = Ta_{desired} - Ta_{actual} \tag{4.50}$$

$$Error(Ts) = Ts_{desired} - Ts_{actual} \tag{4.51}$$

Where $Ta_{desired}$ and Ta_{actual} are the desired and actual incubator air temperatures respectively. Similarly, $Ts_{desired}$ and Ts_{actual} are the desired and actual infant skin temperatures respectively.

ANFIS controller relates the desired incubator air temperature and actual incubator air temperature (from system model), similarly it relates the desired infant skin temperature and actual infant skin temperature (from system model). The main function of this unit is to keep the actual temperatures close to the desired temperatures. The controller has merely two input signal (the difference between the quantities of desired and actual temperatures) and one output signal (control of the state of the heater).

The system design of this paper which is discussed in the above section integrates an ANFIS controller. The controller has a main advantage of turning the heater power, through considering the optimal and actual temperature differences based on the individual preterm infant conditions. After the system is designed we will simulate our system using MATLAB/Simulink tool box. The designed controller output will be compared with fuzzy logic controller.

In this thesis, the fuzzy system is design based on the input-output data pairs and we are following five steps in order to design the fuzzy logic controller.

Step 1: Define fuzzy sets to cover the input and output spaces, we choose 5 fuzzy sets and 5 fuzzy sets for the corresponding input spaces (*Error (Ta)* and *Error (Ts)* respectively) and 5 fuzzy sets for the corresponding output space (*Qheater*) with generalized bell membership function for all fuzzy sets.

Step 2: Generate one rule from each input-output data pairs, for each input-output data pair we also determine the degree of membership values.

Step 3: Assign a degree to each rule generated in Step 2, Since the number of input-output pairs is usually large and with each pair generating one rule, it is highly likely that there are conflicting rules, that is, rules with the same IF parts but different THEN parts. To resolve this conflict, we assign a degree to each generated rule in Step 2 and keep only one rule from a conflicting group that has the maximum degree. In this way not only the conflict problem resolved, but also the number of rules is greatly reduced.

Step 4: Create the fuzzy rule base, the fuzzy rule base consists of the following three sets of rules.

- The rules generated in Step 2 that do not conflict with any other rules.
- The rule from a conflicting group that has the maximum degree, where a group of conflicting rules consists of rules with the same IF parts but different THEN parts.
- Linguistic rules from human experts (due to conscious knowledge).

Step 5: Construct the fuzzy system based on the fuzzy rule base.

CHAPTER 5

SIMULATION STUDIES AND DISCUSSION

4.1 Introduction

This chapter presents a simulation conducted and results obtained from controlling the infant-incubator system. In chapter three we were discussed the reasons and the techniques fuzzy logic and artificial neural networks integrated together. In addition, in chapter four the infant-incubator system and the controllers were also modeled. In this chapter, an adaptive neuro fuzzy inference controller approach for controlling the incubator environment is simulated and based on the simulation results, comparison is made with Fuzzy logic control system. We used Matlab for the generation and design of the ANFIS controller and fuzzy logic controller, the overall block diagrams used for demonstrating simulation results during comparison between ANFIS controller and FL controller can be designed using Simulink as shown in figure 5.1 and 5.2. The controllers are implemented with the same reference system model but different selected conditions. As discussed in the previous chapter, the inputs to the controller are *Error (Ta)* (the difference between desired and actual incubator air temperatures) and *Error (Ts)* (the difference between desired and actual infant skin temperatures). The errors are then fed to the controller and the output is the variation of *Qheater* (heater power rating).

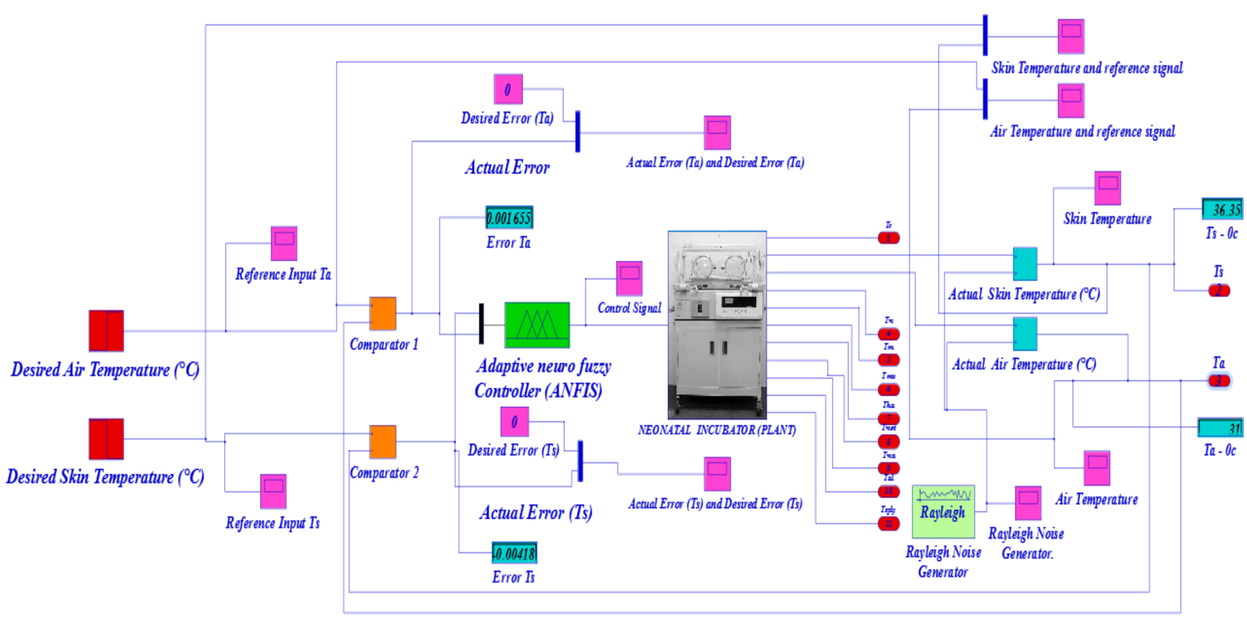

__Figure 5.1__: ANFIS based control system with infant-incubator model

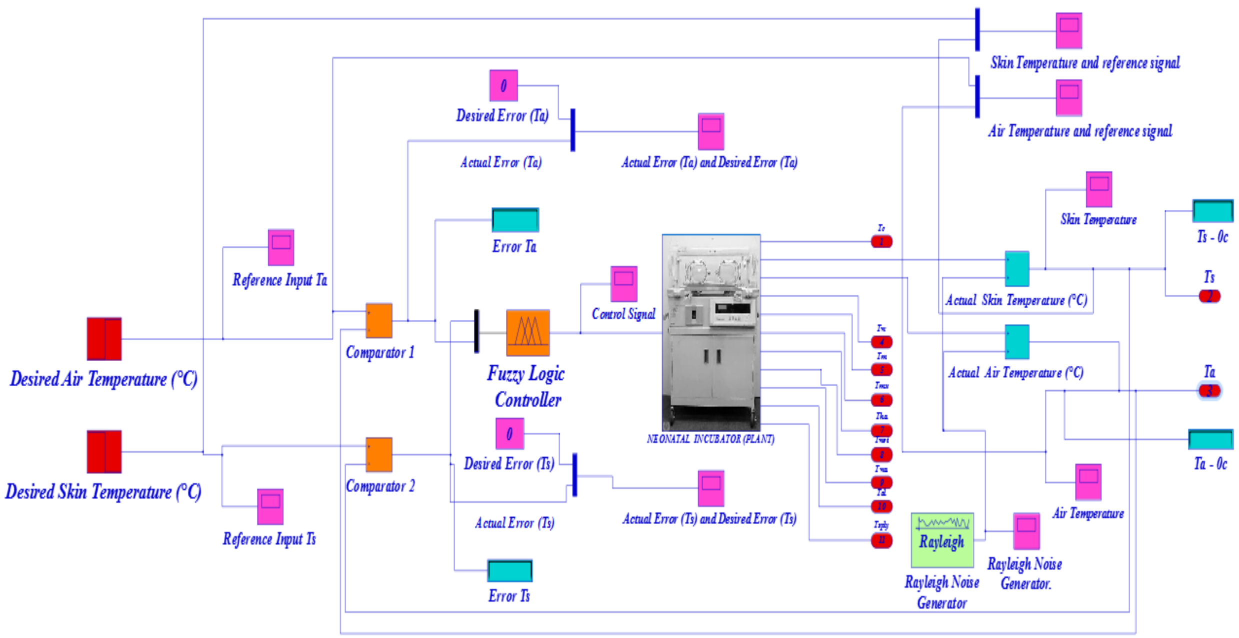

Figure 5.2: Fuzzy logic based control system with infant-incubator model

5.2 Training and checking data sets generation

The training and checking data sets were generated from the modeled infant incubator system and saved as a file. A total of 239 data sets were generated, by setting the desired incubator's air and infant's skin temperatures for the system model and compare the desired temperatures to the actual temperatures, which are the outputs of the modeled system. Then record all the errors, which are related to the difference between the desired and actual temperatures, and the corresponding rated powers of the heater for various conditions (considering different infant masses, postnatal ages and gestational ages) of the infant-incubator system.

From a total of 239 data sets, we assign 208 data sets for training the ANFIS network, in order to enhance the generalization capability of the network, and the remaining 31 data sets, which are unknown input/output patterns for the ANFIS network, were assigned for checking of the trained ANFIS network.

5.3 Training and Checking stages of ANFIS controller

The first thing to do in the training stage of the ANFIS network is export the input-output data sets to the workspace, after that, load the data sets to the anfis editor tool from the workspace as shown in the figure 5.3.

***Figure 5.3**: Loading training data sets from the workspace*

Once the data file is loaded, the network has to be trained by selecting an appropriate initial fuzzy inference system and optimization method. After some training period of time, the neural network can be applied for selection of an optimized rule bases and appropriate determination of the tuned parameters of corresponding inputs and outputs membership functions.

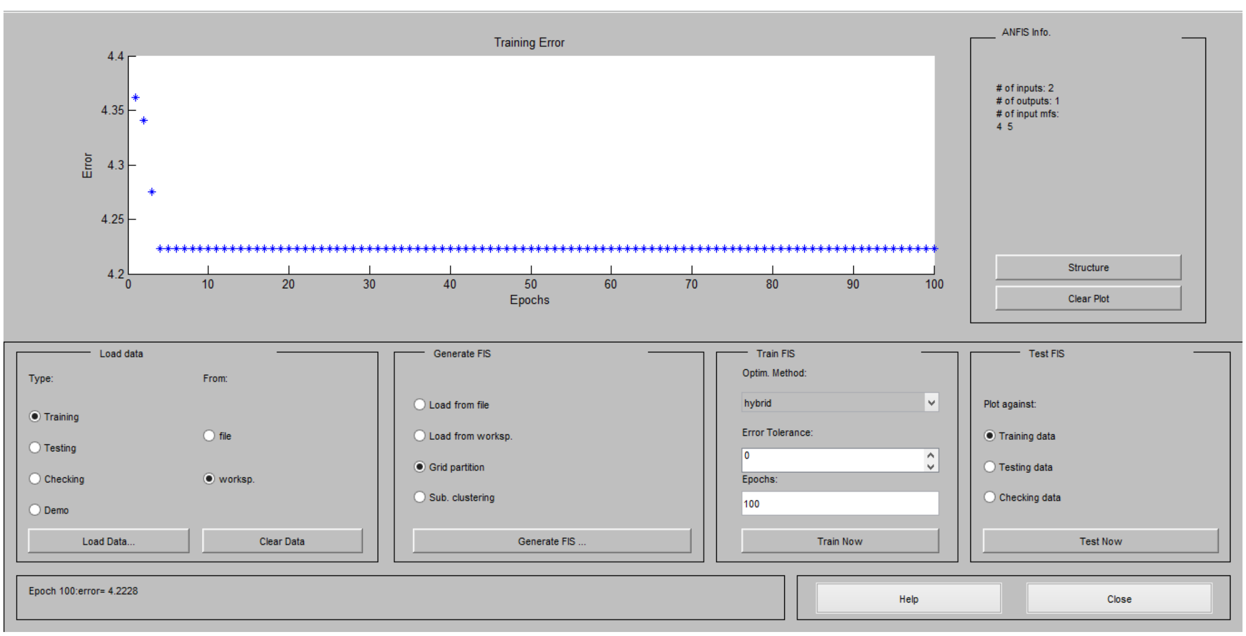

***Figure 5.4**: Training error over 100 epochs*

***Figure 5.5**: Training data Vs ANFIS output*

We proceed to the checking stage of the trained ANFIS network, in this stage the first thing to do is export checking input-output data sets to the workspace, after that, load the data sets to the anfis editor from the workspace in order to validate the trained network as shown in the figure 5.6

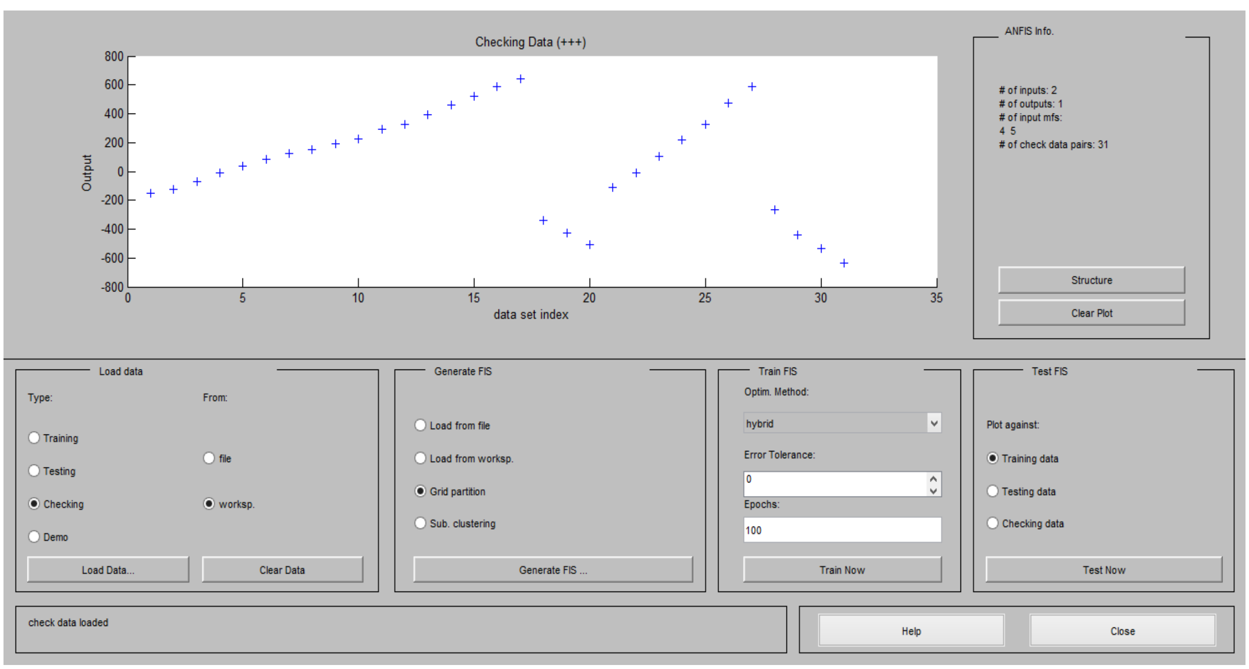

***Figure 5.6**: Loading checking data sets from the workspace*

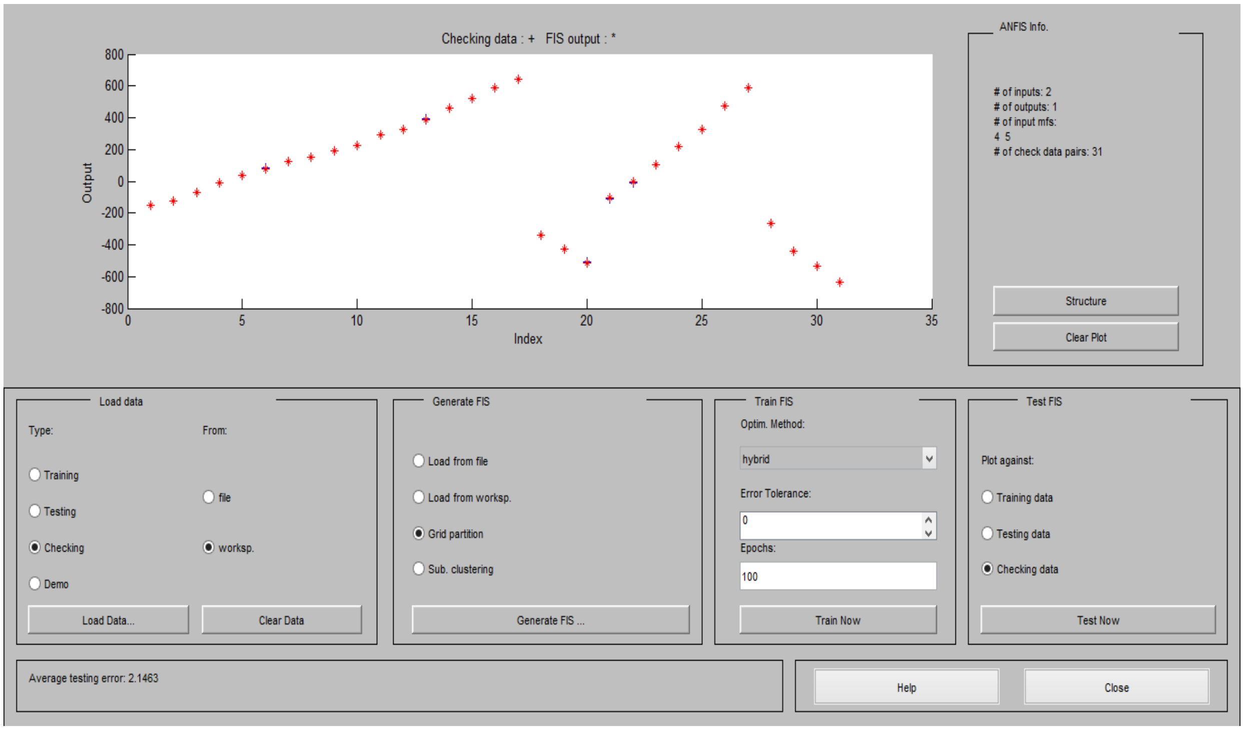

. ***Figure 5.7****: Checking data Vs ANFIS output*

Now the ANFIS network complete its training stage and the network is ready for implementation, the detailed structure of the network shown in the figure 5.8.

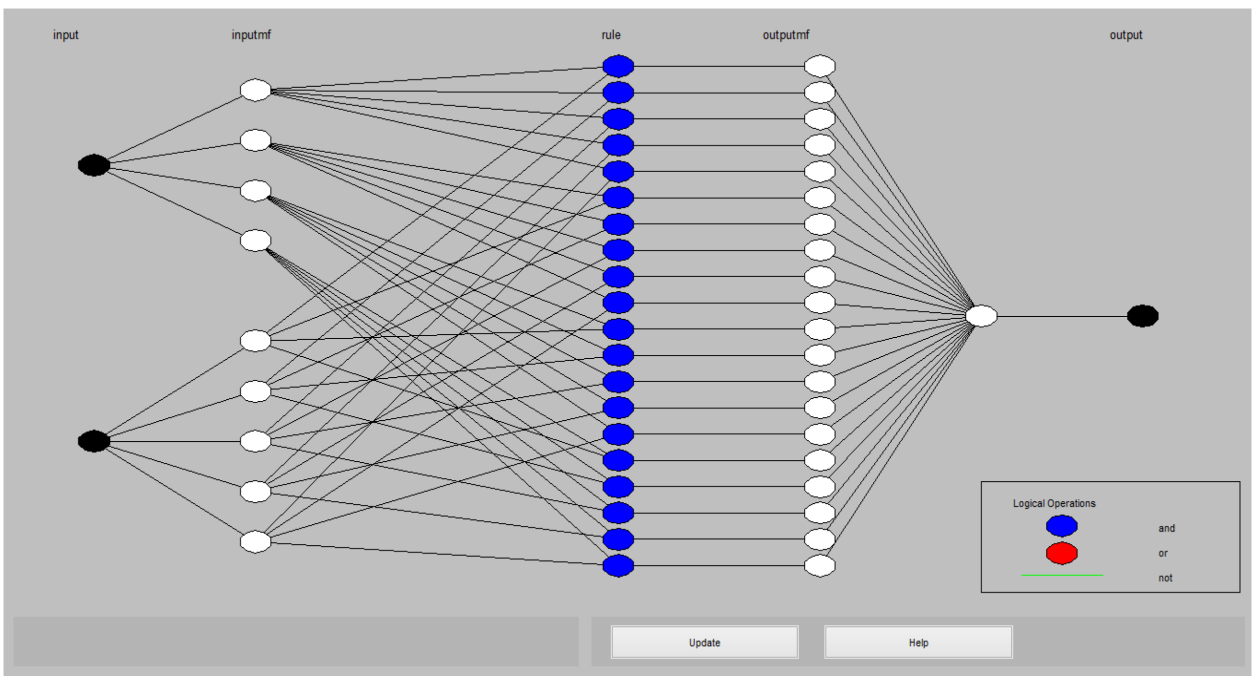

Figure 5.8*: ANFIS Structure*

In addition the corresponding inputs membership functions, output membership functions, surface viewer and rule viewer of the ANFIS network shown in the figure 5.9, 5.10 and 5.11 respectively.

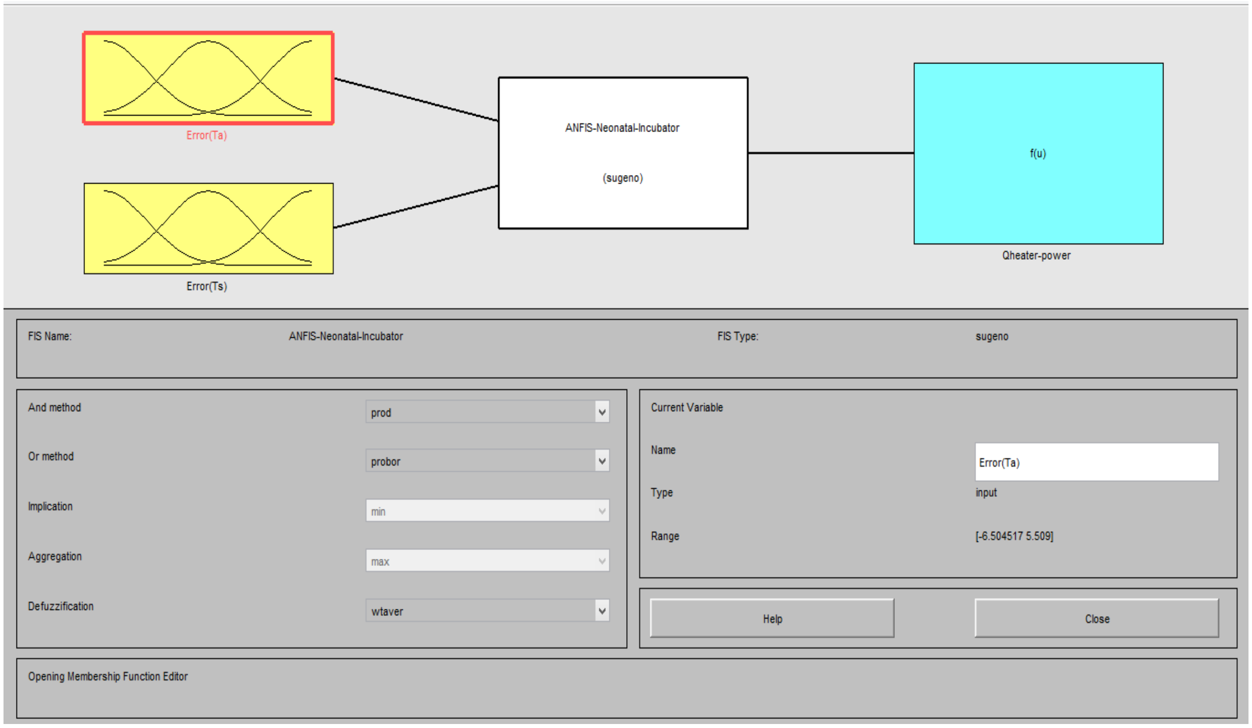

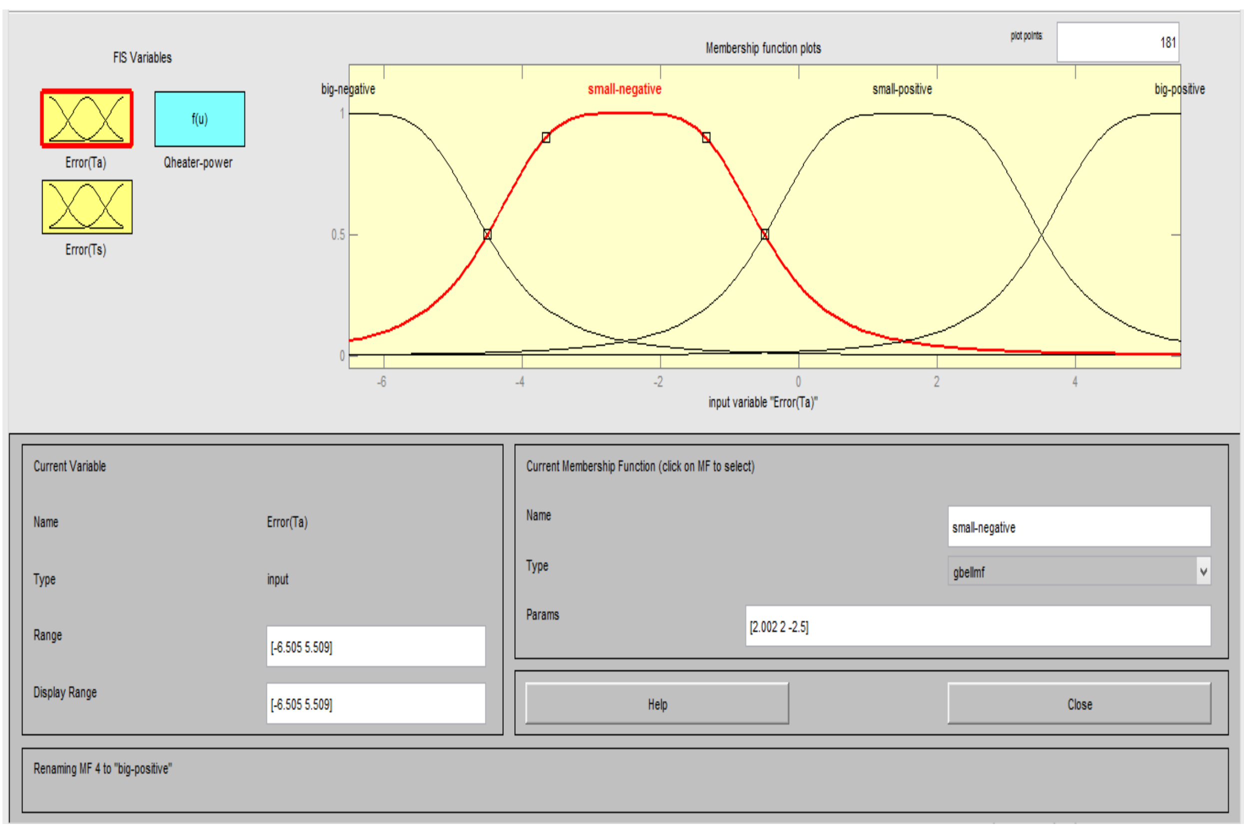

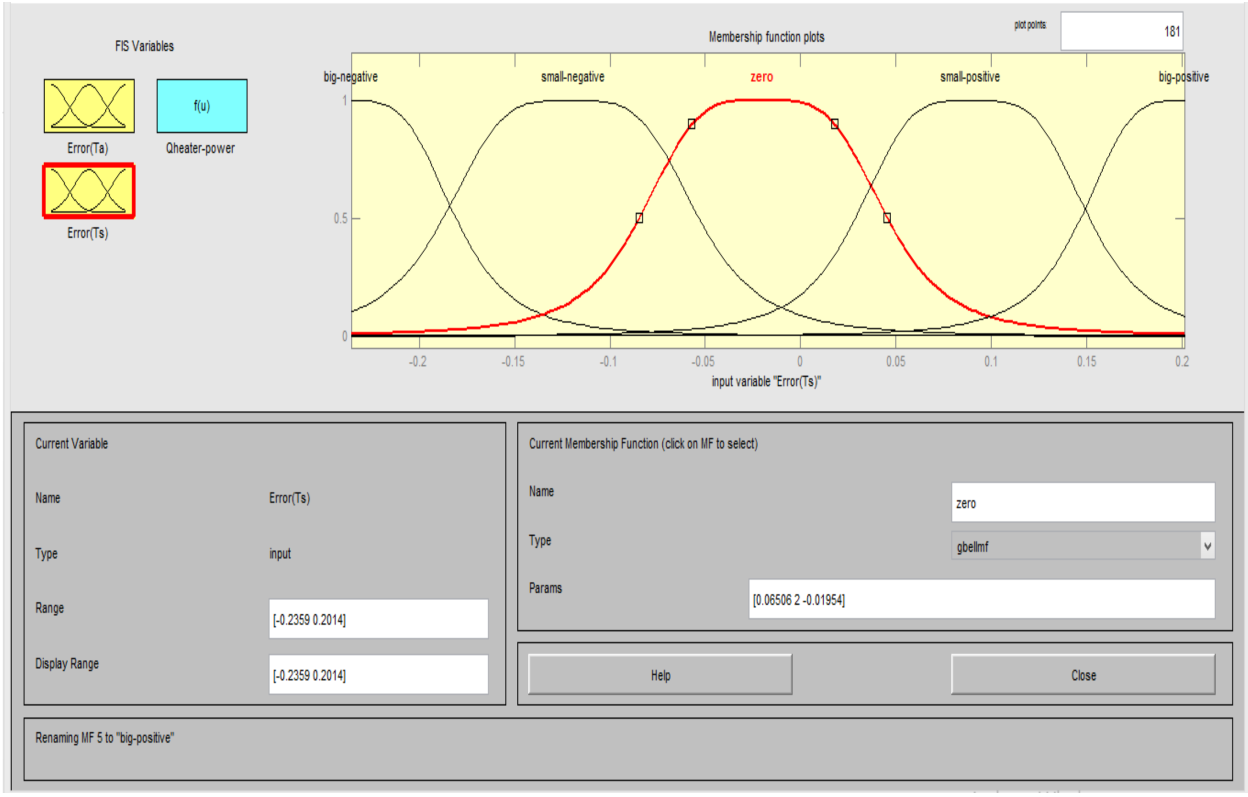

Figure 5.9: *Membership Functions for inputs of ANFIS controller*

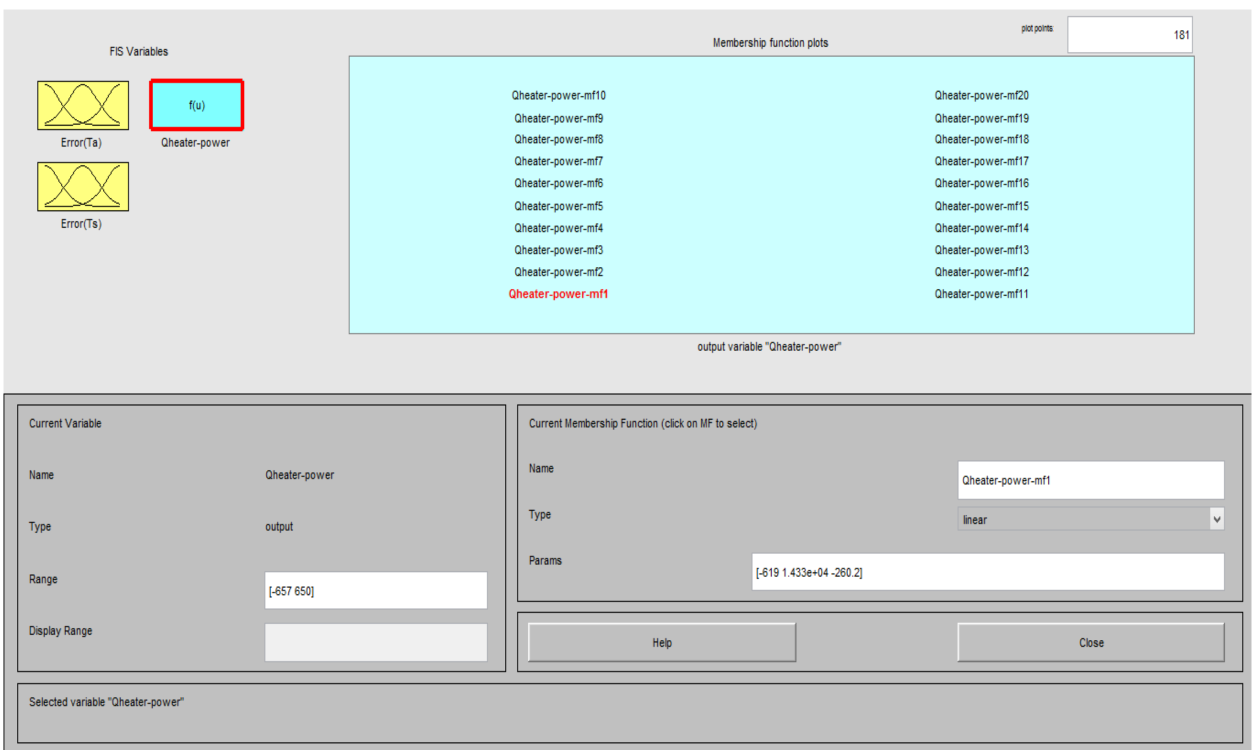

Figure 5.10: *Membership Functions for output of ANFIS controller*

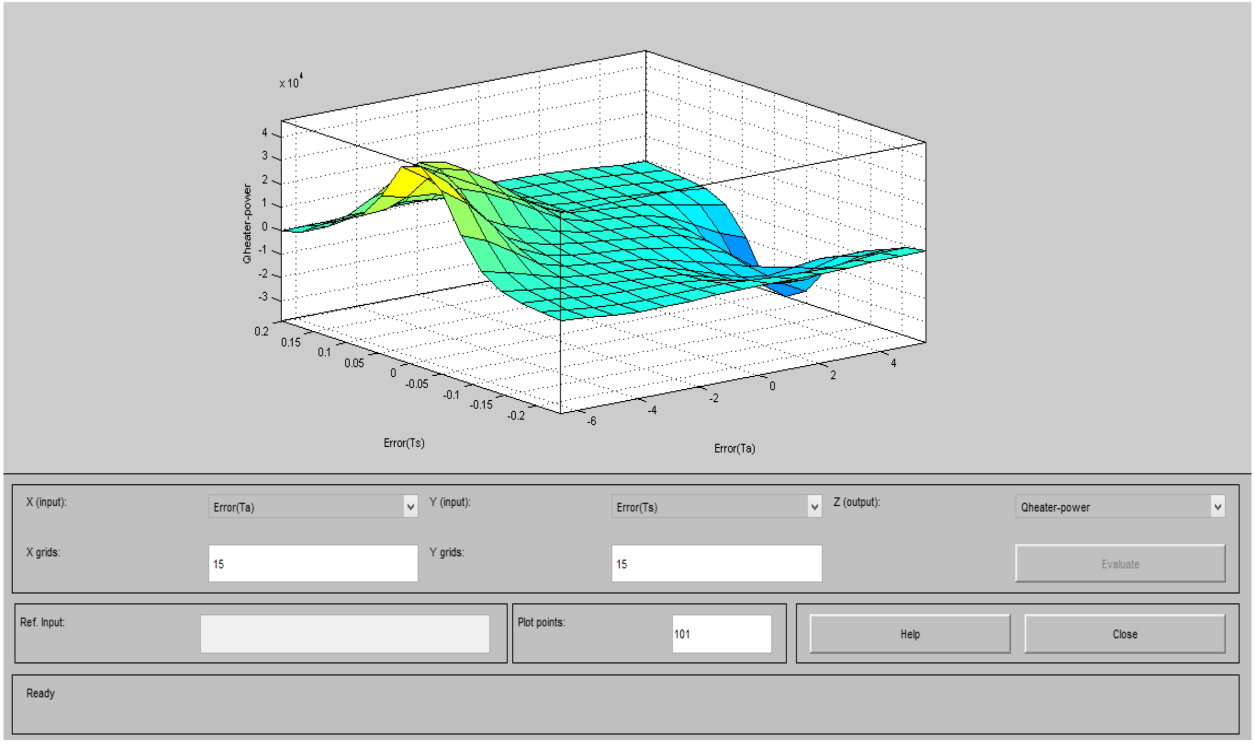

***Figure 5.11**: Surface viewer of the three parameters (two input and one output parameters) of ANFIS*

According to the errors (*Error (Ta)* and *Error (Ts)*), there are 20 rules for the ANFIS in order to make the optimum output decision i.e. heater power (*Qheater*).

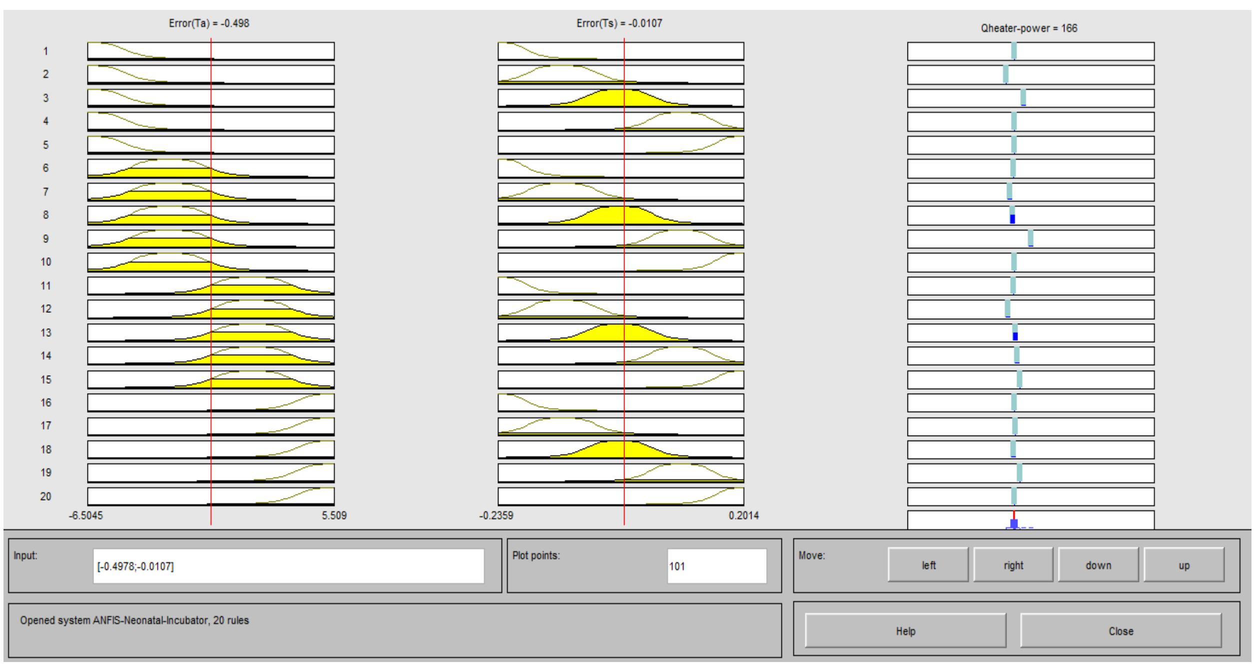

***Figure 5.12**: Rule viewer of ANFIS network*

5.4 Inputs, Output and Rule bases of FLC

Mamdani type fuzzy logic controller membership functions and rule bases are designed based on the input-output data sets, this data sets were used to train the ANFIS network. As we know it, the input and output variables for the FLC are the same as those of the ANFIS controller. The input variables for the fuzzy system are *Error (Ta)* and *Error (Ts)*, which are shown in figure 5.13.

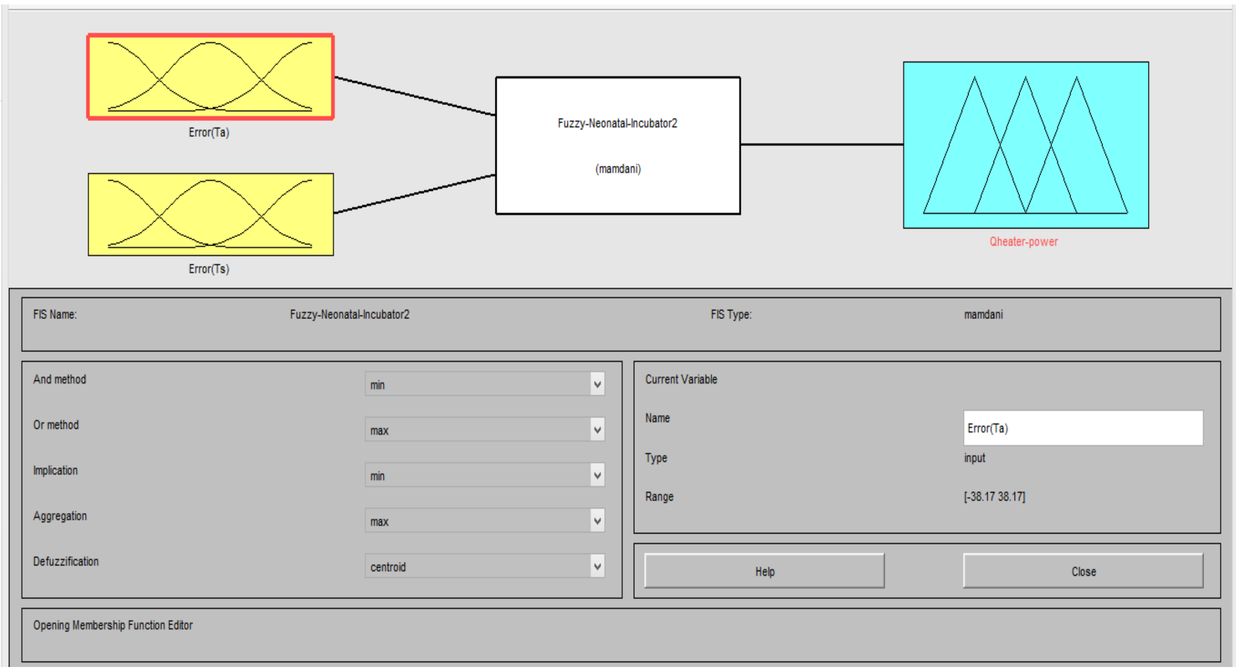

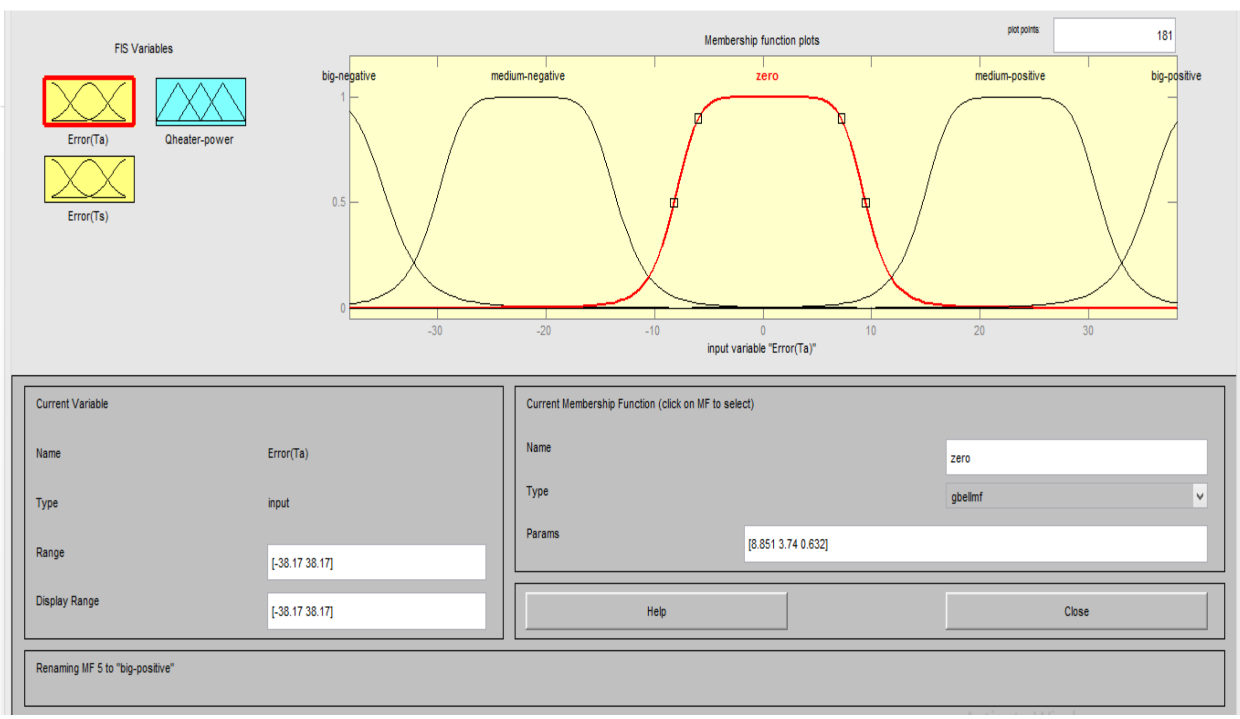

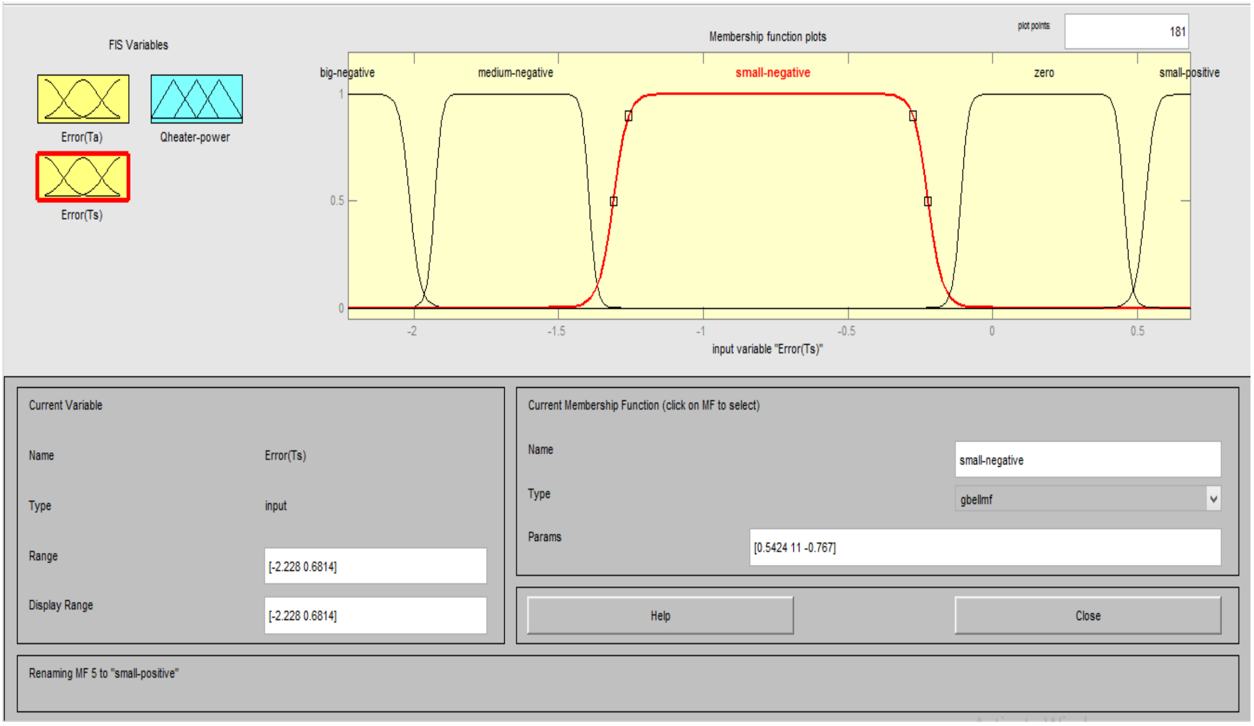

***Figure 5.13**: Membership Functions for inputs of FLC*

The output variable for the fuzzy system is *Qheater* and the corresponding membership functions for this variable is shown in figure 5.14. In addition, the surface viewer and the rule viewer for the FLC is shown in figure 5.15 and 5.16 respectively.

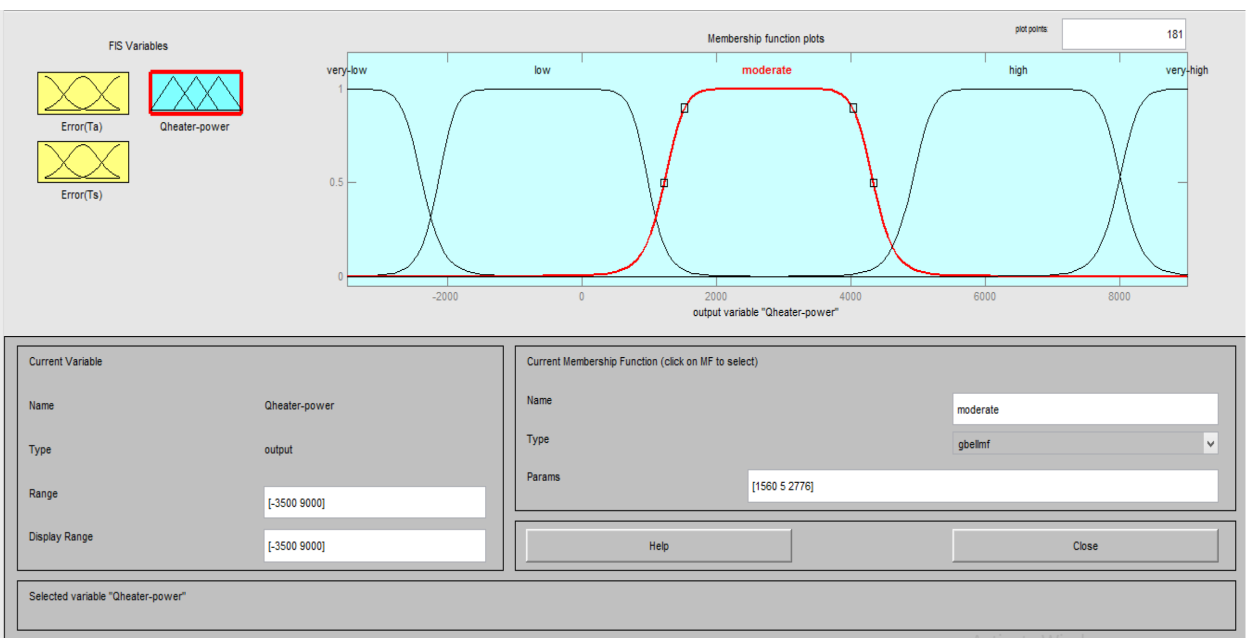

***Figure 5.14**: Membership Functions for output of FLC*

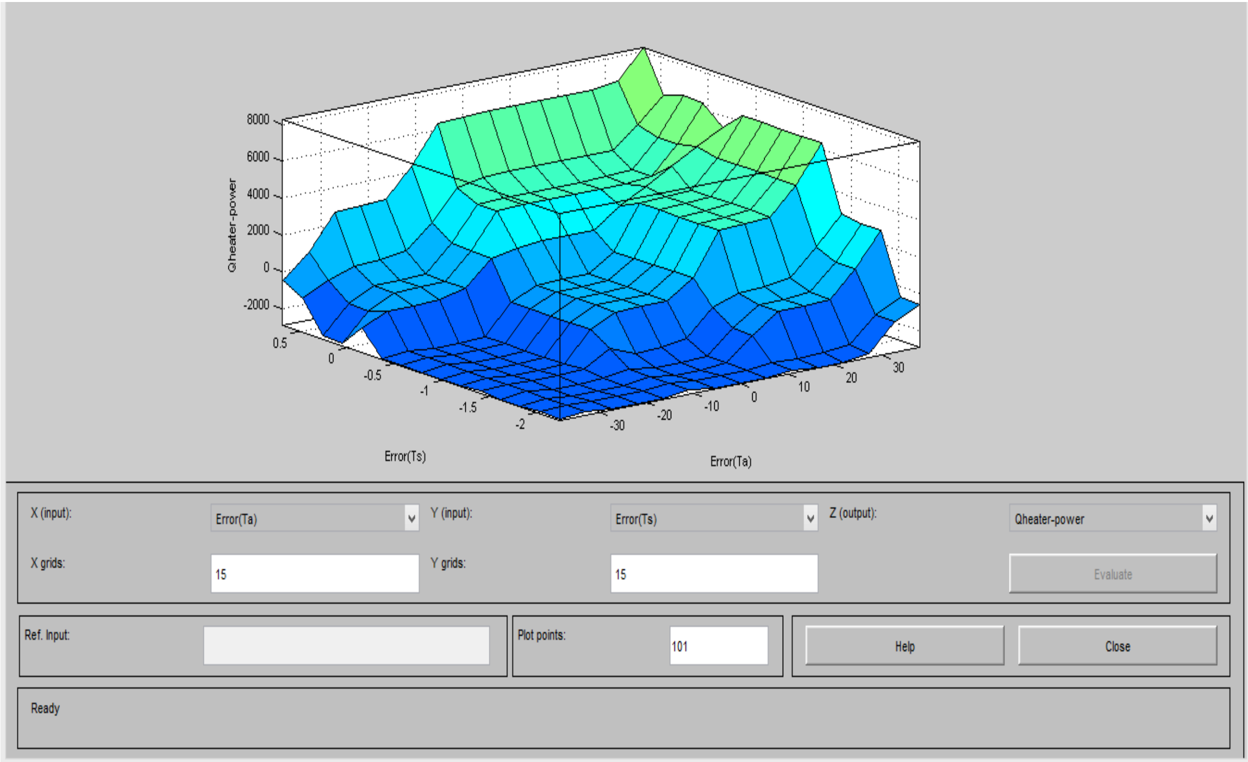

Figure 5.15: *Surface viewer of the three parameters (two input and one output parameters) of FLC*

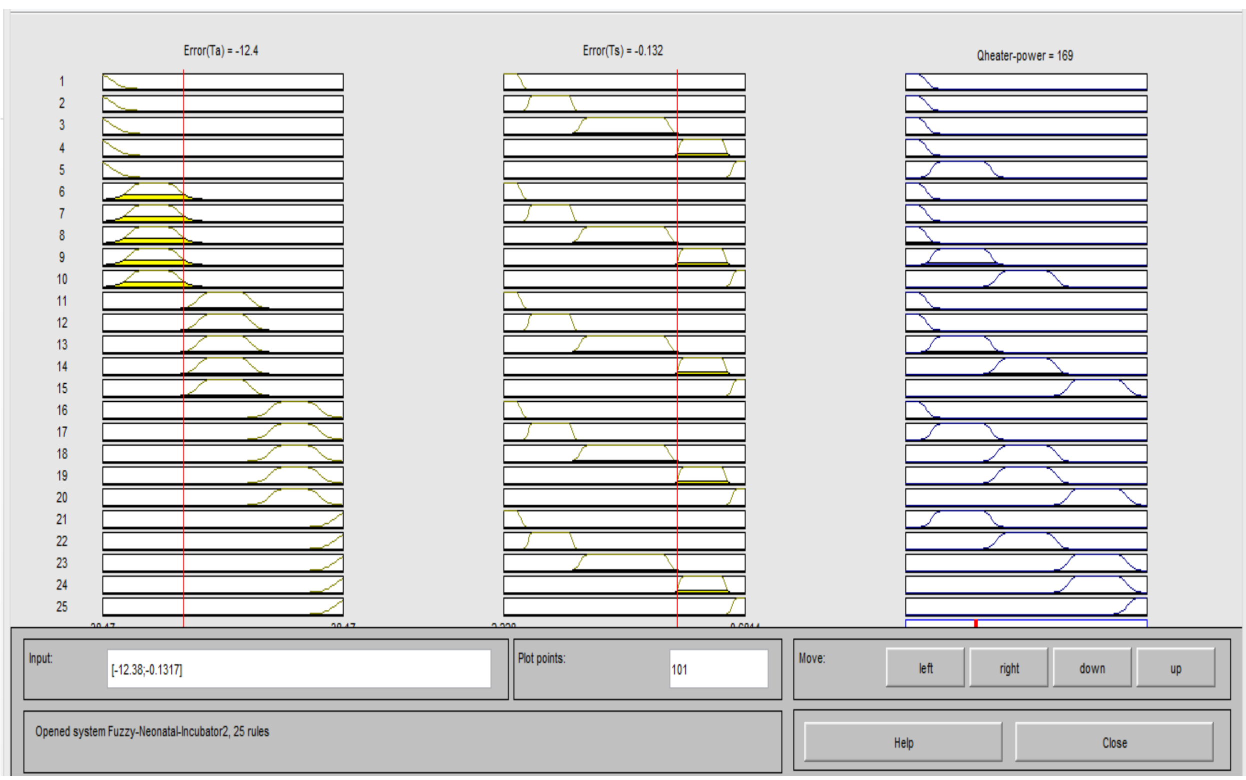

Figure 5.16: *Rule viewer of FLC*

According to the errors (*Error (Ta)* and *Error (Ts)*), there are 25 rules for the FLC in order to make the optimum output decision i.e. heater power (*Qheater*). These rules are given in table 5.1

***Table 5.1**: Fuzzy rules look up table*

Error(Ts)* \ *Error(Ta)	***BN***	***MN***	***Z***	***MP***	***BP***
BN	*VL*	*VL*	*VL*	*VL*	*L*
MN	*VL*	*VL*	*VL*	*L*	*M*
SN	*VL*	*VL*	*L*	*M*	*H*
Z	*VL*	*L*	*M*	*M*	*H*
SP	*L*	*M*	*H*	*H*	*VH*

The linguistic fuzzy variables BN, MN, SN, Z, MP, SP, BP, VL. L, M, H and VH stands for big-negative, medium-negative, small-negative, zero, medium-positive, small-positive, big-positive, very-low, low, moderate, high and very-high respectively.

Look up table was changed several times to get the desired combination of rules. Different membership functions were investigated to get the desired shape and range. System was tuned by changing the width and overlapping of the membership functions. Finally, decent performance of the system is achieved.

5.5 Simulation results

In order to analyze the performance of ANFIS controller and FLC on the infant-incubator control system, we select certain conditions for the system, so that based on the response of the closed loop system for those selected conditions, we will reach out to conclusions.

Incubator air and infant skin temperatures control for 0.9 kg infant-mass and postnatal-age of 1 day: In order to attain the thermo-neutral environment for the preterm infant, we consider clinically suggested incubator air and infant skin Temperatures for 0.9 kg infant mass and postnatal age of 1 day, which is around 35^{o}C and 36.6 ^{o}C respectively. As a result, the system response for both controllers simulate and the results shown in the figures below.

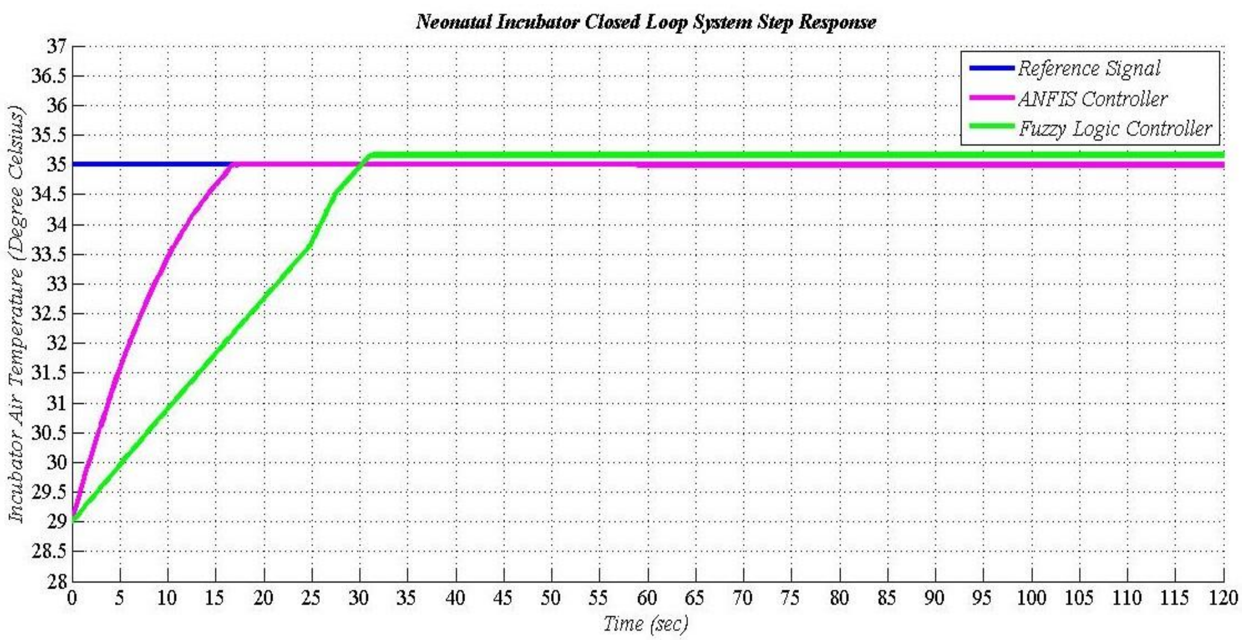

***Figure 5.17**: Incubator air temperature control for 0.9 kg infant-mass and postnatal-age of 1 day*

The performance of both controllers analyzed based on the transient and steady-state response characteristics of the system for step input signal. For the transient response analysis we choose settling time and maximum percent overshoot. For the steady-state response analysis we consider steady-state error.

Table 5.2*: Performance evaluation of both controllers, in controlling the incubator air temperature for 0.9kg infant-mass and postnatal-age of 1 day*

Performance Parameters	ANFIS Controller	Fuzzy Logic Controller
Steady-state Error	0.0039°C	-0.1663°C
Settling Time (sec)	16.1sec	31sec
Maximum Percent Overshoot (%)	0%	17%

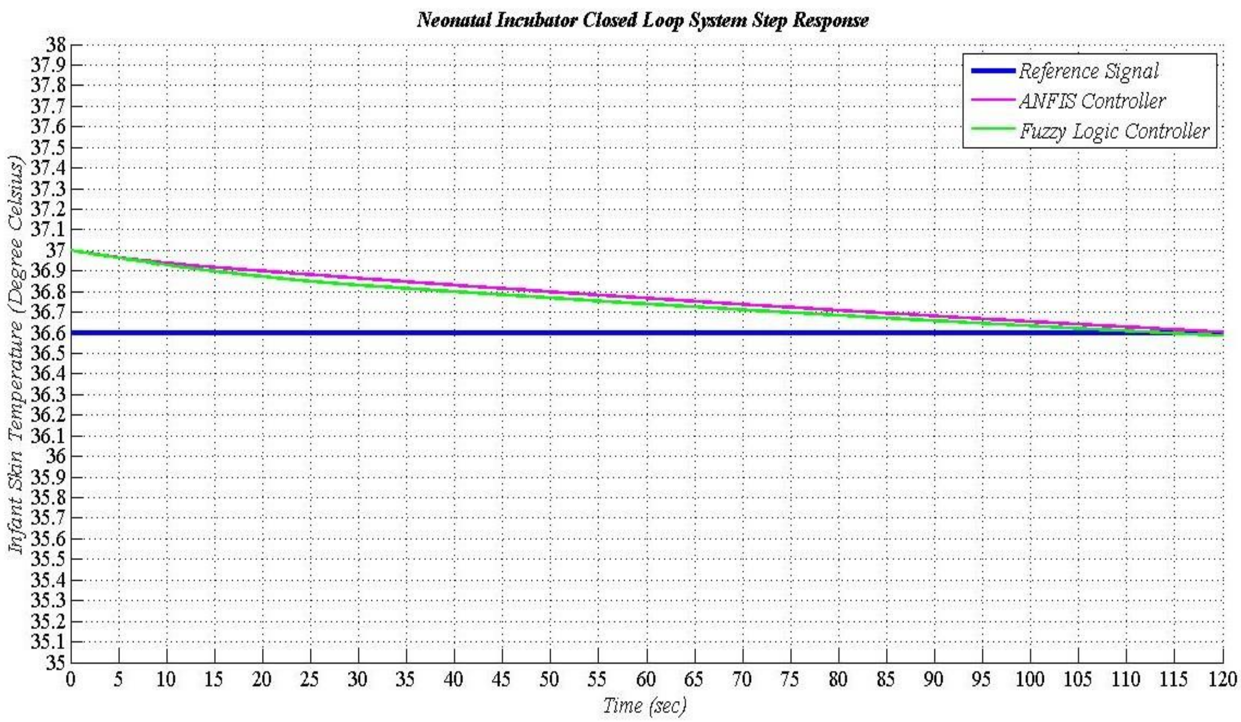

Figure 5.18*: Infant skin temperature control for 0.9 kg infant-mass and postnatal-age of 1 day*

Table 5.3*: Performance evaluation of both controllers, in controlling the infant skin temperature for 0.9kg infant-mass and postnatal-age of 1 day*

Performance Parameters	ANFIS Controller	Fuzzy Logic Controller
Steady-state Error	-0.002982°C	0.0147°C
Settling Time (sec)	105sec	104.4sec
Maximum Percent Overshoot (%)	0.003%	1.37%

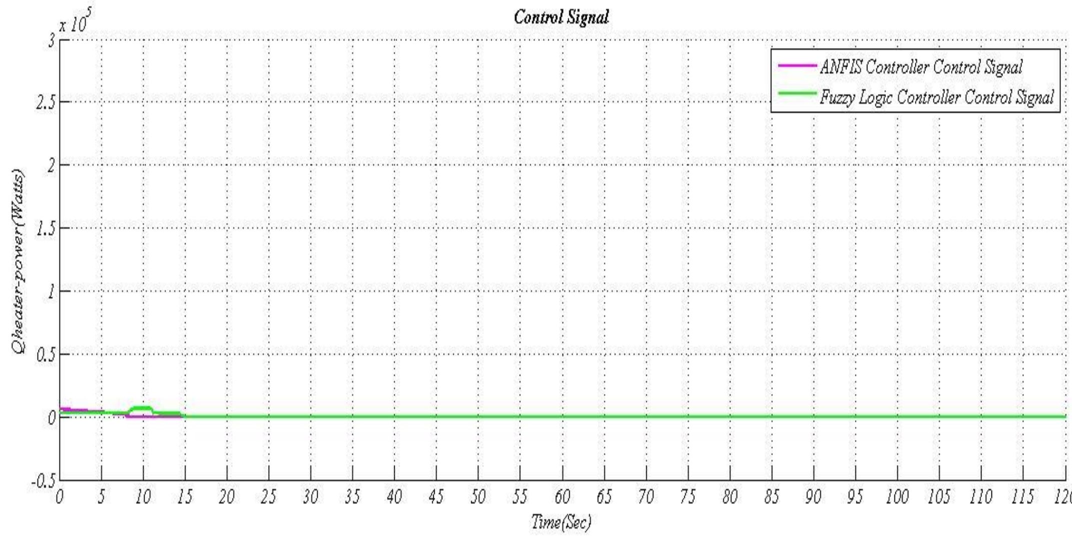

***Figure 5.19**: Control signals of both controllers for 0.9 kg infant-mass and postnatal-age of 1 day*

Incubator air and infant skin temperatures control for 2 kg infant-mass and postnatal-age of 5 days: In order to attain the thermo-neutral environment for the preterm infant, we consider clinically suggested incubator air and infant skin temperatures for 2 kg infant mass and postnatal age of 5 days, which is around 32°C and 36.4 °C respectively. As a result, the system response for both controllers simulate and the results shown in the figures below.

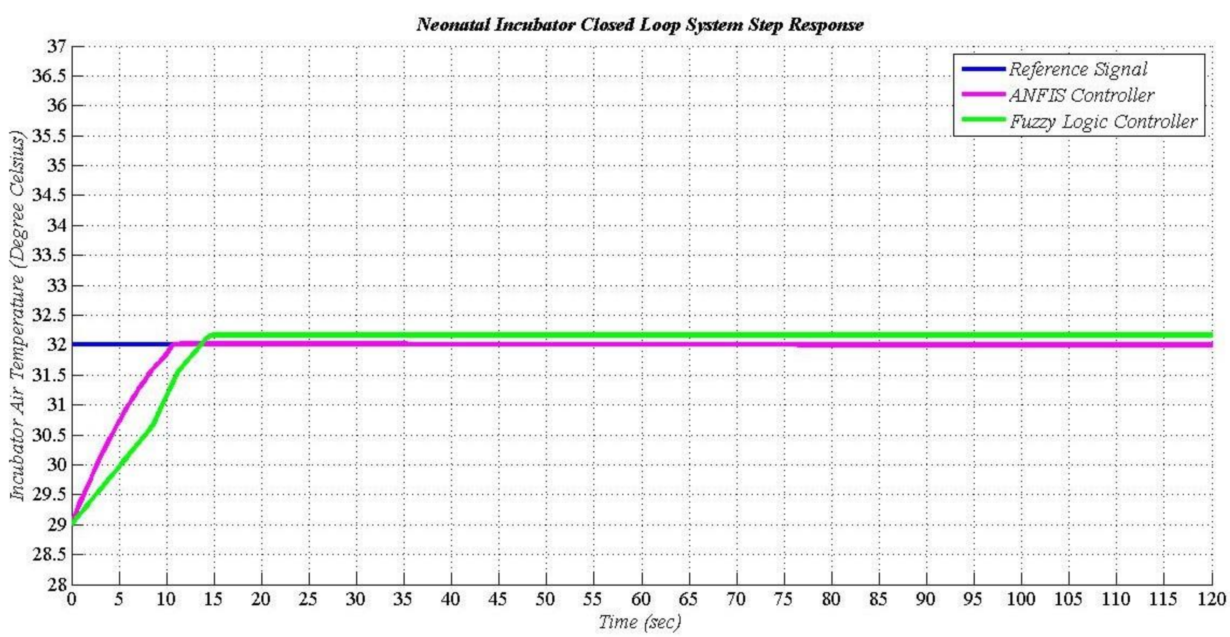

***Figure 5.20**: Incubator air temperature control for 2 kg infant-mass and postnatal-age of 5 days*

Table 5.4*: Performance evaluation of both controllers, in controlling the incubator air temperature for 2kg infant-mass and postnatal-age of 5 days*

Performance Parameters	ANFIS Controller	Fuzzy Logic Controller
Steady-state Error	0.001857°C	-0.1678°C
Settling Time (sec)	10.3sec	14.1sec
Maximum Percent Overshoot (%)	0%	16%

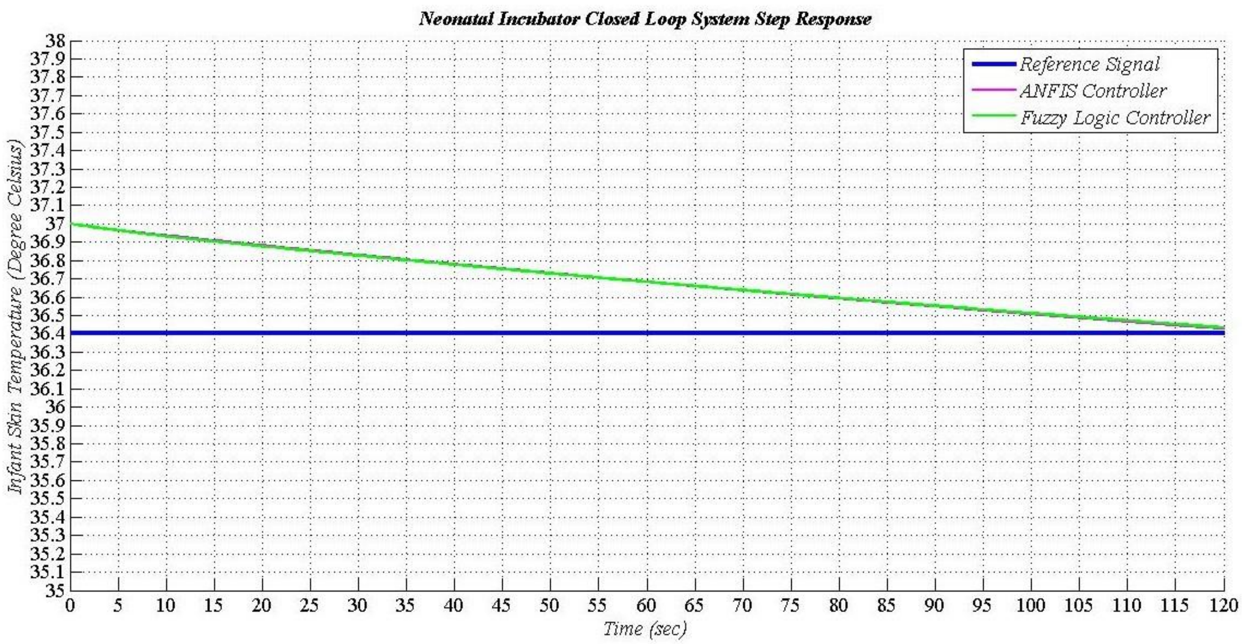

Figure 5.21*: Infant skin temperature control for 2 kg infant-mass and postnatal-age of 5 days*

Table 5.5*: Performance evaluation of both controllers, in controlling the infant skin temperature for 2kg infant-mass and postnatal-age of 5 days*

Performance Parameters	ANFIS Controller	Fuzzy Logic Controller
Steady-state Error	-0.01709°C	-0.0289°C
Settling Time (sec)	116sec	115.82sec
Maximum Percent Overshoot (%)	1.68%	1.731%

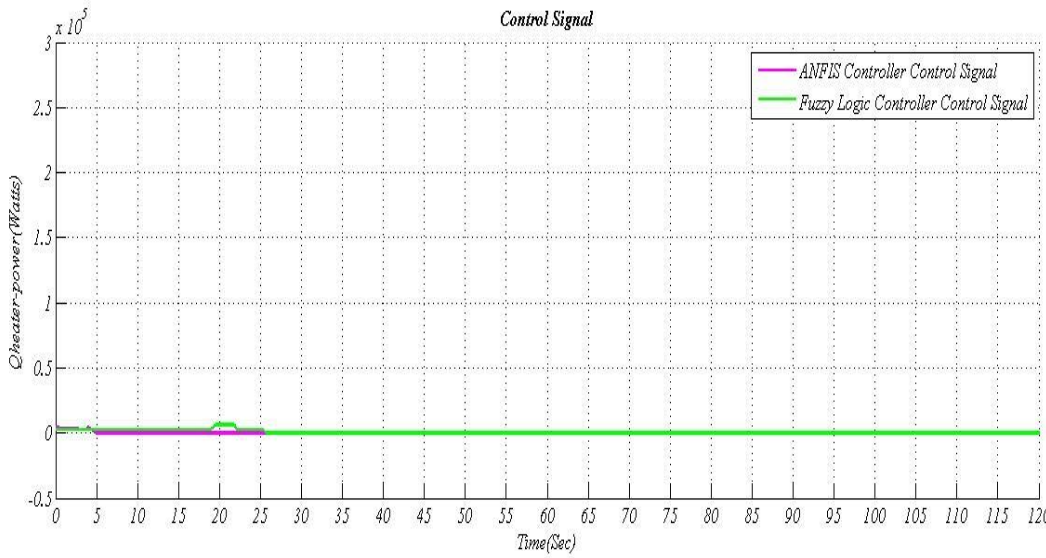

Figure 5.22*: Control signals of both controllers for 2 kg infant-mass and postnatal-age of 5 days*

Finally the overall system dynamic performance is evaluated. For this purpose, a sinusoidal wave with amplitude of 5 degree Celsius, frequency of 0.2 rad/sec and the constant deviation of 31 degree Celsius is used for incubator air temperature. This signal generates a wave which at its maximum can reach 36°C and at its minimum can reach 26°C.

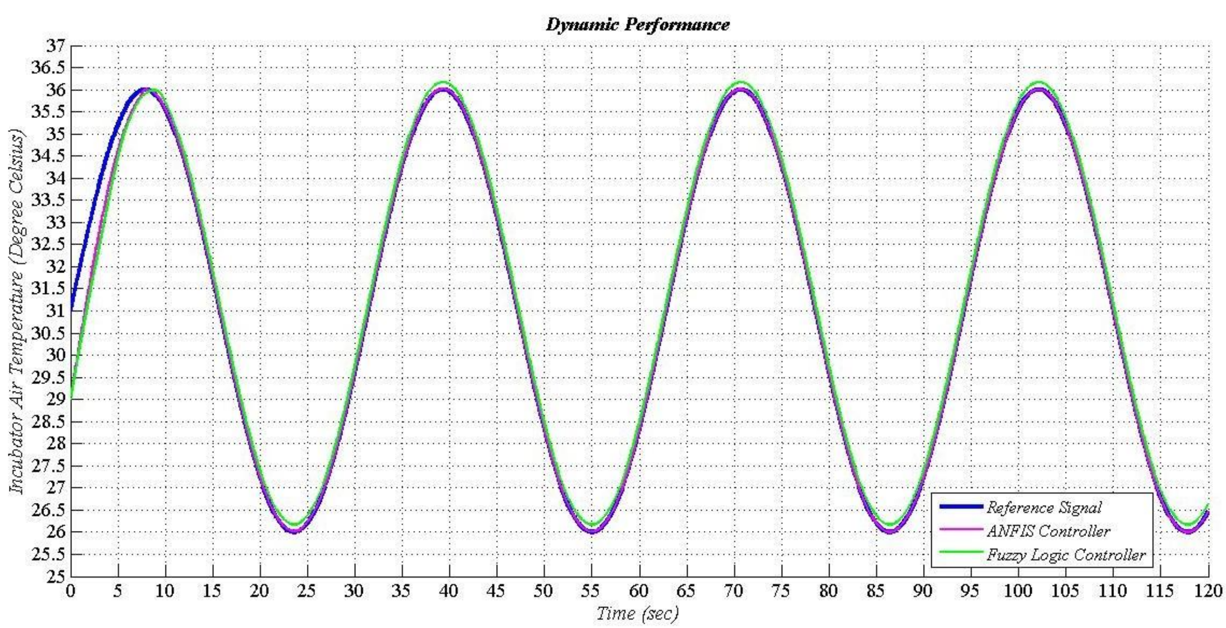

Figure 5.23*: Dynamic response of both controllers for sinusoidal incubator air temperature input signal*

Similarly, a sinusoidal wave with amplitude of 0.8 degree Celsius, frequency of 0.2 rad/sec and the constant deviation of 36.3 degree Celsius is used for infant skin temperature. This signal generates a wave which at its maximum can reach 37.1°C and at its minimum can reach 35.5°C.

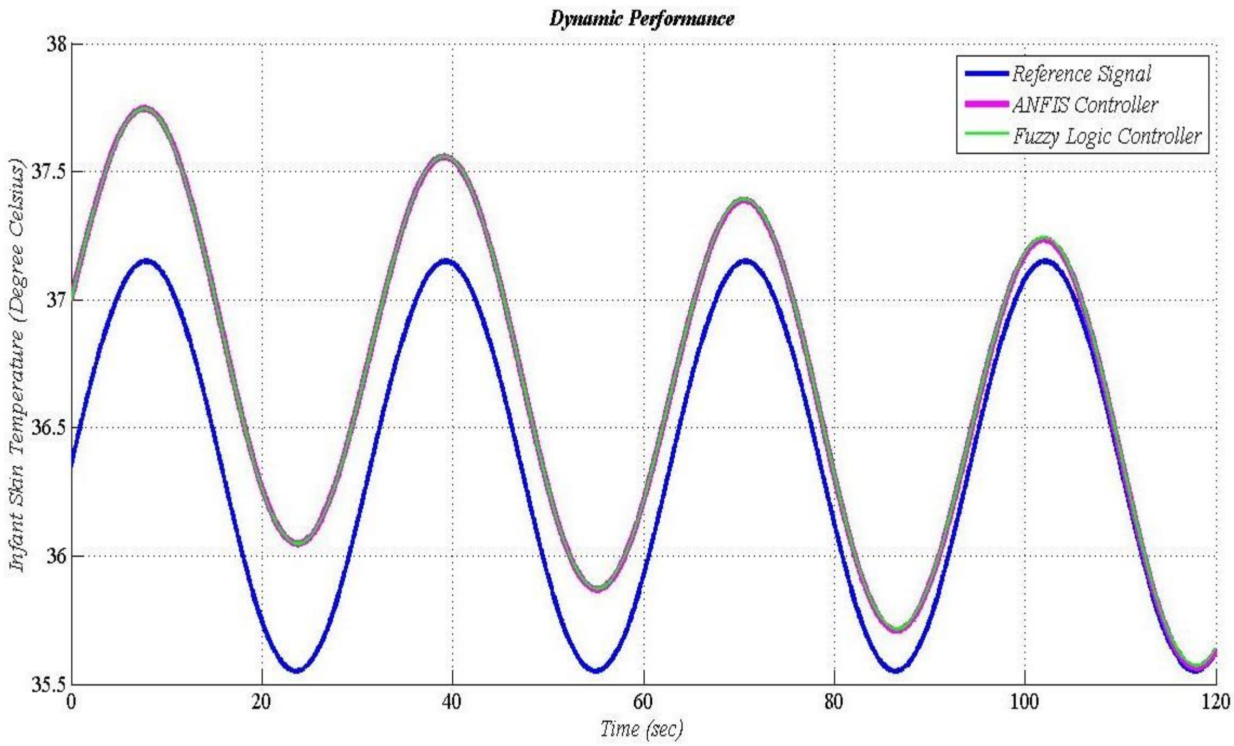

Figure 5.24*: Dynamic response of both controllers for sinusoidal infant skin temperature input signal*

In addition there are small ports in the incubator walls which can be opened to clean and feed the neonate. When these small doors are opened to nurse the neonate, the insulation of the system is broken and thermo neutrality of the system is disturbed. A lot of cold air at the environment temperature starts flowing into the incubator air space and the incubator air loses its heat to the environment by convection. Due to this disturbance, here may be fluctuations in incubator air temperature and infant skin temperature. In this thesis we consider the system under environmental disturbance and analyze the behavior of the control systems under this condition, simulation results are illustrated in the following figures.

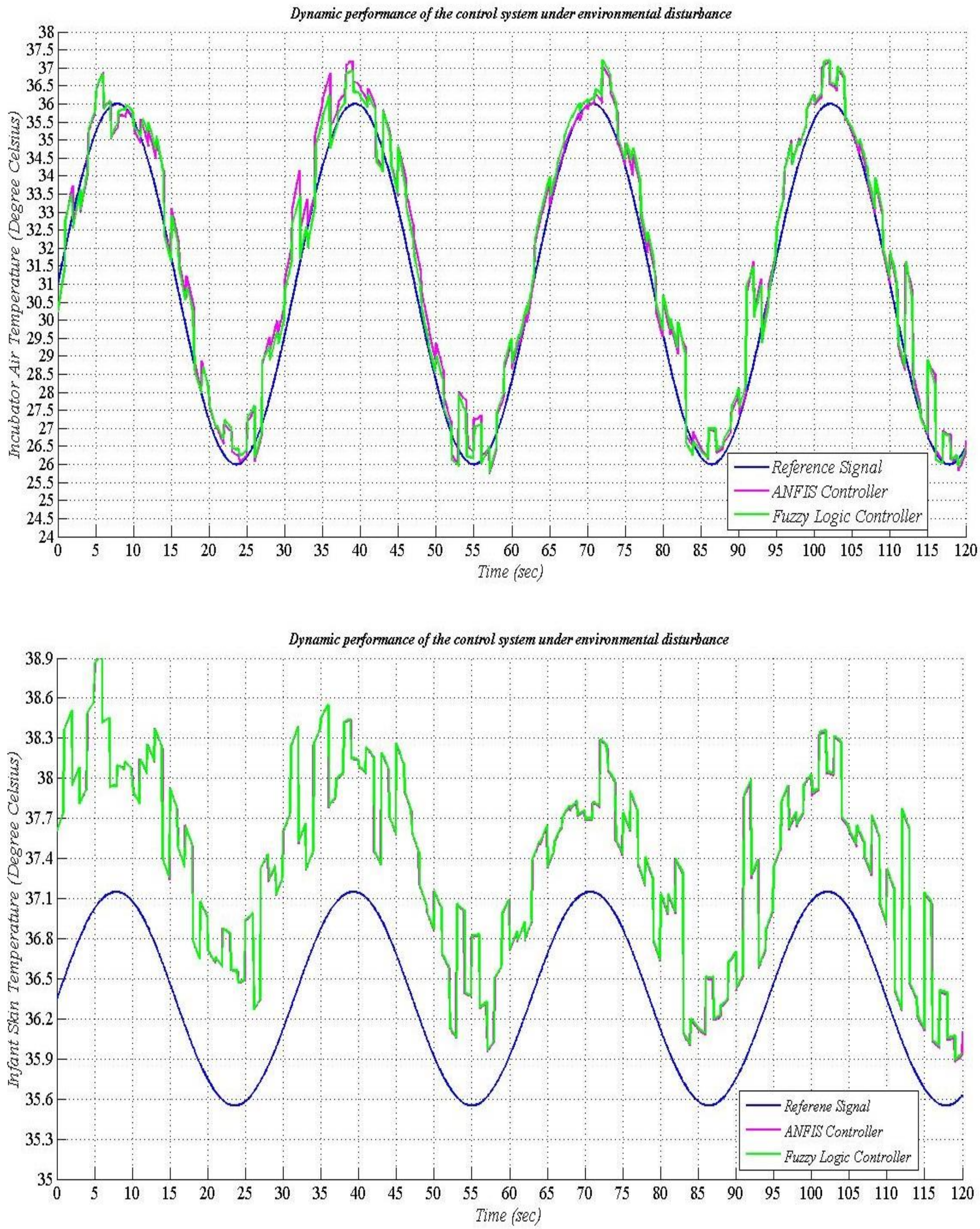

***Figure 5.25**: Dynamic response of both controllers under environmental disturbance*

5.6 Discussions

As we have discussed in the previous sections, the simulation processes conducted in this thesis justifies the performance of ANFIS controller and Fuzzy logic controller on neonatal incubator control system. In order to analyze the performance of both controllers, we select certain conditions on the control system and analyze the performance on the bases of the transient and steady-state response characteristics of the system for step input signals.

When the infant mass inside the incubator is considered as 0.9kg and postnatal age of 1 day, the step responses of ANFIS based and Fuzzy logic based infant-incubator system for the predefined set values of the incubator air temperature was analyzed on the bases of the transient and steady-state response characteristics. As a result, the settling time for the ANFIS based and Fuzzy logic based control system responses were 16.1sec and 31sec respectively. From this result we can analyze that, the ANFIS based control system is faster and greatly reduce the settling time without any overshoot in comparison to Fuzzy logic based control system. Similarly the steady-state error for the ANFIS based and Fuzzy logic based control system responses were 0.0039^{o}C and -0.1633^{o}C respectively. From this result we can also analyze that, the ANFIS based control system greatly reduce the steady-state error in comparison to the Fuzzy logic based control system.

When the infant mass inside the incubator is considered as 2kg and postnatal age of 5 days, the step responses of ANFIS based and Fuzzy logic based infant-incubator system for the predefined set values of the incubator air temperature was analyzed on the bases of the transient and steady-state response characteristics. As a result, the settling time for the ANFIS based and Fuzzy logic based control system responses were 10.3sec and 14.1sec respectively. From this result we can analyze that, the ANFIS based control system is faster and greatly reduce the settling time without any overshoot in comparison to Fuzzy logic based control system. Similarly the steady-state error for the ANFIS based and Fuzzy logic based control system responses were 0.001857^{o}C and -0.1678^{o}C respectively. From this result we can also analyze that, the ANFIS based control system greatly reduce the steady-state error in comparison to the Fuzzy logic based control system.

Generally the step responses of ANFIS based and Fuzzy logic based infant-incubator system for the predefined set values of the infant skin temperatures were somehow identical output responses, but still the ANFIS based control system has a little bit better output response than that of Fuzzy logic based control system.

The heater power rating of the system is supplied according to *Error (Ta)* and *Error (Ts)* introducing to the controller. Both controllers action in the above phenomena was smoothly decreasing the heater power rating from a certain corresponding power rating to the equilibrium position, but we can analyze that there were some offsets on the control signal of Fuzzy logic based control system and the system is a little bit slow in order to reach the equilibrium power rating relative to the ANFIS based control system.

The dynamic performance analysis of ANFIS based and Fuzzy logic based control systems, studied under the implementation of sinusoidal input signals for both desired incubator air temperature and infant skin temperature, as a result we can analyze that the actual incubator air temperature and infant skin temperature track the reference input signals in both control systems, but the ANFIS based control system has better tracking capability than those of Fuzzy logic based control system.

Finally, considering the system under environmental disturbance, in this situation we can realize that ANFIS based and Fuzzy logic based control systems reject and control the effect of environmental disturbance under consideration in a very well manner, but we can observe that there is a little bit fluctuations on the infant's skin temperature control relative to the incubator's air temperature control.

CHAPTER 6

CONCLUSIONS, RECOMMENDATIONS AND FUTURE WORK

6.1 Conclusions

An infant incubator model was simulated without implementing any temperature controlling mechanisms and the stability characteristics of both heater power to incubator air temperature (air mode) and heater power to infant skin temperature (skin mode) of the plant were analyzed on the bases of root locus and bode plot analysis mechanisms. It was observed that all the poles of both air mode and skin mode transfer functions lies in the left half of the S-plane. Similarly both air mode and skin mode systems have also positive phase margin and infinity gain margin, which is obvious that, most of the time for second order and above systems the phase plot does not cross -180^0 line, so that the gain margin of the system become infinity. As a result, for such systems the appropriate relative stability measure is the phase margin rather than gain margin.

The closed loop system integrate the proposed ANFIS controller and Fuzzy logic controller, in order to process *Error (Ta)* (the difference between actual incubator air temperature and desired incubator air temperature) and *Error (Ts)* (the difference between actual incubator air temperature and desired incubator air temperature) simultaneously and used this to vary the supply power rating. As a result, simulation results of both controllers for the variation of infant mass and postnatal age of the infant inside the incubator, reveals that the performance of ANFIS controller is better and superior over Fuzzy logic controller. In addition simulation results for the addition of environmental disturbance to the system and the dynamic performance analysis of both controllers also reveals that the performance of ANFIS controller is better than that of Fuzzy logic controller.

The main concept behind this improvement on the performance of the fuzzy logic system is that, the learning and generalization capability of artificial neural networks greatly reduce the time, which is consumed by the fuzzy logic system during the design and tuning process of the governing rules and membership functions in order to generate the optimum rule-base and membership functions for better performance.

6.2 Recommendation

In this thesis, we implement an existing mathematical model of infant-incubator system with temperature variations of the various compartments of the system as an output variable. However, by the consideration of system identification techniques it is possible to obtain the approximate mathematical model of the infant-incubator system from the input-output data sets with various output variables, such as the relative humidity and oxygen concentration of the incubator micro environment. As a result, controlling these output variables together with temperature controlling will improve the performance of the control system and provide better thermo neutral environment for the preterm infants.

6.3 Future work

In this thesis, we explore the feasibility of a neuro-fuzzy based temperature control of neonatal incubator, it is believed that there are a lot of ideas for further research studies. Some possible directions are the following:

- Design a suitable control system for transport incubators by considering the optimization of the power source supply, this incubators are used when a preterm infant is moved from one hospital to another and most units also carry their own backup power supplies.
- In addition to the controller design, wireless communication integrated with the controllers could be a solution to monitor the preterm infants remotely.
- Evaluation of the overall efficiency of the proposed control system for specific application.
- Other intelligent control algorithms like Genetic Algorithm can also be adopted in order to tune the rule bases and membership functions of fuzzy logic systems.

REFERENCES

1. World Health Report, "*Life in the 21st century: A vision for all*", Report of the director general, World health organization, Geneva, 1998.
2. Premature infants [Online]. Available: http://en.wikipedia.org/wiki/Premature_(preterm) infants , Accessed on January 26 2016.
3. Interprofessional Education and Research Committee of the Champlain Maternal Newborn Regional Program (CMNRP), "Newborn thermoregulation", Self-learning module, June 2013.
4. World Health Organization, Maternal and newborn health/ Safe motherhood unit, Division of reproductive health (Technical Support) "*Thermal Protection of newborn: a practical guide*", Geneva, (2nd Edition, WHO/RHT/MSM/1997).
5. Guler and M. Burunkaya, "Humidity control of an incubator using the microcontroller based Active humidifier system employing an ultrasonic nebulizer", Journal of Medical Engineering & Technology, Vol. 26, No.2, 2002, pp.82– 88.
6. Garima Mathur, "Fuzzy logic control for infant incubator system", University of Akron, August 2006.
7. Ajay B. Patil, "*Adaptive Neuro Fuzzy Controller for Process Control System*", 978-1-4244-2806-9/08/2008, IEEE.
8. Prasanga D., Hiniduma Lokuge, Yael Maguire and Aileen Wu, "*Design of a Passive Incubator for Premature Infants in the Developing World*", Massachusetts Institute of Technology, Cambridge, U.S.A, 2002.
9. Varuninder Singh, "*Design and development of micro controller based temperature and humidity controller for infant incubator*", Thapar Institute of Engineering and Technology, Patiala, June 2006.
10. Lyon A.J., Pikaar M.E., Badger P. and McIntosh N., "*Temperature control in very low birth weight infants during first five days of life*", Arch dis childhood; Vol.76, 1997, pp.F47-F50.
11. Shin D.I., Shin K.H., Kim I.K., Park K.S., Lee T.S., Kim S.I., Lim K.S., and Huh S.J., "*Low-power hybrid wireless network for monitoring infant incubators*", Medical Engineering and Physics, Vol. 27, No. 8, October 2005, pp. 713-716.

12. Reddy Narender P., Mathur Garima and Hariharan, "*Toward a fuzzy logic control of the infant incubator*", Annals of Biomedical Engineering, Vol. 37, No. 10, October 2009. pp. 2146 – 2152.
13. Thomas K.A. and Burr R., "*Preterm infant thermal care: Differing thermal environments produced by air versus skin servo control incubators*", Vol.19, 1999, pp.264-270.
14. T. A. Tisa, Z. A. Nisha and M. A. Kiber, "*Design of an enhanced temperature control system for neonatal incubator*", Bangladesh Journal of Medical Physics, University of Dhaka, Bangladesh, Vol.5, No.1, 2012.
15. P. J. Sauer, H.J.D. and H. A. Visser, "*New standards for neutral thermal environment of healthy very low birth-weight infants in week one of life*", Arch Dis Child, Vol. 59, 1984, pp.18-22.
16. E. N. Hey and G. Katz, "*The optimum thermal environment for naked babies*", Arch Dis Child, Vol. 45, 1970, pp. 328-334.
17. Barry N. Simon Jr., Narender P. Reddy and Anand Kantak, "*A theoretical model of infant incubator dynamics*" Journal of biomedical engineering, Vol. 116, August 1994.
18. Yasser Amer Al-Taweel and Ahmed Al-jumaily, "*A simulation model of infant incubator feedback system with humidification and temperature control*", The Faculty of Engineering and Science of Auckland University of Technology, August 2006.
19. Ghada M. Amer and Kasim M. Al-Aubidy, "*Novel technique to control the premature infant incubator system using ANN*", Third International Conference on Systems, Signals and Devices, Sousse, Tunisia, March 21-24, 2005.
20. Hüseyin Arpaci and Ö Faruk Özgüven, "*ANFIS & fractional order PID controller design and comparison for overhead cranes*", Indian Journal of Engineering & Materials Sciences, Vol. 18, June 2011, pp. 191-203.
21. J. Godjevac, "*Comparative study of fuzzy control, neural network control and neuro-fuzzy control*" Computer science department, TR No.103/95, February 1995.
22. B. Krose and P.V. Smagt, "*An introduction to neural network*", University of Amsterdam, *8th* edition, November 1996.
23. J. Vieira, F. M. Dias and A. Mota, "*Neuro-Fuzz systems: A survey*", Aveiro, Portugal.
24. D. Nauck, F. Klawon and R. Kruse, "*Foundations of Neuro-Fuzzy systems*", J. Wiley and Sons, 1997.

25. T. C. Lin and C. S. Lee, "*Neural network based fuzzy logic control and decision system*", IEEE Transactions on Computers, Vol.40, No. 12, 1991, pp. 1320-1336.
26. B. Kosko, "*Neural networks and fuzzy systems: A Dynamical System Approach to Machine Intelligence*", Prentice Hall, Englewood Cliffs, New Jersey, 1992.
27. A. Abraham and Baikunth Nath, " *Hybrid intelligent systems: A review of a decade of Research*", School of Computing and Information Technology, Faculty of Information Technology , Monash University, Australia, TR Series5/2000, 2000, pp. 1-55.
28. N. Kasabove and Q. Song, "*Dynamic Evolving Fuzzy Neural Networks with 'm-out-of-n' Activation Nodes for On-Line Adaptive Systems*", Technical Report TR99/04, Department of Information Science, University of Otago, March 1999.
29. E. Czogala and J. Leski, "*Neuro-Fuzzy intelligent Systems: Studies in Fuzziness and Soft Computing*", Springer Verlag, Germany, 2000.
30. H. R. Berenji and P. Khedkar, "*Learning and tuning Fuzzy Logic controllers through Reinforcements*", IEEE Transactions on Neural Networks, Vol.3, No.5 1992, pp. 724-740.
31. M. Figueiredo and F. Gomide, "*Design of Fuzzy Systems using Neuro-Fuzzy networks*", IEEE Transactions on Neural Networks, Vol.10, No. 4, 1999, pp. 815-827.
32. J.S. Rojer Jang, "*Neuro-Fuzzy modelling: Architectures, Analysis and Applications*", PhD. Thesis, University of California, Berkley, July1992.
33. J.S. Rojer Jang, "*ANFIS: Adaptive network-based fuzzy inference systems*", IEEE Transactions on Systems, Man and Cybernetics, Vol. 23, No.3, June 1993, pp. 665–685.
34. R.D. Rojas, E.F. Bell and E.L. Dove, "*A mathematical model of premature baby thermoregulation and infant incubator dynamics*", International Conference on Simulation Modelling in Bioengineering, Vol. 3, 1996, pp. 23-38.
35. Jan A.J. Stolwijk, "*Physiological and behavioral temperature regulation*", Vol.48, Springfield, Thomas, 1970, pp. 703-721.
36. James S. Ultman, "*Computational model for insensible water loss from the newborn pediatrics*", Vol. 79, No.5, 1987, pp.760-765.
37. Yunus A. Cengel, "*Heat transfer: A practical Approach*". *2nd* edition, McGraw-Hill.
38. Michael H. LeBlanc, "*The physics of thermal exchange between infants and their environment*", AAMI Technology Assessment Report, vol.21, No.1, Feb. 1987, pp.11-15.

APPENDICES

APPENDIX A: Neonatal incubator model

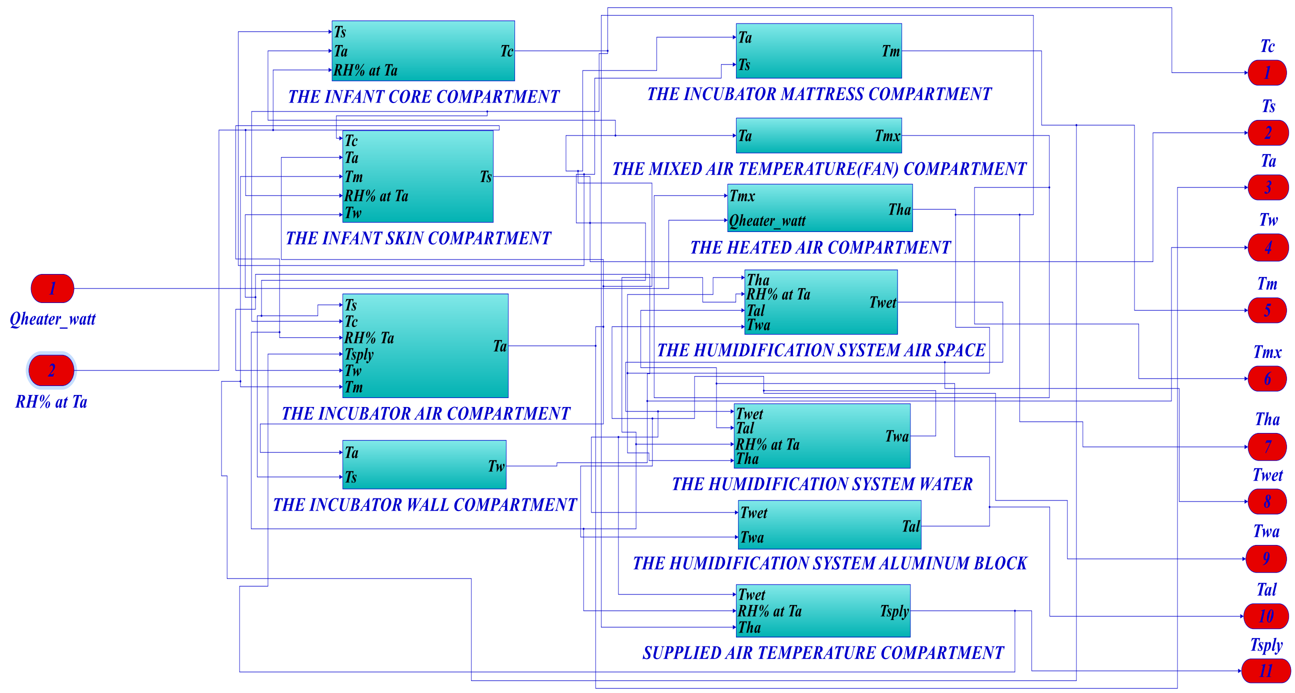

***Figure A.1**: Neonatal Incubator model*

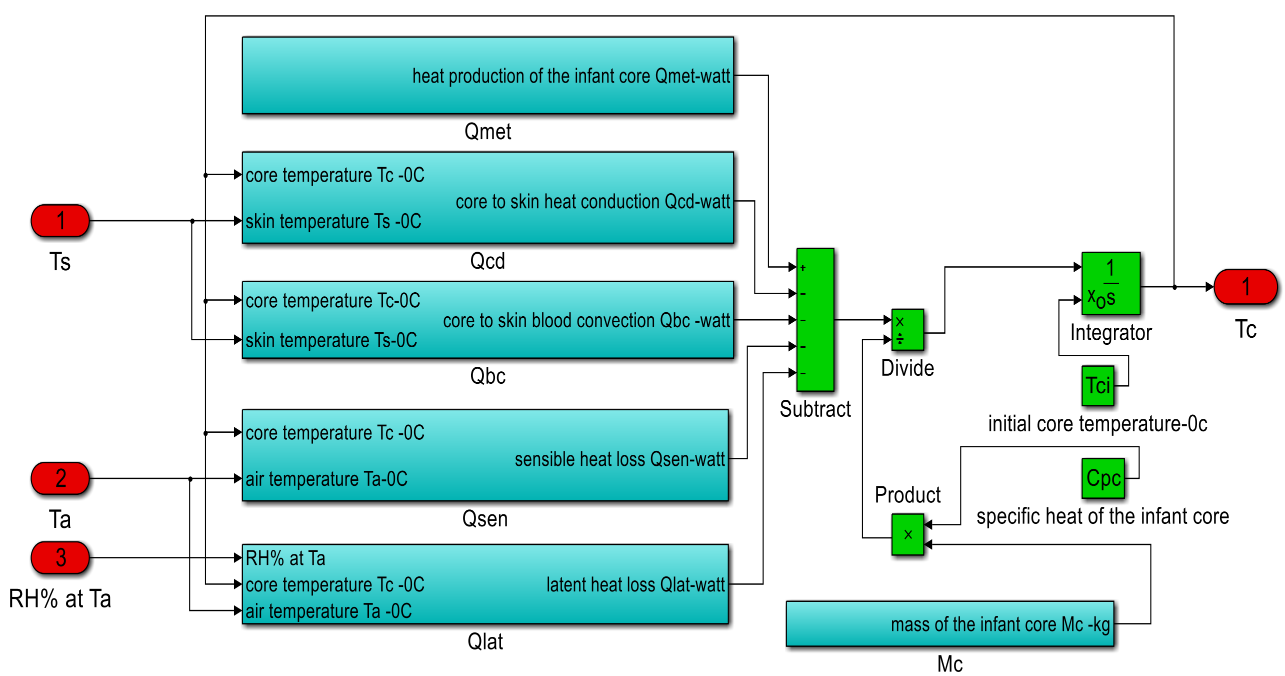

***Figure A.2**: Infant core compartment model*

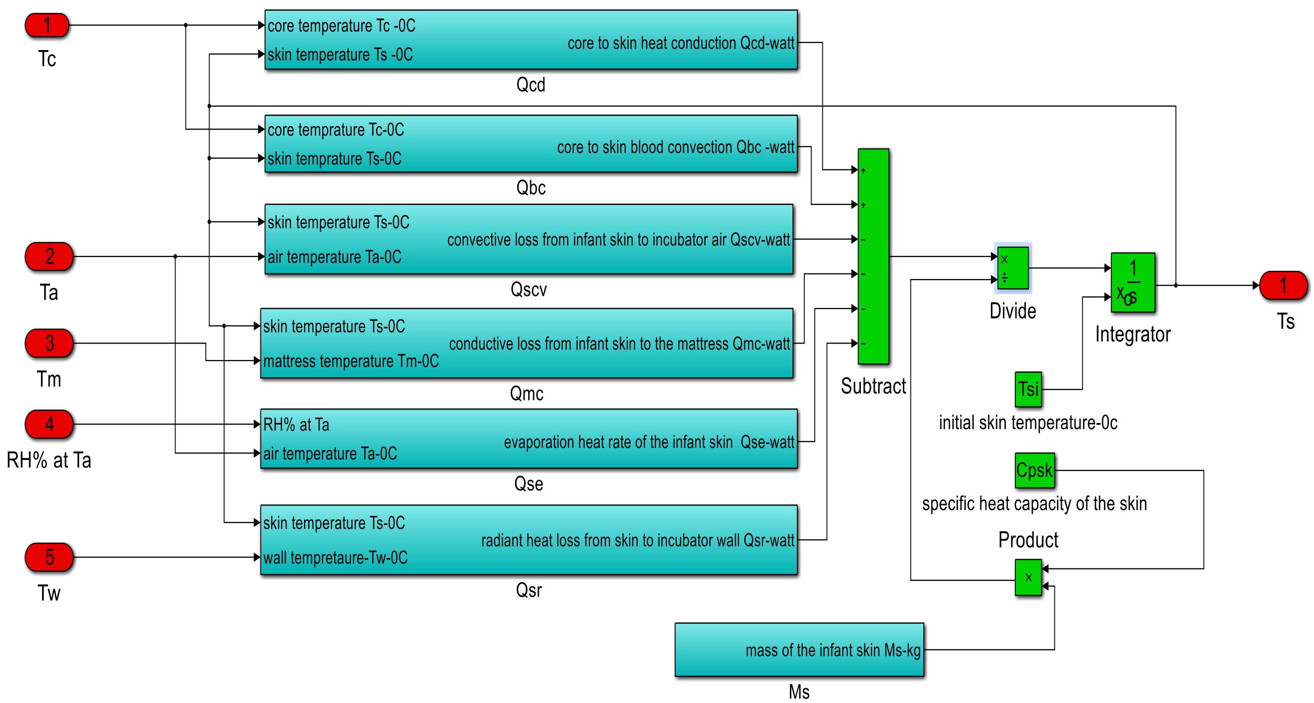

Figure A.3: *Infant skin compartment model*

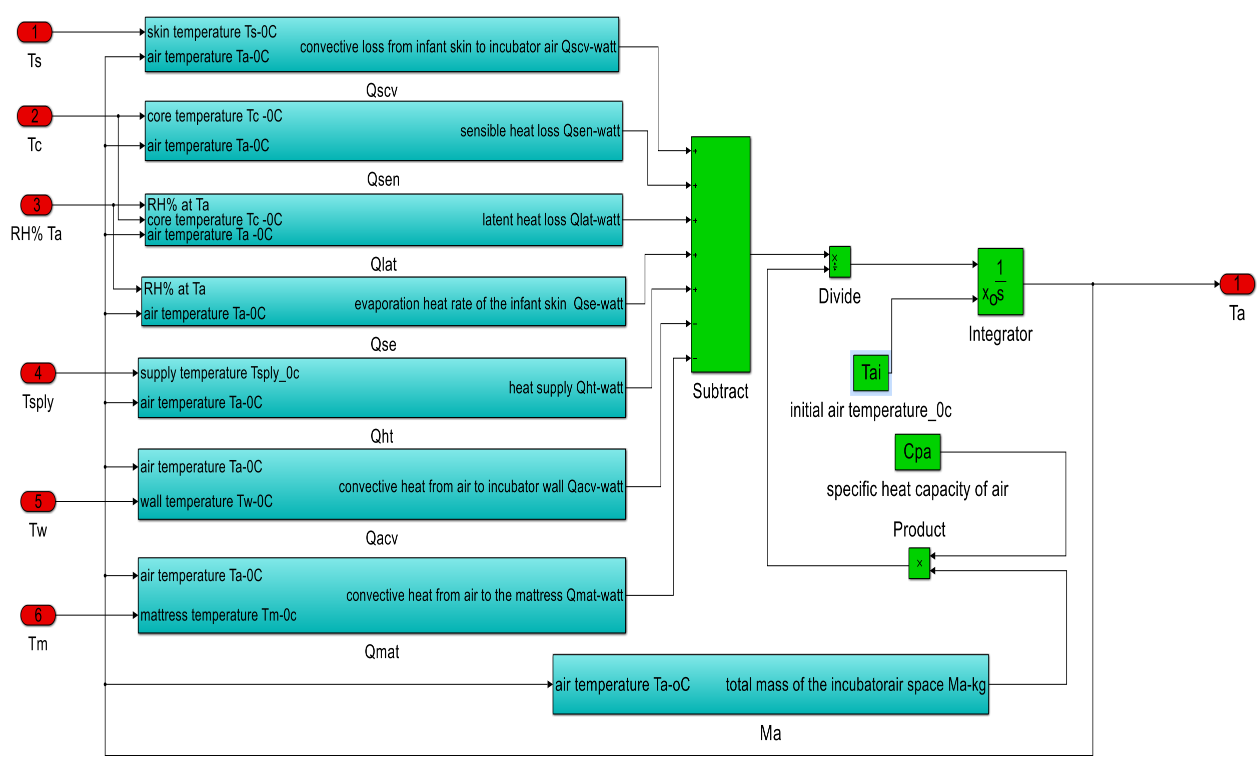

Figure A.4: *Incubator air compartment model*

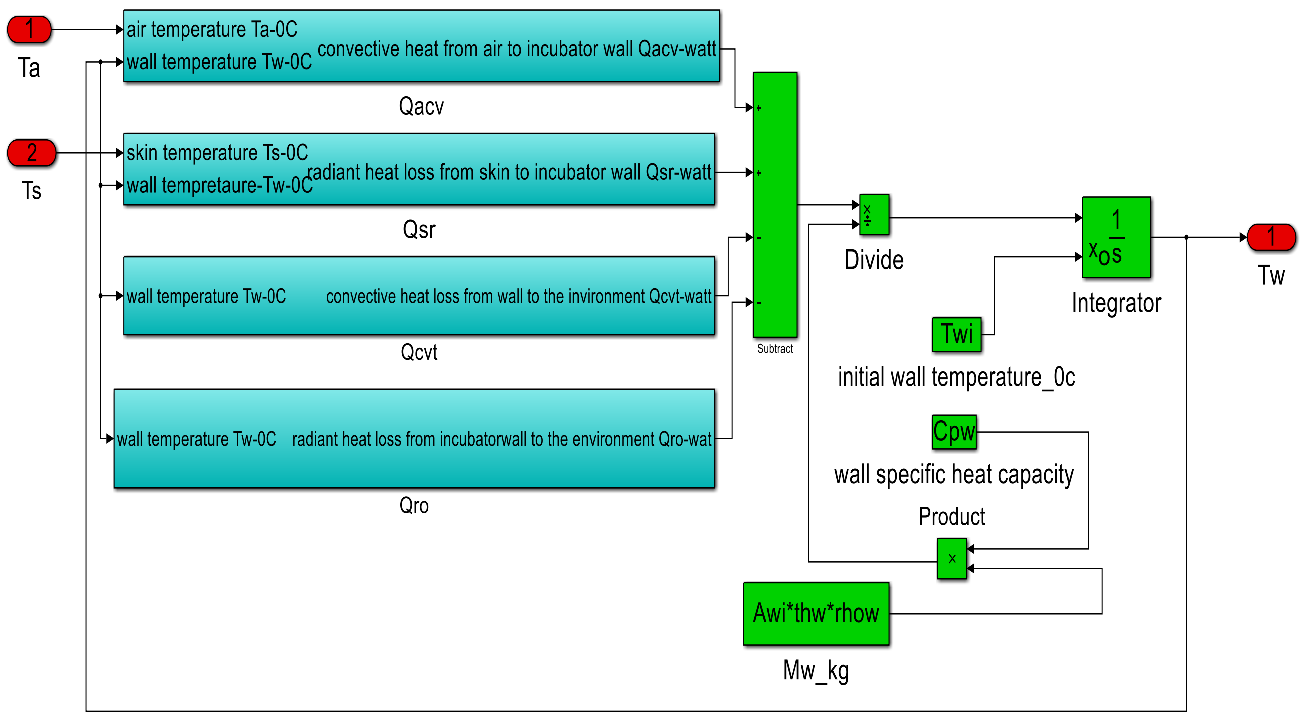

***Figure A.5**: Incubator wall compartment model*

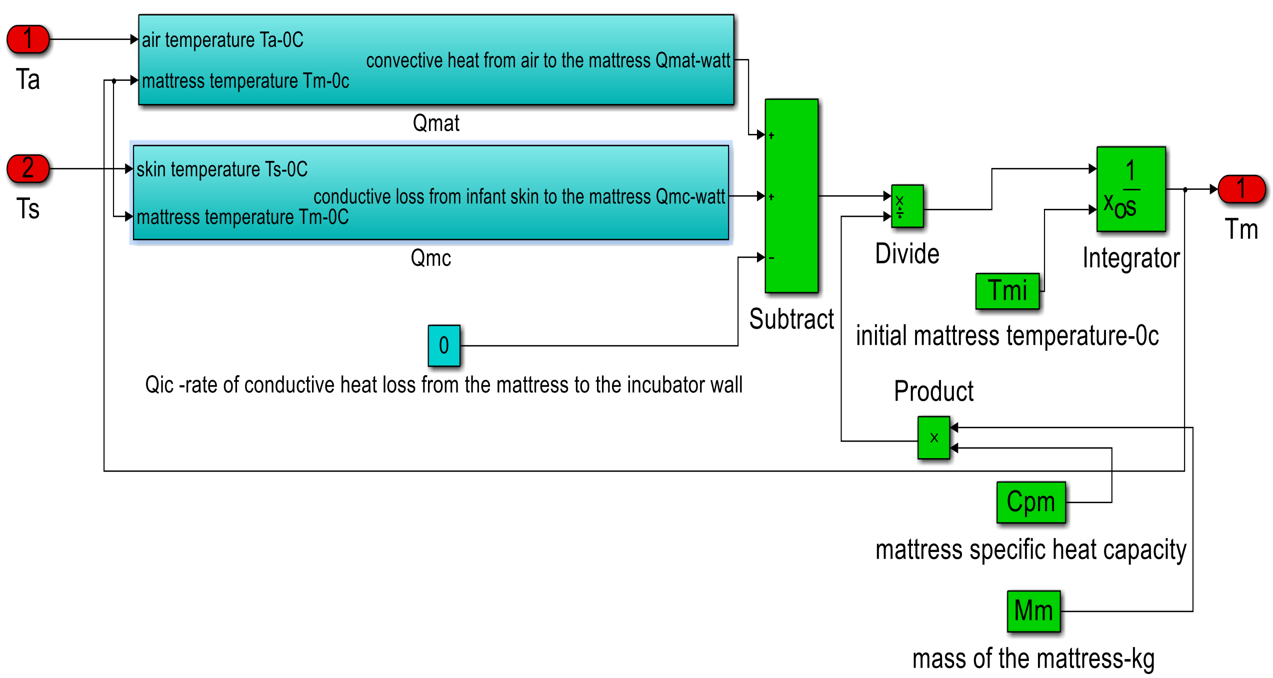

***Figure A.6**: Incubator mattress compartment model*

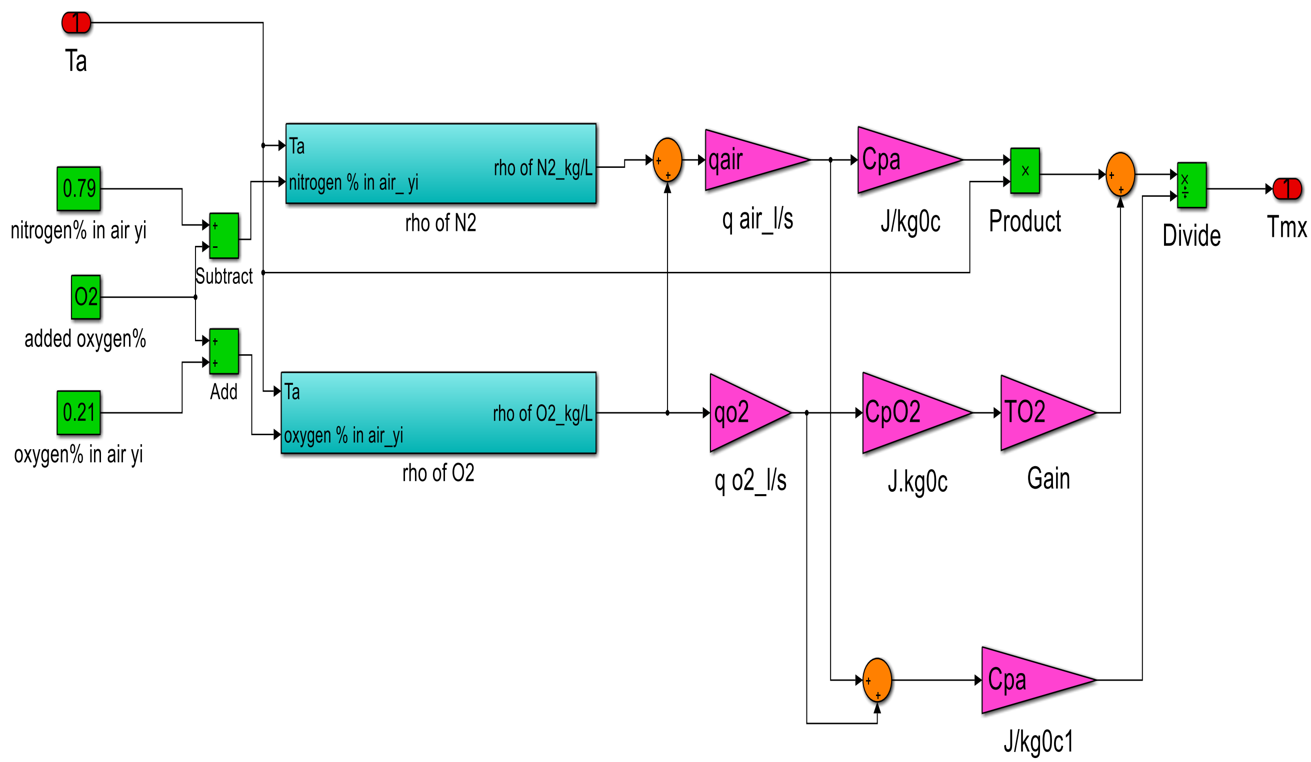

Figure A.7: *Mixed air temperature (Fan) compartment model*

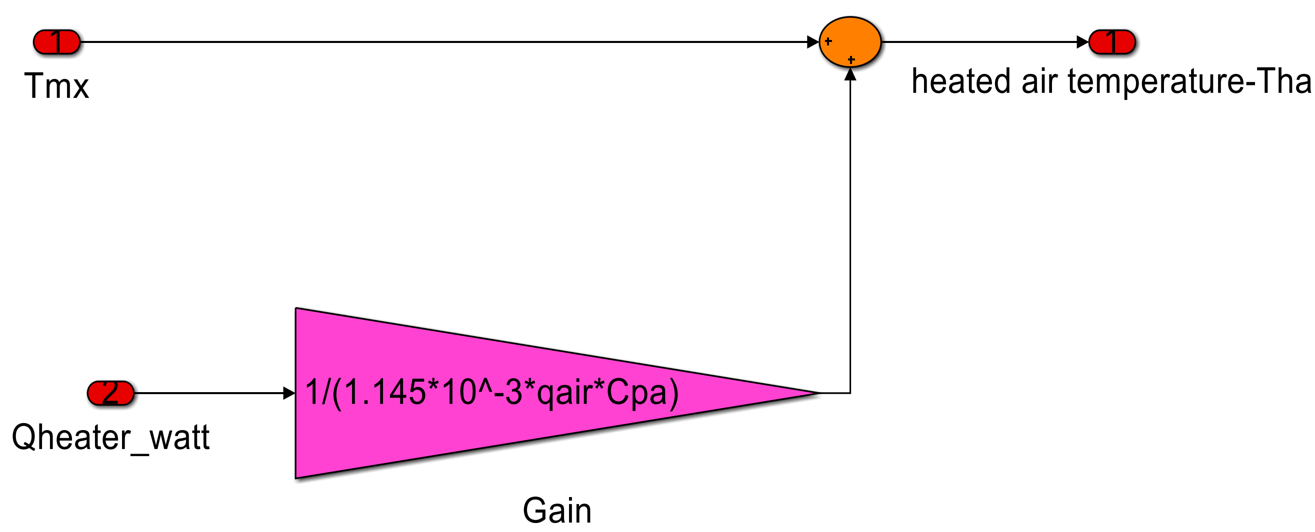

Figure A.8: *Heated air compartment model*

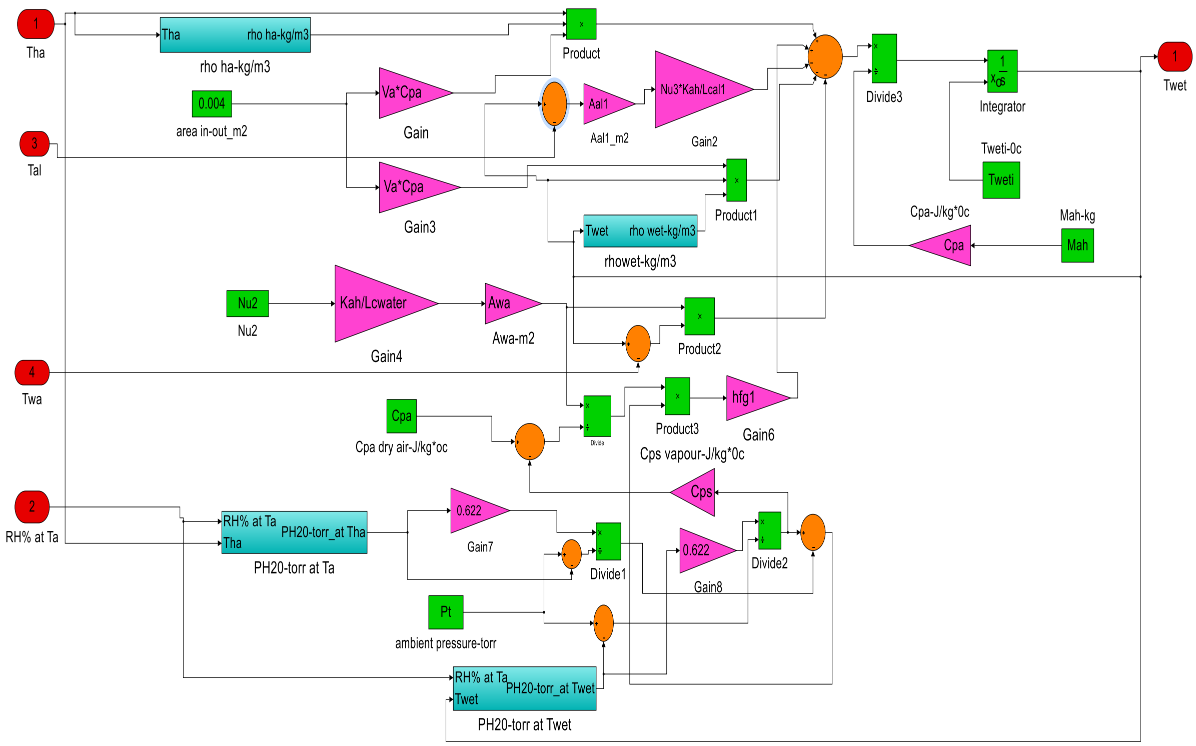

***Figure A.9**: Humidification system air compartment model*

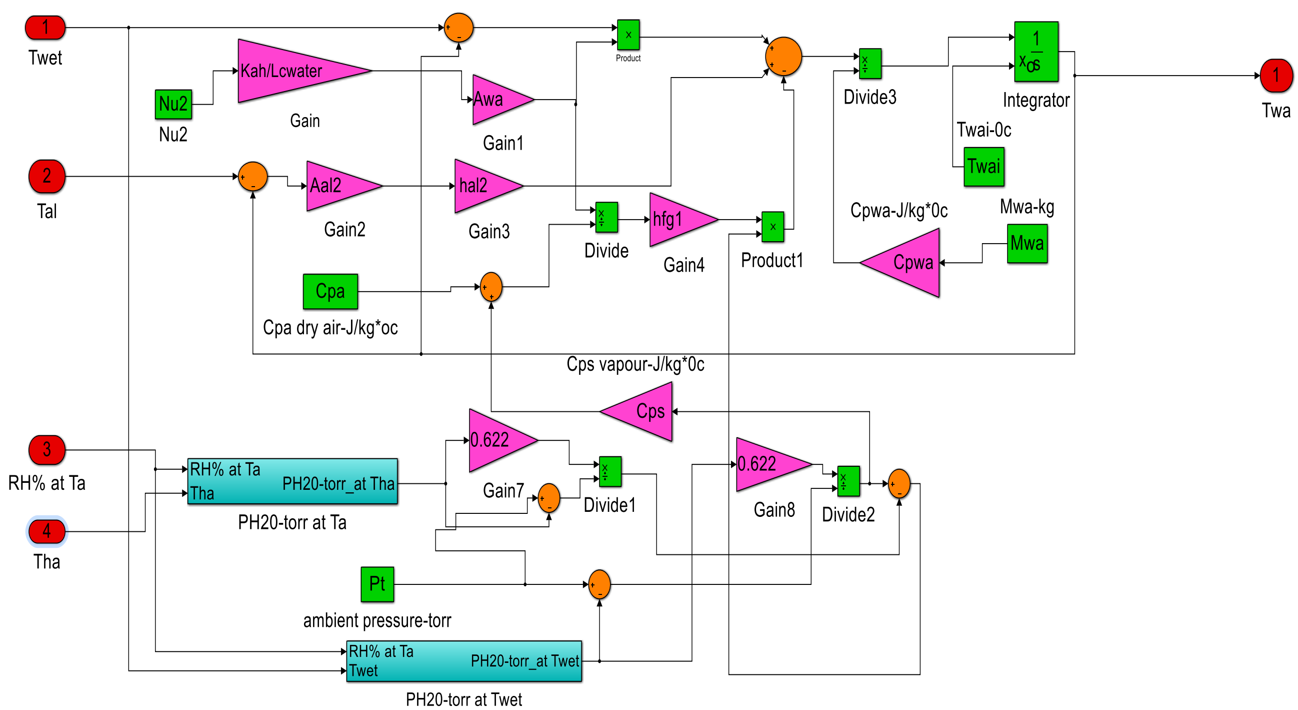

***Figure A.10**: Humidification system water compartment model*

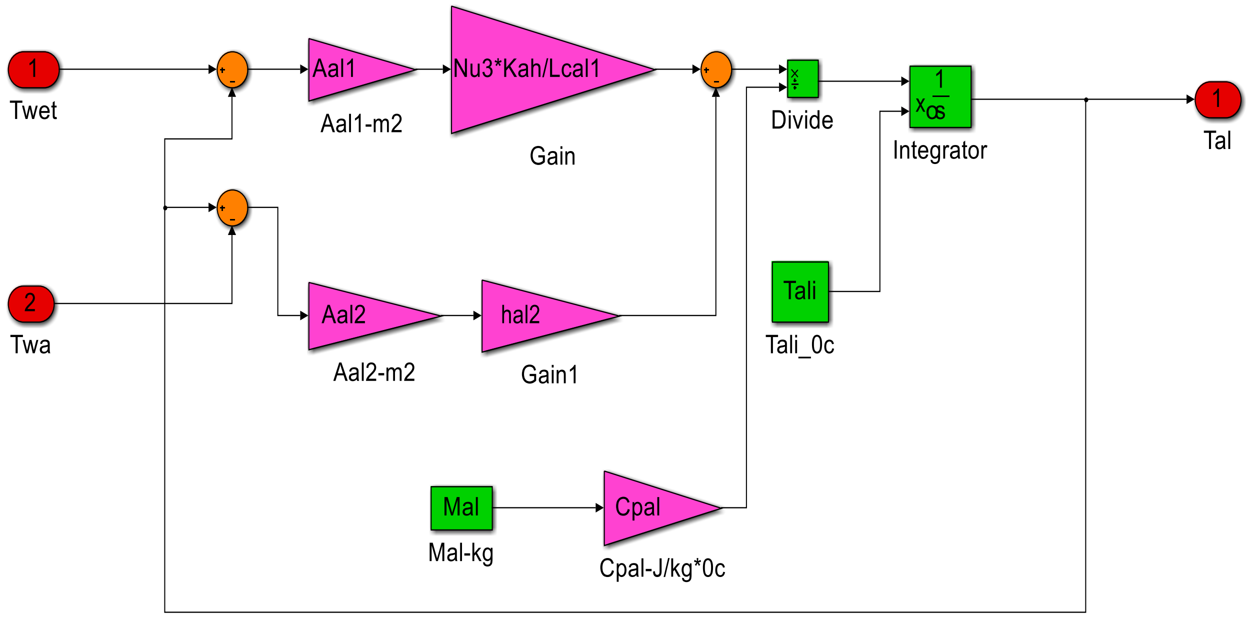

Figure A.11*: Humidification system aluminum block compartment model*

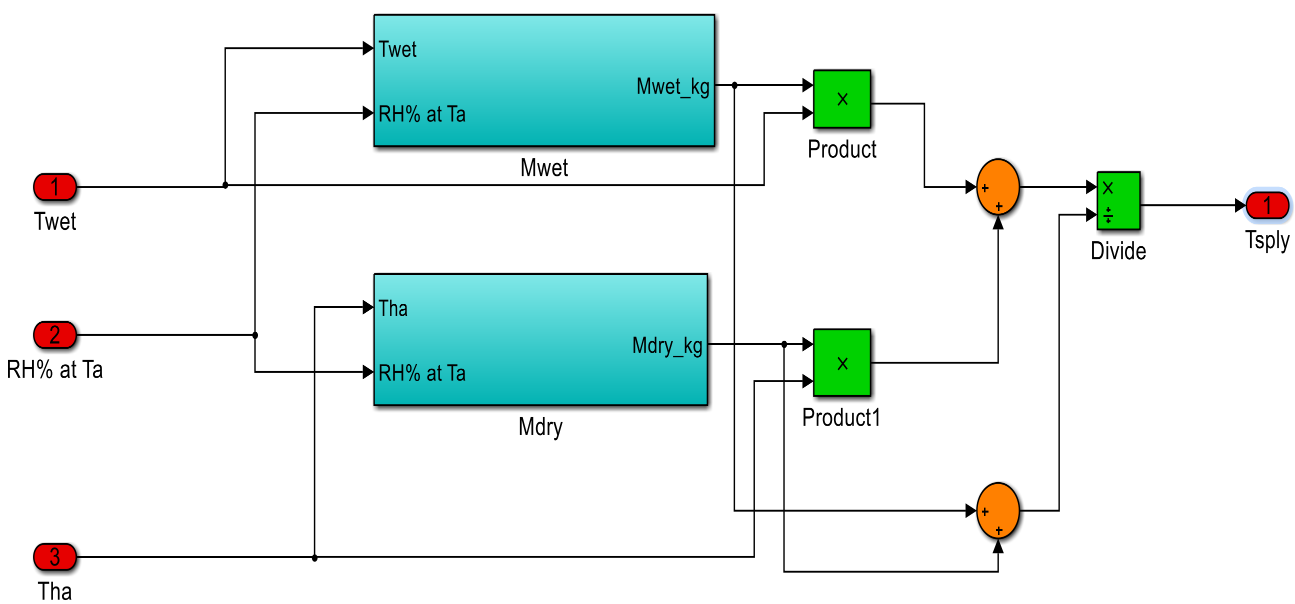

Figure A.12*: Supplied air temperature compartment model*

APPENDIX B: Parameters for the infant-incubator Simulink model

```
% INFANT RELATED VARIABLES
m=0.900;       % kg infant mass
Mrst=24.8;     % W/m2 resting metabolic rate
age=1;         % day postnatal age
GA=28;         % weeks gestational age
ths=0.0005;    % m skin thickness of the infant
Vcb=80*m;      % mL volume of the blood
bf=0.0035;    % sec^-1 blood flow rate parameter
IV=3.667;      % mL/kg*sec inspired minute volume
% INCUBATER RELATED VARIABLES
Amat=0.61*0.345;    % m2 total area of the mattress
Awi=2*(0.403*0.42)+2*(0.853*0.42)+(0.853*0.403); % m2 surface area of the
incubator walls
thw=0.006;            % m thickness of the incubator wall
thm=0.02735;          % m thickness of the mattress
Mm=0.2575;            % kg mass of the mattress
qair=21/60;           % 1/sec volumetric air flow rate
qo2=0;                % 1/sec volumetric oxygen flow rate
Vinc=0.403*0.42*0.835;  % m3 incubator volume
O2=0;                   % O2% percentage of the added oxygen
Aal1=5*2*(0.2*0.028);  % m2 surface area of the exposed part of the finned
aluminium block
Aal2=5*2*(0.2*0.04)+4*0.02163*0.2; % m2 surface area of the submerged part of
the finned aluminium block
Awa=0.335*0.127-0.0035*0.2*5;  % m2 total surface area of the water surface
in the water chamber
Mah=(0.028*0.335*0.127)*1.092;  % kg mass of the air inside the water chamber
Mwa=(0.04*0.335*0.127)*0.001*10^(6); % kg mass of the water inside the water
chamber
Mal=0.88183;          % kg mass of the aluminum block
Ru=8.31447;         % KJ/Kmol universal gas constant
%% VARIOUS THERMAL CONDUCTIVITIES AND CONVECTIVE HEAT TRANSFER COEFFICIENTS
Kc=0.51;        % w/m*0c thermal conductivity of the core
Kmat=0.04184;  % ..................................mattress
Ka=0.02625;    %..................................incubator air at 35 0c
%% VARIOUS DENSITIES
rhoc=1080;     % kg/m3 core density
rhos=1000;     % .....skin.........
rhoa=1.145*10^-6;  % ........air....at 35 0c
rhow=1190.236;     % ........wall...
rhob=1.06E-3;      % ........blood..
rhowater=0.001;    % kg/mL water......
%% PRESSURE DATA
Pt=760;            % torr ambient pressure at 35 0c
%% NATURAL COVECTION PARAMETERS
Awh=0.403*0.853;   % m2 surface area of the horizontal wall of the incubator
g=9.81;          % m/sec^2 gravitational acceleration
Beta=3.356*10^-3;  % 1/k volume expansion coefficient at 30 0c
```

```
Lc=Awh/(0.403+0.853); % m characteristic length of the horizontal surface
mueao=1.872*10^-5;    % kg/m*sec dynamic viscosity at 30 0c
Cpao=1007;            % J/kg*0c specific heat of the air 30 0c
Kao=0.02588;          % W/kg*0c thermal conductivity of the air at 30 0c
v=1.608*10^-5;         % m^2/sec kinematic viscosity of the air at 30 0c
Lc1=0.420;           % m characteristic length of the vertical surface
Awv=0.420*0.853;      % m^2 surface area of the vertical long side
Awv1=0.420*0.403;     % m^2 surface area of the vertical short side
%% NATURAL CONVECTION FOR THE ALUMINIUM BLOCK
hal2=443.33;    %
%% VARIOUS TEMPERATURES AND HUMIDITIES
%Tex=37;              % 0c exhaled air temperature
Te=25;              % 0c environmental air temperature
RH1=1.00;           % relative humidity of the exhaled air
hfg=2419000;         % J.kg latent heat of water at 35 0c_air temperature
hfg1=2383000;        % J.kg latent heat of water at 50 0c_air temperature
%% VARIOUS VARIABLES OF SPECIFIC HEAT TRANSFER
Cpa=1007;           % J/kg*0c specific heat of the air at 35 0c
CpO2=925.2;         % ............................the added oxygen at 25 0c
CpN2=1038.5;        % ............................nitrogen at 25 0c
Cpc=3470;           % ............................core
Cpsk=3766;          % ............................skin
Cpm=1757;           %.............................mattress
Cpb=3840;           % ............................blood
Cpw=1297;           % ............................wall
Cps=1900;           % ..........................vapor at 53.5 0c
Cpwa=4180;          % ........................water
Cpal=900;           % ........................aluminum block
%% NUSSELT NUMBERS FOR CONVECTIVE HEAT TRANSFER COEFFICIENTS
muea=1.895*10^-5;  % kg/m*sec dynamic viscosity of the air at 35 0c
mues=1.8996*10^-5;  % ................................skin 36 0c
Va=0.1;              % m/sec air velocity
Diasph=0.08;         % m approximate infant diameter
Pr=(muea*Cpa)/Ka;   % prandtel number at 35 0c
Re=rhoa*10^6*Va*Diasph/muea;   % reynolds number for infant
Nusph=2+(0.4*Re^(0.5)+0.06*Re^(2/3))*Pr^(0.4)*(muea/mues);  % nusselt number
for infant
Ac=0.42*0.403;            % m2 incubator area based on the direction of the
air flow
P=2*(0.42+0.403);           % m incubator perimeter based on the direction of
the air flow
Dh=(4*Ac)/P;            % m hydraulic diameter of the incubator
f=0.0119;             % friction factor for internal forced convection
Re1=rhoa*10^6*Va*Dh/muea;   % reynold number for incubator
Nu1=((f/8)*(Re1-1000)*Pr)/(1+12.7*(f/8)^(0.5)*(Pr^(2/3)-1));  % nusselt
number for incubator inside
rhoah=1.092;   % kg/m3 air density  at 50 0c
Lcwater=0.335;  % m characteristic length of water surface
mueah=1.963*10^-5;  % kg/m*sec dynamic viscosity of the air at 50 0c
```

```
ReL=(rhoah*Va*Lcwater)/mueah;  % reynolds number for the air passes over the
water surface inside the water chamber
Cpah=Cpa;               % J/kg*0c specific heat of the air at 50 0c
Kah=0.02735;       % W/m*0c thermal conductivity of the air at 50 0c
PrL=(mueah*Cpah)/Kah;  % prandtel number for the air at 50 0c
Nu2=0.664*ReL^(0.5)*PrL^(1/3);  % nusselt number for the water surface in the
water chamber at 50 0c
Lcal1=0.2;    % m characterstic length of the finned aluminum block
ReL1=(rhoah*Va*Lcal1)/mueah;  % reynold number for the air pass over the
fined water surface
Nu3=0.664*ReL1^(0.5)*PrL^(1/3);   % nusselt number for the exposed aluminum
block at 50 0c
%% RADIATION DEPENDENT FACTOR
sigma=5.67*10^-8;     % W/m2*k^4 stephen boltzmann constant
epsilonskin=1.00;     % emissivity of the skin
epsilonwall=0.86;     % .................wall
%% INITIAL CONDITIONS FOR STATE VARIABLES
Tci=36.5;           % deg c
Tsi=37;             % deg c
Tai=29;             % deg c
Tmi=Tai;            % deg c
Twi=25.5;           % deg c
TO2=25;             % deg c
Tweti=45.5;         % deg c
Twai=33;            % deg c
Tali=34;            % deg c
```

APPENDIX C: State space model generation code for skin mode and air mode

```
% run simulink:
sim('Plant1SKINmod');
%linearized the simulink model
[A,B,C,D]=linmod('Plant1SKINmod');
% state space model
PlantSKIN=ss(A,B,C,D);
sisotool(PlantSKIN)
```

```
% run simulink:
sim('Plant2AIRmod');
%linearized the simulink model
[A,B,C,D]=linmod('Plant2AIRmod');
% state space model
PlantAIR=ss(A,B,C,D);
sisotool(PlantAIR)
```